



**Australian Government**

**Department of Defence  
Science and Technology**

**A Review of Australian Investigations on Aeronautical  
Fatigue and Structural Integrity During the Period April  
2015 to March 2017**

*Editors: Phil Jackson and Kevin Walker*

**Aerospace Division  
Defence Science and Technology Group**

**ABSTRACT**

This document has been prepared for presentation to the 35<sup>th</sup> Conference of the International Committee on Aeronautical Fatigue and Structural Integrity (ICAF) scheduled to be held in Nagoya, Japan, 5-6 June 2017. The document contains summaries of the research and associated activities in the field of aircraft fatigue and structural integrity at research laboratories, universities and aerospace companies in Australia during the period April 2015 and March 2017.

A report of the same name will be published by Defence Science and Technology and available for public release.

*Approved for public release*



*Produced by*

*Aerospace Division  
Defence Science and Technology Group  
506 Lorimer Street  
Fishermans Bend VIC 3207, Australia*

*Telephone 1300 333 362*

*© Commonwealth of Australia 2017  
May 2017  
AR-XX-XXXX*

*This information may be subject to privately owned rights.*



# Contents

1. INTRODUCTION.....	8
2. RESEARCH ACTIVITIES .....	9
2.1 Investigation of 3D Stress States at Crack Front; [A. Kotousov and Z. He, [The University of Adelaide].....	9
2.2 Effect of Crack Front Shapes on Fatigue Life Assessment; B. Zakavi and A. Kotousov, [The University of Adelaide, Australia] and R. Branco, [The University of Coimbra, Portugal].....	11
2.3 Evaluation of fatigue crack propagation behaviour in Ti-6Al-4V manufactured by selective laser melting; K. Walker, and Q. Liu [DST Group Australia], and M. Brandt [RMIT University Australia] .....	12
2.4 The Effect of Cold Expansion on the Fatigue Life of Low Load Transfer Joint Coupons Containing Cracked Fastener Holes; P. S. Baburamani, R. Ogden [DST Group], T. J. Harrison [Fortburn Pty Ltd].....	14
2.5 The Effect of Decoupling of Corrosion and Fatigue; D. Tamboli, R. Jones [Monash University], S. Barter [DST Group] .....	16
2.6 Quantitative fractography and modelling of fatigue crack propagation in high strength AerMet®100 steel repaired with a laser cladding process; K.F. Walker [DST Group Australia], J.M. Lourenco, Rio Grande do Norte [Federal Institute of Technology Brazil], S, Sun, M. Brandt, and C.H. Wang [RMIT University Australia] .....	18
2.7 Fatigue Crack Growth of 7075-T651 Aluminium Alloy under Proportional and Non-proportional Mixed Mode I and II Loads, Xiaobo Yu [DST Group], Ling Li and G. Proust [University of Sydney].....	20
2.8 Softening and re-hardening of 7075 Aluminium Alloys under variable amplitude loads; Xiaobo Yu, Chris Wallbrink and Qianchu Liu (DST Group) .....	22
2.9 Constant-Amplitude Fatigue-Crack Growth Behavior on 7075-T6 and 7249-T76511 Aluminum Alloys; K.F. Walker [DST Group Australia], and J.C. Newman Jr. [Mississippi State University USA] .....	23
2.10 Spectrum Truncation or Spectrum Compression? :When time and money matters and nothing less than a fraction of the original spectrum is acceptable; Chris Wallbrink and Beau Krieg [DST Group] .....	27
2.11 Improving fatigue life predictions with a crack growth rate material model based on small crack growth & legacy data; M. Burchill, S. Barter [DST Group] .....	29
2.12 The development of bar-coded marker band load sequences to enhance fatigue test outcomes; M. Burchill, S. Barter, M. McDonald [DST Group] .	32
2.13 Fatigue crack path manipulation for crack growth rate measurement, S. Barter, P. White, M. Burchill [DST Group].....	34
2.14 Automation of Quantitative Fractography for Determination of Fatigue Crack Growth Rates with Marker Loads; W. Hu, S. Barter [DST Group], A. Wiliem, B. Lovell, L. Liu [University of Queensland] .....	37
2.15 Automated Crack Growth Tracking Capability; Dr N. Rajic [DST Group]	38

2.16	A bounded distribution model of equivalent initial flaw size distribution for structural risk analysis; R. Torregosa and W. Hu, [DST Group].....	39
2.17	A comparative evaluation of a deterministic and probabilistic approach for determining safety inspection intervals of airframe structures; R. Torregosa and W. Hu [DST Group].....	40
2.18	Fatigue Crack Prognosis Using Bayesian iProbabilistic Modelling; W. Wang, W. Hu, and N. Armstrong [DST Group] .....	41
2.19	Aeronautical Fatigue and Structural Integrity Activities at Boeing Aerostructures Australia (BAA); A. Garg, A. Pipilikas, A Sheppard [BAA Melbourne], S. Georgiadis [Boeing Research & Technology, Melbourne] .	45
2.19.1	Introduction.....	45
2.19.2	CFRP Joint Durability with Bolts .....	46
2.19.3	CFRP Joint Durability with Rivets .....	47
2.19.4	Notched Fatigue Behaviour of CFRP Pre-Preg and Resin Infused Laminates.....	48
2.19.5	High Cycle Vibration Fatigue .....	50
2.19.6	Integrated Co-cured Structures and New Materials .....	51
3.	FULL SCALE TEST ACTIVITIES .....	52
3.1	C-130J Wing Fatigue Test Teardown and Forensic analysis; D. Williams [DST Group] .....	52
3.2	Distributed Fibre Optic Strain System for Full-Scale Fatigue Testing; C. Davis, M. Knowles, N. Rajic and G. Swanton, [DST Group].....	55
3.3	Sample Heading Level 2 Blueprint TITANS: A Roadmap towards the Virtual Fatigue Test through a Collaborative International Effort; A. K. Wong [DST Group] .....	57
4.	IN-SERVICE STRUCTURAL INTEGRITY MANAGEMENT .....	61
4.1	Innovative Repair of Classic Hornet Centreline Pylons based on Optimal Shape Reworking; Xiaobo Yu1, Jaime Calero, Simon Barter, Michael Opie [DST Group], Matt Gordon [Defence Aviation Safety Authority] .....	61
4.2	F/A-18A/B Shear Post Coupon Design and Critical Crack Size Estimation, R Evans and X Yu [DST Group], D Tata [QinetiQ] .....	63
4.3	Fatigue Analysis of Transport Aircraft Structures using Advanced Cyclic Plasticity Models - an Assessment; D. Agius, [RMIT], C. Wallbrink, W. Hu [DST Group], K. Kourousis [University of Limerick] and C. Wang [UNSW].....	65
4.4	Simulated Aircraft Spectrum Loading Behavior on 7075-T6 and 7249-T76511 Aluminum Alloys used on the P-3 Aircraft; K.F. Walker [DST Group Australia] and J.C. Newman Jr., [Mississippi State University USA] .....	67
4.5	Research Program Outcome: Interaction of Fatigue and Intergranular Corrosion in the AP-3C Dome Nut Holes; T. J. Harrison, B. R. Crawford, C. Loader, D. Goudie, A. Walliker [DST Group].....	71
4.6	A Study of the Effectiveness of porosity as a fatigue crack initiator in AA7050-T7451; S. Barter and B. Dixon [DST Group].....	74

4.7	An Investigation of the Effectiveness of Adhesively Bonded Doubler Repairs on Existing Fatigue Cracks in Typical Combat Aircraft Structures; G. Swanton, L. Robertson and S. Barter [DST Group] .....	76
4.8	Recent Developments in SHM for Aircraft Structures - an Australian Defence Perspective; S. Galea, N. Rajic, C. Davis, C. Rosalie, J. Smithard, C. Brooks, S. van der Velden and P. Norman; [DST Group].....	77
4.9	F/A-18 Inner Wing Step Lap Joint Phased Array Ultrasonic (PAUT) Inspection Development; S. Trezise [QinetiQ Australia] .....	78
4.10	C-130J WFT Test Interpretation; M. Richmond [QinetiQ Australia] .....	78
4.11	Rotary Wing - Best Practice Fatigue Management; Anthea Mills [QinetiQ Australia] .....	79
4.12	Non-intrusive Flight Test Instrumentation (NIFTI) for Aircraft Structural Integrity Management; S. Galea [DST Group] .....	80
5.	FATIGUE INVESTIGATIONS OF IN-SERVICE AIRCRAFT.....	81
5.1	Propeller “falls off” a Saab 340B Commuter Aircraft; [Civil Aviation Safety Authority].....	81
5.2	RAAF F/A-18 Auxiliary Power Unit (APU) Turbine Hub Cracking; [N. Athinotis DST Group] .....	82
5.3	Helicopter Horizontal Driveshaft Intermediate Bearing Cracked Assembly; [N. Athinotis DST Group] .....	83
5.4	PC-9/A Frame 11 Left Hand Top Fastening Bracket Stress Corrosion Cracking; [N. Athinotis DST Group].....	84
5.5	PC-9/A Nose Landing Gear Folding Strut Cracking; [N. Athinotis DST Group] .....	85

# 1. Introduction

This document presents a review of Australian work related to aeronautical fatigue and structural integrity in the period April 2015 to March 2017, and is made up from inputs from the organisations listed below. The editor acknowledges these contributions with appreciation. Each contribution includes relevant references for further information and enquiries should be addressed to the person identified against the item of interest.

DST Defence Science and Technology Group, 506 Lorimer Street, Fishermans Bend, VIC 3207, Australia

QinetiQ Australia Level 3, 210 Kings Way, South Melbourne, VIC 3205, Australia.

Monash University Dept of Mechanical Engineering, PO Box 72, Monash University, VIC 3800, Australia.

RMIT University Dept of Aerospace, Mechanical and Manufacturing Engineering, PO Box 71 Bundoora, VIC 3083, Australia

University of New South Wales School of Mechanical and Manufacturing Engineering, University of New South Wales, NSW 2052 Australia

The University of Adelaide School of Mechanical Engineering, The University of Adelaide, Engineering South, L1, SA 5005, Australia

Civil Aviation Safety Authority Aviation House, PO Box 2005 Canberra, ACT 2601, Australia

Royal Australian Air Force Deputy Director ASI, Directorate General Technical Airworthiness, RAAF Williams, Laverton, VIC 3027, Australia

## 2. Research activities

### 2.1 Investigation of 3D Stress States at Crack Front; [A. Kotousov and Z. He, [The University of Adelaide].

Theoretical, numerical and experimental studies involving elastic plate components, weakened by through-the-thickness cracks and subjected to loading parallel to the plane of the plate, are often based on plane stress or plane strain simplifications. These simplifications essentially reduce the dimensionality of the physical three-dimensional problem and enable the achievement of effective analytical and numerical solutions for many important practical problems [1]. The influence of various three-dimensional effects, such as the variation of stresses across the plate thickness, effects of the three-dimensional corner (vertex) singularities and coupling of fracture modes II and III, on the deformation and stresses near the crack front are presently largely ignored or viewed as negligible for all practical purposes [2]. As a result of this perception, the outcomes of experimental studies and fracture tests are also commonly analysed within the framework of the plane theories of elasticity. Nevertheless, a number of theoretical and experimental studies over the past two decades have demonstrated that the predictions made within these theories can be unsatisfactory and the effect of three-dimensional stress states at the crack front on fatigue and fracture of plate components can be quite significant [3].

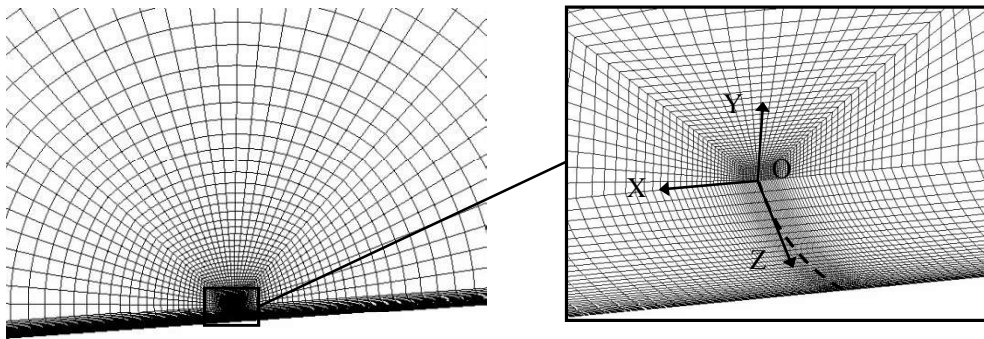


Figure 1: Mesh in vicinity of the curved crack front.

Our recent studies aimed to elucidate the role of three-dimensional stress states in the fracture and fatigue phenomena. The main outcomes achieved so far are: (1) the development and validation of a simplified method for the evaluation of the fatigue crack front shapes and their effect on the steady-state fatigue crack growth rates in plate components [4]. The method is based on a number of implicit and explicit assumptions and utilises the earlier developed analytical model for plasticity-induced crack closure in plates of finite thickness [5] as well as linear-elastic three-dimensional finite element modelling (Figure 1 shows mesh division of the 3D FE model); (2) the development and validation of an experimental approach for accurate evaluation of stress intensity factors from the measurement of the out-of-plane displacements in the near crack tip region, which are affected by three dimensional effects, in particular, by the 3D corner (vertex) singularity [6]. The approach is based on the linear relationships between the remote stress intensity factors and the displacement fields in the area of interest. Digital image correlation (DIC) technique was employed to extract the displacement data around the crack tip region on the surface of testing samples. Figure 2a shows a contour plot of out-of-plane displacement around the crack tip for specimens subjected to mode I loading. The experimental data agrees very well with that obtained from numerical simulations, see Figure 2b, especially in the near crack tip region.

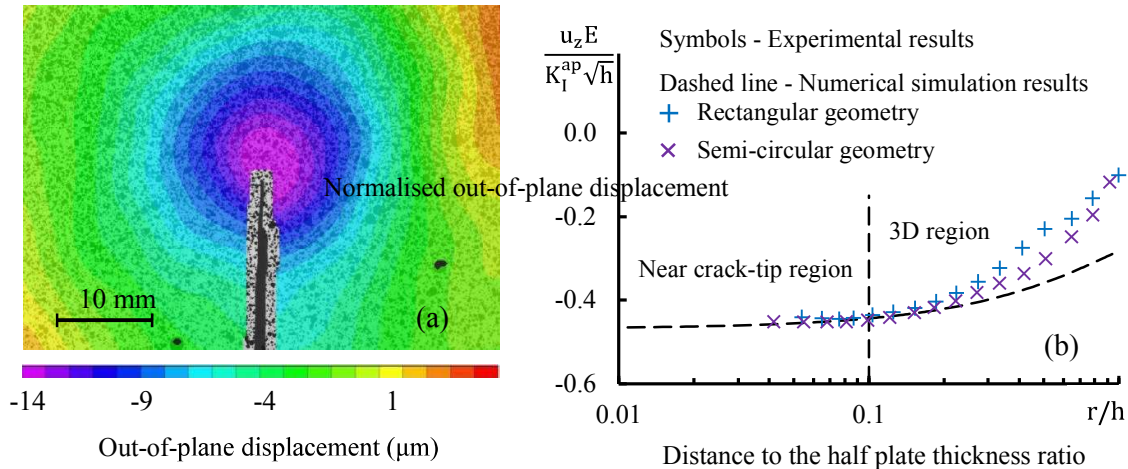


Figure 2: (a) Contour plot of out-of-plane displacement around the crack tip for specimens stressed in mode I. (b) Normalised out-of-plane displacement on the plate free surface as a function of  $r/h$ .

Our efforts in this area could be important in several engineering contexts. For example, the new theoretical model, which takes into account the actual shape of the crack front, can be utilised in advanced fatigue life calculations, as well as in failure investigations. The latter is possible as the shape of the fatigue crack front can be related to the parameters of fatigue loading. The developed experimental approach [6] can be useful in fracture characterisation of thick plate components with through-cracks. This approach specifically addresses the situation when the K-dominance zone, or William's solution convergence domain, are relatively small. In this case, the data extraction region can be affected by the 3D stress states leading to significant errors in the evaluation of the stress intensity factors when using traditional methods.

Email: [andrei.kotousov@adelaide.edu.au](mailto:andrei.kotousov@adelaide.edu.au)

## References

- [1] A Kotousov. Fracture in plates of finite thickness. *International Journal of Solids and Structures*, Vol 44, 2007, pp 8259-8273.
- [2] A Kotousov. Effect of plate thickness on stress state at sharp notches and the strength paradox of thick plates. *International Journal of Solids and Structures*, Vol 47, 2010, pp 1916-1923.
- [3] LP Pook. A fifty year retrospective review of three dimensional effects at cracks and sharp notches. *Fatigue and Fracture of Engineering Materials and Structures*, Vol 36, 2013, pp 699-723.
- [4] Z He, A Kotousov, R Branco. A simplified method for the evaluation of fatigue crack front shapes under mode I loading. *International Journal of Fracture*, Vol 188, 2014, pp 203-211.
- [5] J Codrington, A Kotousov. A crack closure model of fatigue crack growth in plates of finite thickness under small-scale yielding conditions. *Mechanics of Materials*, Vol 41, 2009, pp 165-173.
- [6] Z He, A Kotousov. On evaluation of stress intensity factor from in-plane and transverse surface displacements. *Experimental Mechanics*, Vol 56, 2016, pp 1385-1393.

## 2.2 Effect of Crack Front Shapes on Fatigue Life Assessment; B. Zakavi and A. Kotousov, [The University of Adelaide, Australia] and R. Branco, [The University of Coimbra, Portugal].

Many experimental studies and test results demonstrated that fatigue crack front shapes are not straight but curved as shown in Figure 1 [1]. This phenomenon was discussed in many papers, and several plausible explanations were proposed over the past four decades. In particular, the angle at which the front intersects the free plate surface,  $\gamma$ , is often linked to the presence of the 3D corner singularity [1-3]. Recently, several methods were developed in order to predict the fatigue crack front shape evolution and its effect on the crack growth rates. These include explicit numerical techniques, e.g. [1] as well as simplified procedures, e.g. [4, 5]. However, all these methods were largely focused on through-the-thickness cracks in plate components, which represent a small portion of practically important situations.

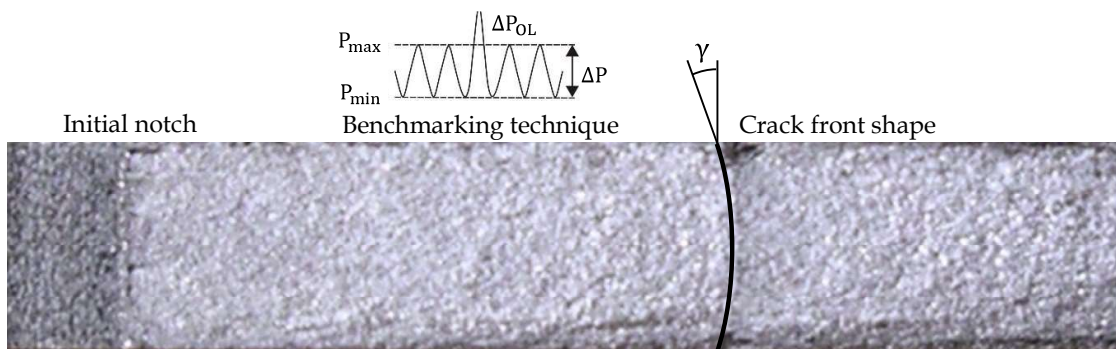


Figure 1: The experimental crack front shape for an Aluminium alloy 6082-T6 plate with a through-thickness crack,  $R=0.25$  [1]

Our long-term goal is to develop advanced fatigue crack growth modelling tools, which are capable to take into account the evolution of the shapes of fatigue cracks in various structural components. It is expected that the achievement of this goal will improve of the accuracy of fatigue life prediction techniques, which currently disregard this phenomenon.

### References

- [1] R Branco, FV Antunes. Finite element modelling and analysis of crack shape evolution in Mode-I fatigue Middle Cracked Tension specimens. *Engineering Fracture Mechanics*, 2008; Vol. 75(10), pp. 3020-3037.
- [2] M Heyder, K Kolk, G Kuhn. Numerical and experimental investigations of the influence of corner singularities on 3D fatigue crack propagation. *Engineering Fracture Mechanics*, 2005; Vol. 72(13), pp. 2095-2105.
- [3] Z He, A Kotousov, F Berto. Effect of vertex singularities on stress intensities near plate free surfaces. *Fatigue and Fracture of Engineering Materials and Structures*, 2015; Vol. 38(7), pp. 860-869.
- [4] J Codrington, A Kotousov. A crack closure model of fatigue crack growth in plates of finite thickness under small-scale yielding conditions. *Mechanics of Materials*, 2009; Vol. 41(2), pp. 165-173.
- [5] Z He, A Kotousov, R Branco. A simplified method for the evaluation of fatigue crack front shapes under mode I loading. *International Journal of Fracture*, 2014; Vol. 188(2), pp. 203-211.

### 2.3 Evaluation of fatigue crack propagation behaviour in Ti-6Al-4V manufactured by selective laser melting; K. Walker, and Q. Liu [DST Group Australia], and M. Brandt [RMIT University Australia]

Total fatigue life performance of high strength titanium alloy Ti-6Al-4V manufactured by Additive Manufacturing (AM) based methods such as Selective Laser Melting (SLM) is of significant interest and has gained much attention recently. Researchers often compare the total fatigue life of materials manufactured from SLM compared with conventional manufacture, and often the SLM lives are reduced because cracks initiate from “defects” such as porosity or Lack of Fusion (LOF). But for repair and alternative manufacture of complex and critical aerospace structures for example, the crack growth/propagation phase of the fatigue process is also very important and it has not been studied as extensively. The aim of the work here was to evaluate and better understand crack propagation under constant amplitude loading in Ti-6Al-4V samples manufactured using SLM with a variety of layer thicknesses and build directions (vertical or horizontal) [1, 2]. The “as-manufactured” condition was studied, with no post heat treatment. Cracks typically initiated at LOF features which had a negative impact on the total fatigue life. The focus here was on the crack growth phase. Modelling was performed with a conventional Linear Elastic Fracture Mechanics approach using literature data [3, 4] obtained from testing on Compact Tension (C(T)) specimens which were also in the as-manufactured condition with a variety of build directions. The fatigue test specimen geometry is shown in Figure 1 and Figure 2.

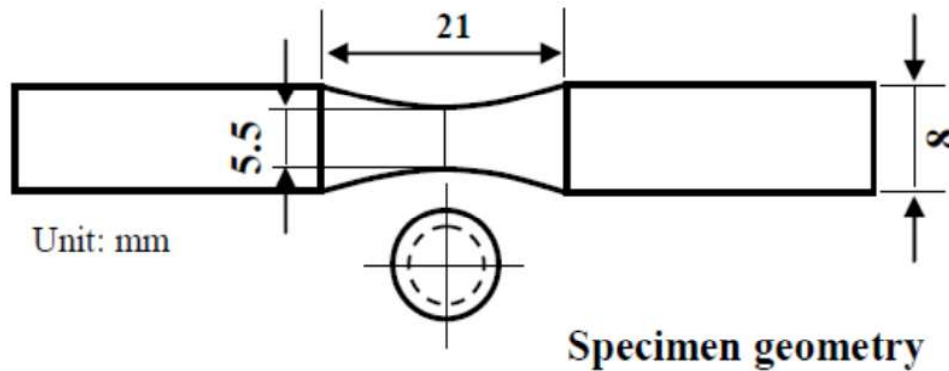


Figure 1 : Fatigue test specimen geometry



Figure 2 : Fatigue test specimen manufacture

The analysis showed that the typical crack initiating lack of fusion/porosity features (see Figure 3) correlated reasonably well as shown in Figure 4.

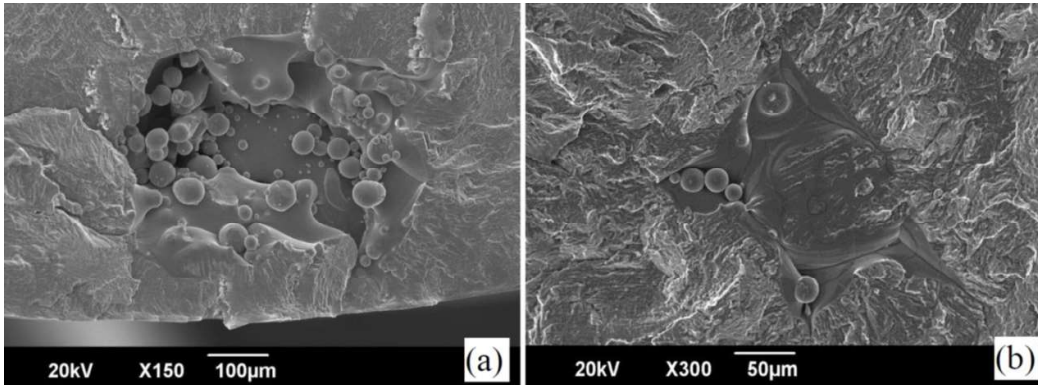


Figure 3 : Typical lack of fusion/porosity features

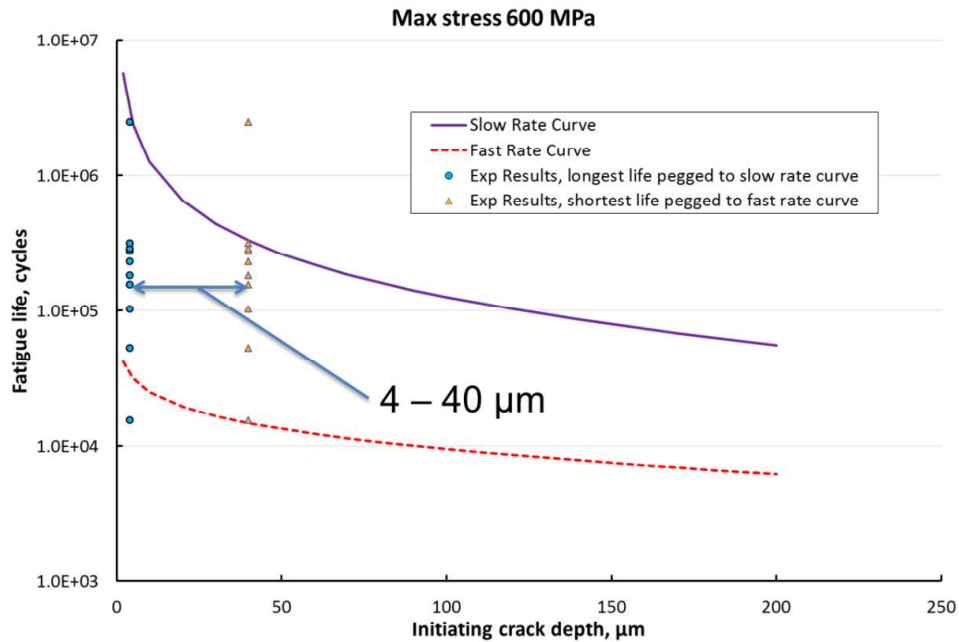


Figure 4 : Equivalent initial crack range to correlate range of observed fatigue lives

The modelling provided a very useful correlation of the data and provided a way of assessing the LOF features in terms of an equivalent initial crack. The crack growth properties of the SLM cases were also compared against literature data for conventionally manufactured material. The work will lead to a better understanding of fatigue crack growth characteristics for components manufactured by AM methods such as SLM. That understanding is an essential requirement for full certification and acceptance into service for critical applications such as aerospace structures.

## References

1. Liu, Q., et al., *The Effect of Manufacturing Defects on The Fatigue Behaviour of Ti-6Al- 4V Specimens Fabricated Using Selective Laser Melting*. Advanced Materials Research, 2014(891-892): p. 1519.
2. Walker, K.F., Liu, Q., and Brandt, M. *Evaluation of fatigue crack propagation behaviour in Ti-6Al-4V manufactured by selective laser melting*. in *International Conference on Fatigue Damage of Structural Materials*. 2016. Hyannis, MA, USA.

3. Dhansay, N.M., R. Tait, and T. Becker, *Fatigue and fracture toughness of Ti-6Al-4V titanium alloy manufactured by selective laser melting*. Advanced Materials Research. Vol. 1019. 2014: Trans Tech Publications Ltd. 248-253.
4. Edwards, P. and M. Ramulu, *Effect of build direction on the fracture toughness and fatigue crack growth in selective laser melted Ti-6Al-4V*. Fatigue and Fracture of Engineering Materials and Structures, 2015. **38**(10): p. 1228-1236.

Contact K. Walker at [kevin.walker@dsto.defence.gov.au](mailto:kevin.walker@dsto.defence.gov.au)

## **2.4 The Effect of Cold Expansion on the Fatigue Life of Low Load Transfer Joint Coupons Containing Cracked Fastener Holes; P. S. Baburamani, R. Ogden [DST Group], T. J. Harrison [Fortburn Pty Ltd]**

### **The description of work and results**

The main objective of this work was to quantify and demonstrate the fatigue life benefits of the Hole Cold Working (HCW) technology, by carrying out laboratory fatigue tests on typical low load transfer joint coupons representative of the fastened joints in transport type aircraft structure. Importantly, these joint coupons also contained pre-cracked fastener holes.

The laboratory fatigue tests in this work were carried out on cracked and pristine low load transfer joint coupons in cold worked and non-cold worked conditions, by applying a variable amplitude wing fatigue test spectrum, a representative loads spectrum generated as part of the RAAF C-130J-30 wing fatigue test program (WFTP) (McCoy and Ogden 2011). The fatigue tests were conducted at a gross maximum applied stress of 150.6 MPa (21.84 ksi), which corresponds to the maximum stress in a C-130J-30 wing fatigue test spectrum at the lower wing panel/fuselage attach angle location with a stress multiplication factor of 1.20. The fatigue test results led to the following conclusion in that the hole cold working technology was seen to be effective in providing fatigue life extension in low load transfer joint coupons, with Hi-Lok™ fasteners even when cracks of up to 3 mm in length were present at the fastener holes in the joint configuration, with an improvement factor at a minimum of 9 and a maximum of 35 (Table 1). Coupons with no pre-existing crack (0.00 mm) or just the EDM notch (0.40 mm) reached run out stage (i.e. no failure of the coupons) at close to 200,000 equivalent number of flights when the fastener holes in the coupons were cold expanded. The laboratory test results presented (Figures 1 and Table 1) in this summary provide a positive trend in reinforcing the benefits of hole cold working in the presence of cracks in the fastener holes. This outcome provides an opportunity for the application of hole cold working technology to in-service transport aircraft structures or similar with cracked fastener holes (see also Baburamani et al. 2016). A fatigue crack growth curve derived from fractographic progression mark measurements, for a coupon with an EDM notch, and a pre-crack length of 3.00 mm and the coupon was hole cold worked is shown in Figure 2.

### **Conclusion and Recommendation**

The laboratory coupon fatigue test results on cracked and pristine low load transfer joint coupons in cold worked and non-cold worked conditions, using realistic variable amplitude spectrum loading, and representative of the RAAF C-130J-30 aircraft loads led to the following conclusion and recommendation:

- a. Hole cold expansion (hole cold working) technology is shown to be effective in providing fatigue life extension in low load transfer joint coupons even when cracks of up to 3 mm in length were present at the fastener holes in the joint configuration.

- b. The fatigue life improvement factors attributable to hole cold working in the low load transfer joint coupons with a 3 mm pre-existing crack have been estimated to be at a minimum of 9 and a maximum of 35.
- c. The technology insertion could be considered during scheduled or unscheduled inspection and when the presence of small (< 3 mm) cracks is evident, to future proof the fastened assemblies from potential, catastrophic failures. The laboratory test results presented in this report provide a positive trend in reinforcing the benefits of hole cold working in the presence of cracking damage at the fastener holes, to provide a basis for consultation with respective ASIP managers and SPOs, and the RAAF Defence Aviation Safety Authority.

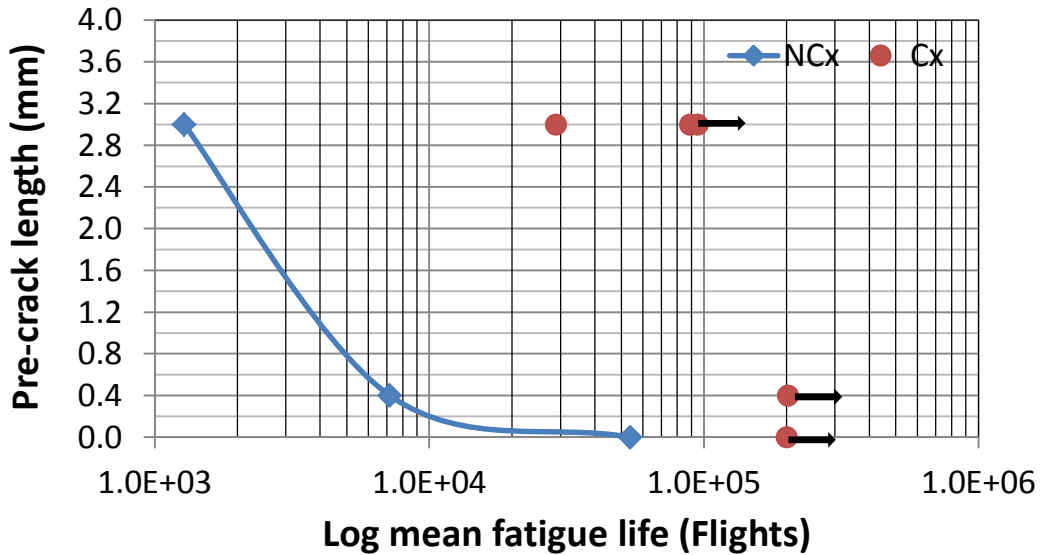


Figure 1 Log mean fatigue life results for variable amplitude, spectrum loading at 150.6 MPa gross stress, including run out coupons marked by arrows in respect of cold worked coupons

Table 1 Fatigue life improvement factors due to cold expansion of low load transfer joint coupons with a 3 mm pre-crack length, as indicated, subject to variable amplitude, spectrum loading, at a maximum applied gross stress of 150.6 MPa (21.84 ksi)

Pre-crack length (mm)	Log mean fatigue life (Flights), not cold expanded, NCx	Log mean fatigue life (flights), cold expanded, Cx	Fatigue life improvement factor (LIF)
No pre-crack, 0.00	53,861.18	Coupon run out #	---
EDM notch, 0.40	7,165.82	Coupon run out #	---
3.00	1,290.40	46,263	35.85
3.00	1,290.40	43,190.62	33.47
3.00	1,290.40	12,010.57	9.31

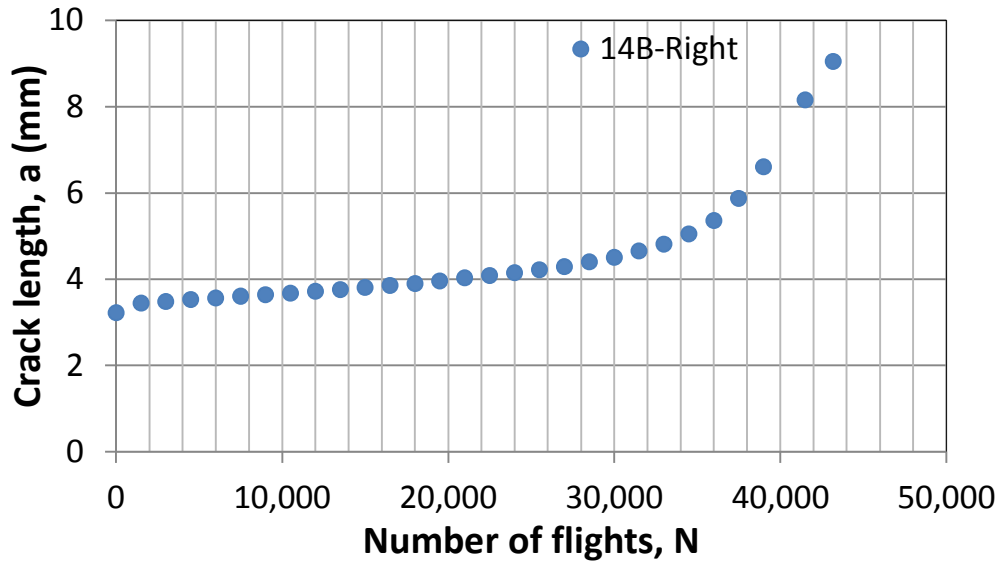


Figure 2 Fatigue crack growth curve derived from fractographic progression mark measurements, for a coupon with an EDM notch, and a pre-crack length of 3.00 mm and the coupon hole cold worked. Note the crack retardation to nearly 30,000 flights due to the effect of hole cold working and the compressive residual stress.

#### References:

- Baburamani, P. S., Ogden, R. and Harrison, T. J., The Effect of Cold Expansion on the Fatigue Life of Low Load Transfer Joint Coupons Containing Cracked Fastener Holes, DST-Group-TN-1572, Defence Science and Technology Group, October 2016, 33p.
- McCoy, M. and Ogden, R., Coupon test Program in Support of the Royal Australian Air Force C-130J-30 Hercules Full Scale Fatigue Test Interpretation, DSTO-TR-2557, June 2011, Defence Science and Technology Organisation, Commonwealth of Australia, 191p.

### 2.5 The Effect of Decoupling of Corrosion and Fatigue; D. Tamboli, R. Jones [Monash University], S. Barter [DST Group]

The degradation produced by corrosion has been identified as a major source of fatigue cracking in aluminium alloy aircraft structures and has been shown to lead to the failure by fatigue in many components. Studies thus far have indicated that a major concern where corrosion is implicated is that a corrosive environment could accelerate the fatigue crack growth that has nucleated from corrosion damage. However, more recent studies have indicated that in combat aircraft at least, there appears to be little corrosion in flight, and that fatigue cracking dominates over any corrosion assisted mechanism. This came to pass when Trathen [1] reported the corrosion rates measured in internal bays of several RAAF aircraft and found that there appeared to be little corrosion activity during flight. Barter and Molent [2] subsequently showed that for cracking in AA7050-T7451 in operational RAAF F/A-18 Hornet aircraft, an observation of the fracture surface revealed that corrosion was only apparent during extended periods of downtime (inactivity). These independent findings suggest that for combat aircraft there appears to be a decoupling of fatigue and environment i.e. the growth of fatigue cracks is not assisted by the environment.

Here, research results are presented to substantiate these findings viz. that for high performance combat aircraft, there appears to be little interaction between corrosion on ground and fatigue

crack growth in flight. In line previous work that examined the Hartman-Schijve equation [3] as a method for the prediction of cracks in the material examined here, it was found that the growth rate of the cracks that had been grown from corrosion pitting could be captured well by this approach.

## Results

Four hour-glass test specimens were prepared by placing an approximately 50  $\mu\text{L}$  droplet of 0.606 M Sodium Chloride (NaCl) solution on the surface in the test section of the specimen and holding these specimens in an environmental chamber maintained at 20°C and 98% relative humidity (RH) for a week. After specimen removal they were tested in a 100kN servo hydraulic fatigue testing machine. One specimen which acted as the baseline test, was simply fatigued to failure after this initial exposure. All tests were carried out at a nominal frequency of 10 Hz. Constant amplitude loading was applied with the addition of a markerband at the end of every 15,000 cycles to aid in Quantitative Fractography (QF). The loading was: 15,000 cycles at  $R = 0.8$  with a marker of 250 cycles at  $R = 0.1$ . Maximum stress in each case was targeted at 250 MPa (slight variation due to the variable location of the pitting that started the main cracks and the hour-glass shape of the specimen). This stress level was targeted since it was a typical peak stress that may be found in a critical component of an F/A-18 thick aluminium plate bulkhead. The remaining 3 specimens were cycled and corroded intermittently. For the intermittent corrosion specimens, they were cycled for 15.5 blocks or 236,375 cycles and then removed from the fatigue machine, wetted and placed in an environmental chamber at 20°C and 98% RH for one week to simulate moisture exposure while an aircraft is on the ground. Thereafter, the coupons were cycled and intermittently exposed every 15 blocks or 228,750 cycles. This procedure of cycling and exposure to the environment (15 blocks + 1-week exposure) was repeated until failure by fatigue.

The resulting crack growth curves were obtained by QF (post failure measurements of the repeating block pattern on the fracture surface) and the results are presented in Figure 1a below.

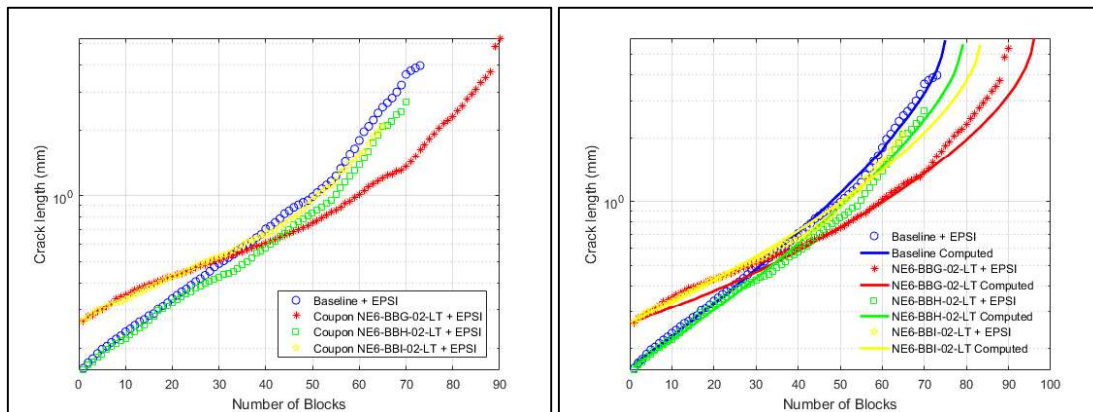


Figure 1. (a) QF measurements for intermittent corrosion and fatigue data + EPS Type I and (b) Measured and Computed crack growth histories for cracks growing from corrosion pits.

The curves all roughly follow an exponential pattern. When the specimens that were intermittently corroded are compared with the baseline test specimen that was only exposed to the initial corrosive environment to grow corrosion pits and then fatigued to failure, there is very little difference in the growth rates. A comparison of these results indicates that intermittent exposure to moisture did not have any appreciable effect on fatigue crack growth. These results thus substantiate that intermittent exposure to the environment while any fatigue loads are not being

applied has little effect of the fatigue crack growth. Therefore, the claims made in [1-2] that fatigue and corrosion appear to be decoupled in combat aircraft allows the problem to be isolated i.e. once fatigue cracking has commenced, the influence of any further corrosion exposure is minimal of that the remaining life of the component can be calculated using an appropriate crack growth model. To demonstrate this, the test results obtained above were modelled using the Hartman-Schijve crack growth equation [3] given below

$$\frac{da}{dN} = 7 \times 10^{-10} \left( \Delta K - \Delta K_{thr} / \sqrt{1 - K_{max}/47} \right)^2 \quad (1)$$

The resulting plots are given in Figure 1b. The solid lines show the computed data using Equation 1. Small variations (between 0.08 and 0.4) in the threshold stress intensity factor,  $\Delta K_{thr}$ , could capture each of the measured test data reasonably well.

## Conclusion

It can thus be concluded that exposing a test specimen intermittently to a corrosive environment causes no significant change in the crack growth rate where the exposure is decoupled for the fatigue cycling and that the growth of the fatigue cracks so produced can be captured well by the Hartman-Schijve equation. These findings are consistent with previous studies conducted at DST Group.

## References

- [1] Trathen, P. (2011). Corrosion monitoring systems on military aircraft in *Proceedings of the 18<sup>th</sup> International Conference on Corrosion*, Perth, Australia.
- [2] Barter, S.A. and Molent, L. (2012). Investigation of an in-service crack subjected to aerodynamic buffet and manoeuvre loads and exposed to a corrosive environment in *Proceedings of the 28<sup>th</sup> International Congress of the Aeronautical Sciences*, Brisbane, Australia.
- [3] Jones, R., Molent, L. and Walker, K. (2012). Fatigue crack growth in a diverse range of materials, *International Journal of Fatigue*, Vol 40, pp 43-50.

## **2.6 Quantitative fractography and modelling of fatigue crack propagation in high strength AerMet®100 steel repaired with a laser cladding process; K.F. Walker [DST Group Australia], J.M. Lourenco, Rio Grande do Norte [Federal Institute of Technology Brazil], S, Sun, M. Brandt, and C.H. Wang [RMIT University Australia]**

Ultra-high strength steels employed in safety-critical applications, such as AerMet®100 used in aircraft landing gear structures, are managed on very conservative rejection criteria for small defects and repair options are limited. A novel repair technique using laser cladding has recently been developed [1]. The present work [2] investigated the fatigue endurance of AerMet®100 steel components repaired by the laser cladding process, and developed a fracture mechanics based model to predict the fatigue endurance of repaired components. Three different types of samples were tested; baseline AerMet®100 sample with a small electro-discharge machining notch to initiate a crack, as-clad repaired, and as-clad repaired followed by heat treatment to relieve

residual stresses. The specimens were subjected to cyclic loading under a special sequence consisting of constant amplitude segments at two different stress-ratios (ratio of minimum to maximum cyclic stress). Fatigue cracking always initiated at the surface rather than at the interface between the clad and the substrate, see Figure 5

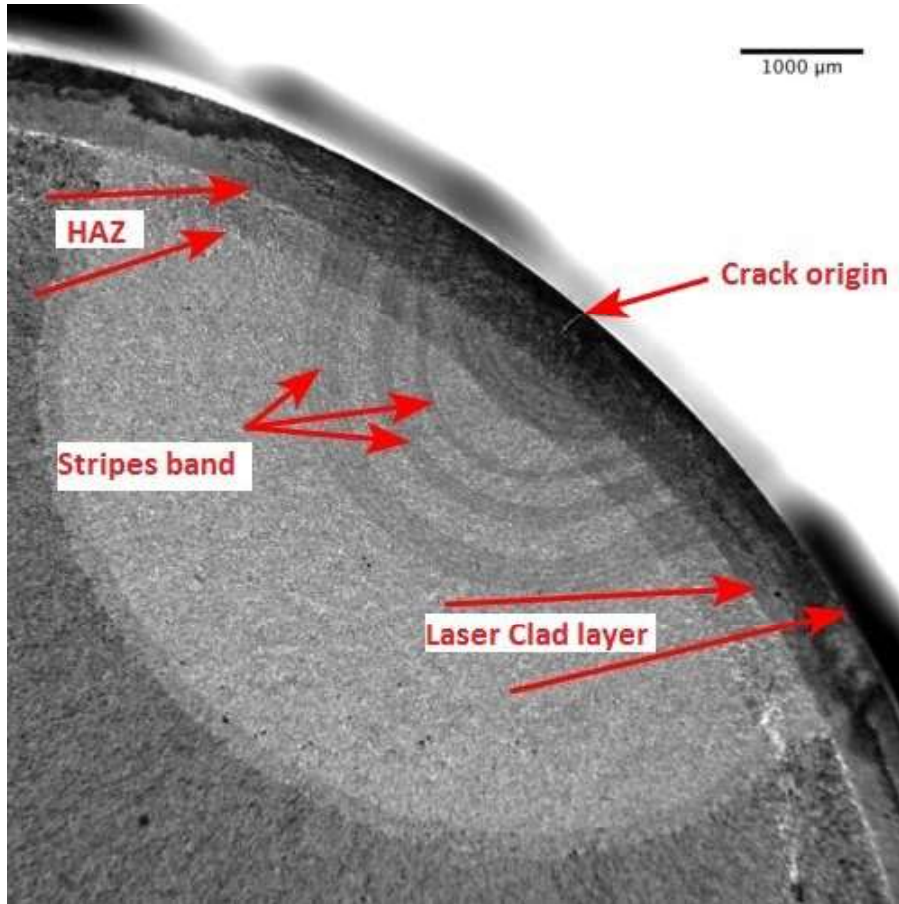


Figure 5 : Typical fatigue surface for clad specimen

The test results (see Figure xx) showed that the crack propagation lives from a common initial depth of 0.25 mm for the as-clad samples were significantly longer than the baseline samples by a factor of three to four. The longer life is attributed to the beneficial compressive residual stresses resulting from the repair process. The model predictions are found to correlate well with the results of quantitative fractography measurements from samples tested under variable amplitude cyclic loads.

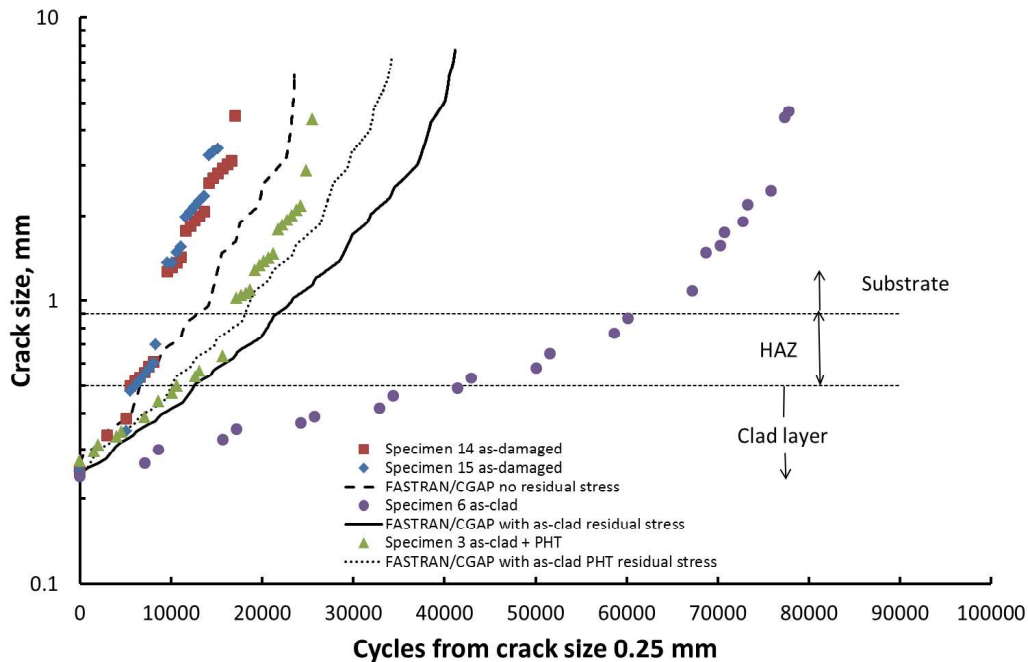


Figure 6 Comparison of analysis and QF for all three conditions from smallest available initial crack size of 0.25 mm

## References

1. Liu, Q., et al., *Laser cladding as a potential repair technology for damaged aircraft components*. International Journal of Structural Integrity, 2011. 2(3): p. 314-331.
2. Walker, K.F., Lourenco, J.M., Sun, S., Brandt, M., and Wang, C.H., *Quantitative fractography and modelling of fatigue crack propagation in high strength AerMet100 steel repaired with a laser cladding process*. International Journal of Fatigue, 2017. 94(<http://dx.doi.org/10.1016/j.ijfatigue.2016.06.031>): p. 288-301.

Contact K. Walker at [kevin.walker@dsto.defence.gov.au](mailto:kevin.walker@dsto.defence.gov.au)

## 2.7 Fatigue Crack Growth of 7075-T651 Aluminium Alloy under Proportional and Non-proportional Mixed Mode I and II Loads, Xiaobo Yu [DST Group], Ling Li and G. Proust [University of Sydney]

Fatigue of aircraft structures is traditionally managed based on the assumption of uniaxial loads. This is a simplified and acceptable approach for most fatigue critical locations where the local stress field is predominantly uniaxial due to load path restrictions. Nevertheless, as evidenced in recent durability analysis of surveillance aircraft, severe multiaxial loads may exist at some of the primary structural locations [1]. Multiaxial fatigue analysis, including fatigue crack growth (FCG) analysis under non-proportional mixed mode I and II loads, is needed for these locations.

At present, experimental FCG investigations are predominantly under mode I or proportional mixed mode loads. Very few test results are available for FCG under non-proportional mixed mode loads. Limited results on A106-93 mild steel [2], as shown in Fig. 1, indicate that a long, stable and small scale yielding shear mode FCG - which is significantly different from the commonly understood open mode FCG - could be produced by non-proportional loads. In open

literatures, no similar tests have been reported for aluminium alloys. This study [3] aims to clarify whether the shear mode FCG, as produced by the non-proportional loads, also occurs to aluminium alloy (AA) 7075-T651 that is typically used for aircraft structures.

Fatigue tests were performed under cyclic tension and torsion using a thin-walled tubular specimen with a key-hole style crack starter. After the generation of a single-side mode I pre-crack, varied forms of mixed mode loads were applied, which in most cases led to coplanar growth for a short distance followed by a long and stable crack path deviation. Fig. 2 shows the typical results of the crack path under two of the load cases. These two load cases are identical to those referred in Fig. 1. These result clearly indicate that the crack path - and therefore the crack growth mechanism - depends on the relative phase between the tension and torsion variations. Such dependency is observed both in the case of the mild steel [2] and aluminium alloy (this study [3]).

Further analysis of the test results indicates that under most of the non-proportional mixed mode load cases, the direction of the deviated crack path could not be reasonably predicted using the commonly accepted maximum tangential stress criterion. Meanwhile, in some cases, the crack path directions could be approximately predicted using the maximum shear stress criterion. It was also confirmed for the first time that a long, stable and non-coplanar shear mode fatigue crack growth could be produced in AA7075-T651 under non-proportional mixed mode I and II loads.

The implications of transient co-planar as well as stable shear-mode fatigue crack growth reveal the need for further investigations over two areas: (i) effects of delayed response to change of load mixture, in particular under in-service multiaxial loading spectra; and (ii) enhanced description of FCG, other than simply referred as open or shear mode FCG, and associated criterion for prediction of crack path.

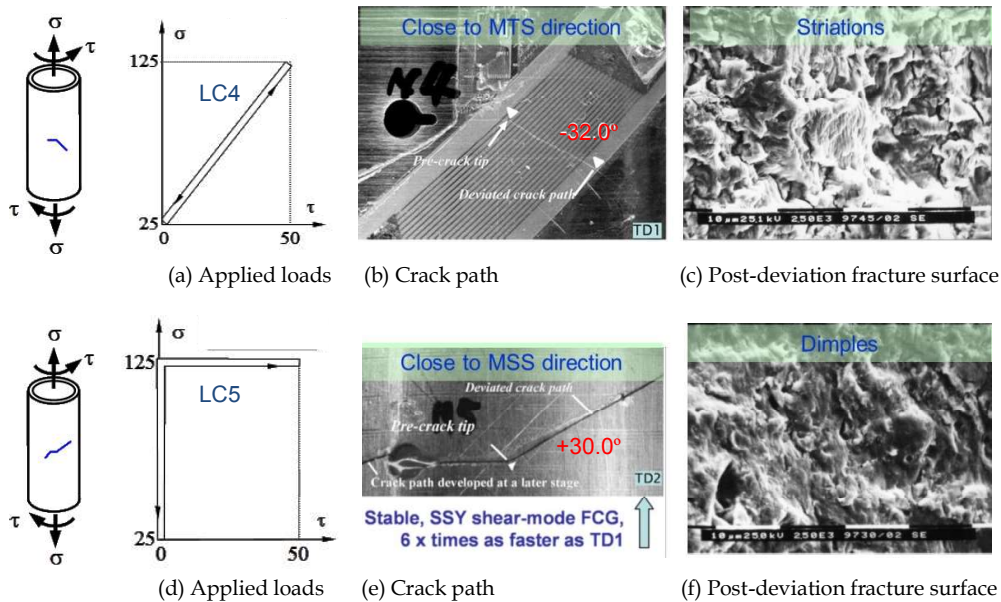


Figure 7. FCG in A106-93 mild steel [2] from a mode I pre-crack, under proportional (a–c), and non-proportional (d–f), mixed-mode loads (SSY refers to small scale yielding).

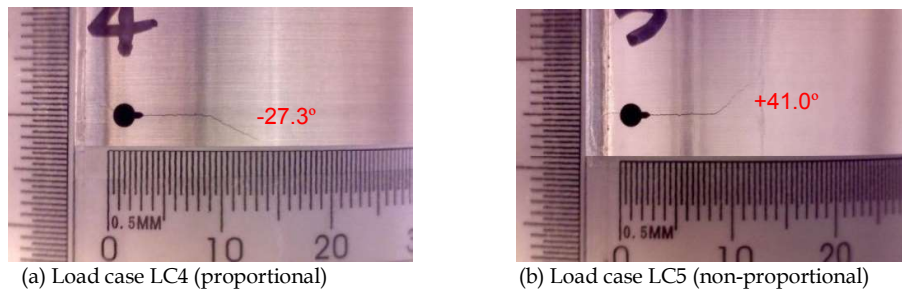


Figure 8. FCG in AA7075-T651 (current study [3]) from a mode I pre-crack, under proportional (a), and non-proportional (b), mixed-mode loads.

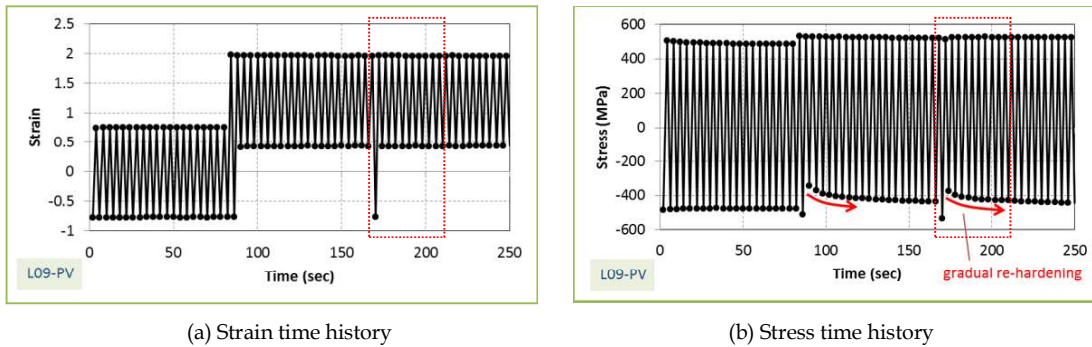
## References

1. Yu X. On the fatigue crack growth analysis of spliced aircraft wing panels under sequential axial and shear loads, *Engineering Fracture Mechanics in press*, 123 (2014) pp116-125.
2. Yu X. *Fatigue crack propagation under mixed mode loads. Ph.D thesis. Sydney: The University of Sydney; 1999.*
3. Yu X, Li L and Proust G. Fatigue crack growth of aluminium alloy 7075-T651 under proportional and non-proportional mixed mode I and II loads, *Engineering Fracture Mechanics, Engineering Fracture Mechanics*, 174 (2017) 155-167.

## 2.8 Softening and re-hardening of 7075 Aluminium Alloys under variable amplitude loads; Xiaobo Yu, Chris Wallbrink and Qianchu Liu (DST Group)

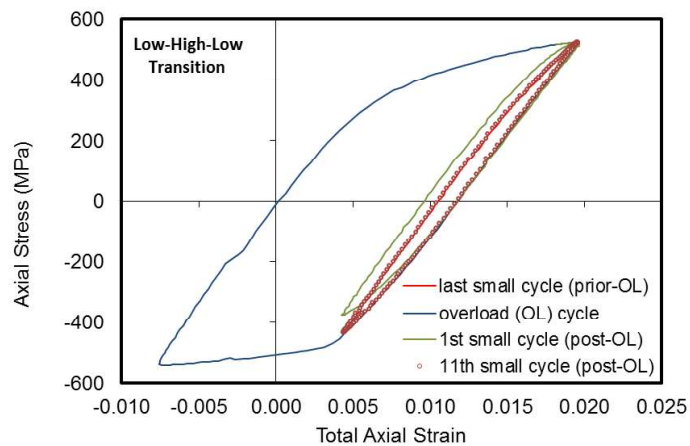
The Defence Science and Technology Group in Australia is interested in achieving a more accurate prediction of fatigue life of airframe components under variable amplitude loads. To achieve this, a better understanding of material plastic behaviour under variable amplitude loading is needed. In a previous study [1], the apparent difference between the monotonic and hysteresis plasticity was investigated by the authors using strain-controlled tests on AA7075-T651 flat dog-bone coupons. Preliminary results showed that the transition between monotonic and hysteresis plastic behavior was reversible, and consistent with the softening and re-hardening process as observed under low-high-low strain amplitude cycles.

The present study [3] further investigated the softening and re-hardening behaviour of the 7075 aluminium alloys, with an extended range of temper, coupon type and loading spectrum. Here, two tempers and coupon types were tested: (i) T651, 6.35 mm thick flat plate dog-bone coupon, and (ii) T7351, 6.35 mm diameter round bar dog-bone coupon. The tests were performed under strain control, using variable amplitude spectra including: single- and multiple-cycle overloads, in-spectrum changes of mean strain, and block-wise step-up and step-down of strain amplitudes. The results confirmed that for both tempers of 7075 aluminium alloy: (i) under low-high cyclic loads, the material softened in the first cycle that follows, which was in line with the monotonic to hysteresis transition; and (ii) under high-low cyclic loads, the material re-hardened gradually. This softening and re-hardening behaviour is different from conventional cyclic softening or hardening. A typical result is shown in Figure 9.



(a) Strain time history

(b) Stress time history



(c) Strain - stress relationship during a low-high-low transition (for the time period indicated by dashed-line rectangular box in (a) & (b))

Figure 9. Typical result of softening and re-hardening observed in a variable amplitude strain-controlled test (AA7075-T651, flat dog-bone coupon, peak-valley data)

#### References:

1. Yu X, Liu Q and Wallbrink C. Unifying monotonic and hysteresis material properties for notch plasticity analysis under variable amplitude loads, *Advanced Materials Research*, 891 (2014) pp500-505.
2. Yu X, Wallbrink C and Liu Q. Softening and re-hardening of 7075 aluminium alloys under variable amplitude loads, presented at: *International Symposium on Plasticity and Its Current Applications*, Hawaii, 3-9 January 2016, Objective ID: AV12583566.

## 2.9 Constant-Amplitude Fatigue-Crack Growth Behavior on 7075-T6 and 7249-T76511 Aluminum Alloys; K.F. Walker [DST Group Australia], and J.C. Newman Jr. [Mississippi State University USA]

The wings on the P-3C Maritime surveillance aircraft are made from 7075-T6 aluminum alloy. The current wings for the United States fleet have been replaced with 7249-T76511 alloy due to its improved corrosion resistance over the 7075 alloy. The P-3C fleet in Australia has maintained the 7075 alloy wings. The objective of this study was to conduct fatigue-crack-growth tests on middle-crack-tension, M(T), specimens made of thin-sheet 7075 and 7249 alloys under constant-amplitude (CA) loading to compare with test data previously generated on compact, C(T), specimens [1, 2].

There were five (5) M(T) specimens made of the 7075-T6 and 7249-T76511 alloys each that were 96.5 mm (2w) wide and 2 mm (B) thick. Two specimens were used to generate constant-amplitude test data, while the other three specimens of each material were used for spectrum crack-growth tests. All specimens had an electrical-discharged-machined (EDM) notch that was 10 mm in length. The objective was to compare the M(T) test data only in the mid-rate regime, and not in the threshold or near-threshold regime due to the very limited number of test specimens. One specimen of each material was tested at  $R = 0.1$  and the other was tested at  $R = 0.7$ . The test frequency was 10 Hertz. Prior to conducting the CA tests, the load frame was tuned. The FTA crack-monitoring system [3] was used to monitor the crack-length-against-cycles data using two crack-mouth-opening displacement (CMOD) gages (front and back). These gages were removed when the crack length reached about 70-75% of the width, and then the specimen was pulled to failure to obtain some fracture toughness data.

Figures 1 and 2 show the Linear-Elastic Fracture Mechanics,  $\sqrt{K}$  against rate data on the 7075 and 7249 alloys for  $R = 0.7$  and  $0.1$ , respectively. The solid (dark) symbols show the M(T) results, which agreed very well with the compact, C(T), test data. The C(T) test data in the near-threshold regime were generated with the new compression pre-cracking test procedures [4]. Figure 3(a) and 3(b) show a comparison between the two materials for  $R = 0.7$  and  $0.1$ , respectively. The 7249 alloy had a much lower threshold ( $\sqrt{K}_{th}$  at rate of  $10^{-10}$  m/cycle) than the 7075 alloy, but in the mid-to upper region, the crack-growth rate for the 7249 alloy was about a factor-of-2 slower than the 7075 alloy.

To generate fracture test data, all of the (10) test specimens ( $B = 2$  mm) were either pulled to failure or cycled to failure. In addition, some additional M(T) test specimens ( $B = 6.35$  mm) made of the 7249-T76511 alloy were tested under both CA and spectrum loading. (These tests were not sponsored by the DST, but tested at MSU.) Figure 4 shows the elastic stress-intensity factor,  $K_{Ie}$ , at failure against crack-length-to-width ( $c/w$ ) ratio. Generally, all of the test data fell in the  $c/w$  range of 0.6 to 0.8, except two tests. One test was at a low  $c/w$  ratio, which fractured under the double- (or V-) shear failure mode. Double-shear will always produce a higher fracture toughness (or failure load) than single-shear fracture. Another specimen had a very unsymmetrical deep crack, so an estimate was made for the  $K_{Ie}$  value. Although there was limited fracture data, an estimate was made for the two-fracture parameters,  $K_F$  and  $m$ , from the Two-Parameter Fracture Criterion (TPFC [5]). The solid curves are calculated from the TPFC for  $K_F = 209$  MPa-m<sup>1/2</sup> and  $m = 1$ . The correlation was well within  $\pm 10\%$  for the 96.6-mm wide specimens. The upper and lower solid curves are predictions for larger and smaller width specimens. Ideally, fracture tests at different widths would have been better to establish the two fracture parameters.

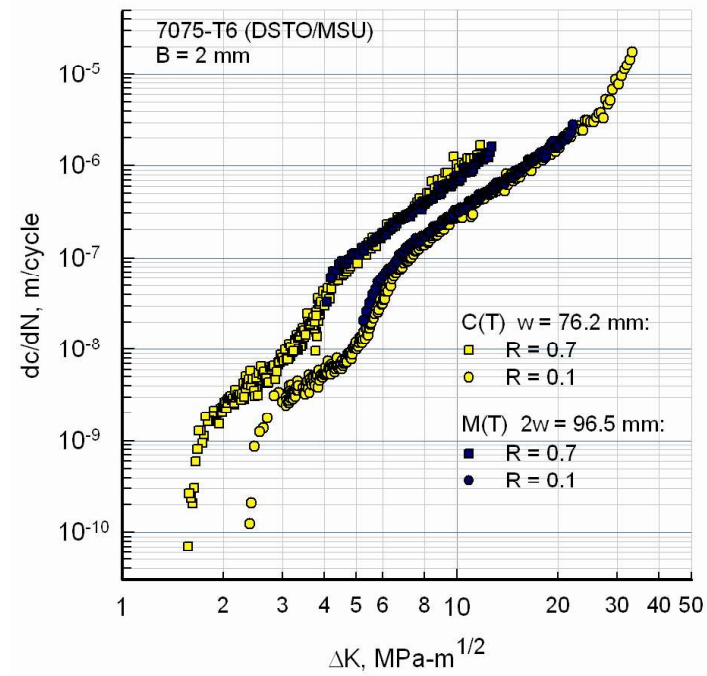


Figure 1. Comparison of C(T) and M(T) crack-growth rate data on 7075-T6.

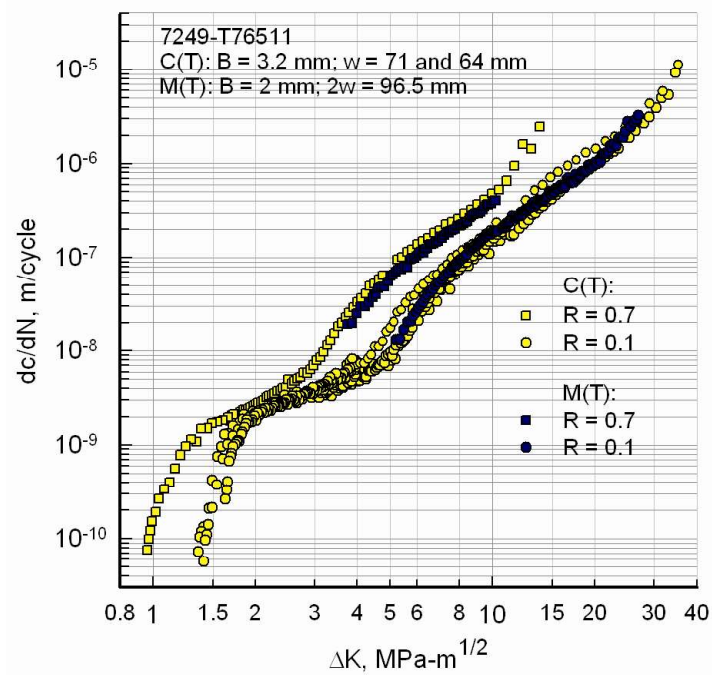
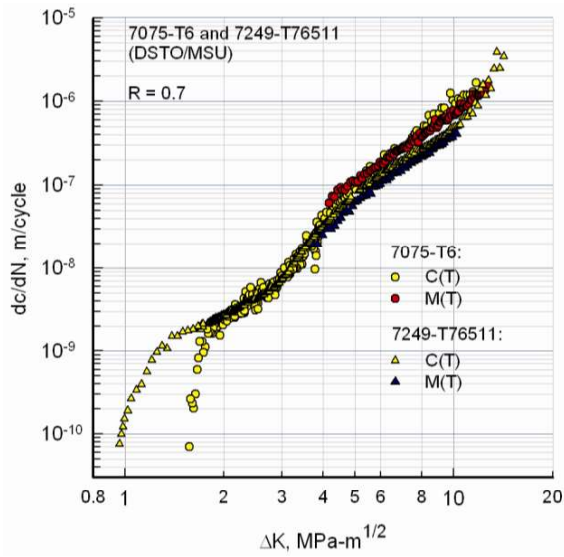
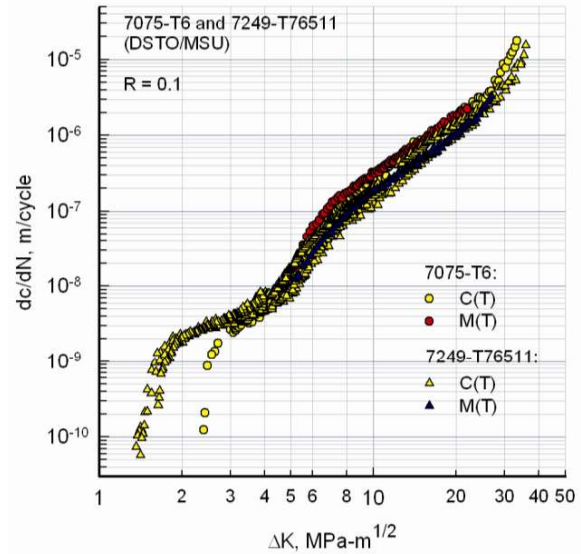


Figure 2. Comparison of C(T) and M(T) crack-growth rate data on 7249-T76511.



(a)  $R = 0.7$



(b)  $R = 0.1$

Figure 3. Comparison of 7075-T6 and 7249-T76511  $\Delta K$ -rate results at high and low stress ratios.

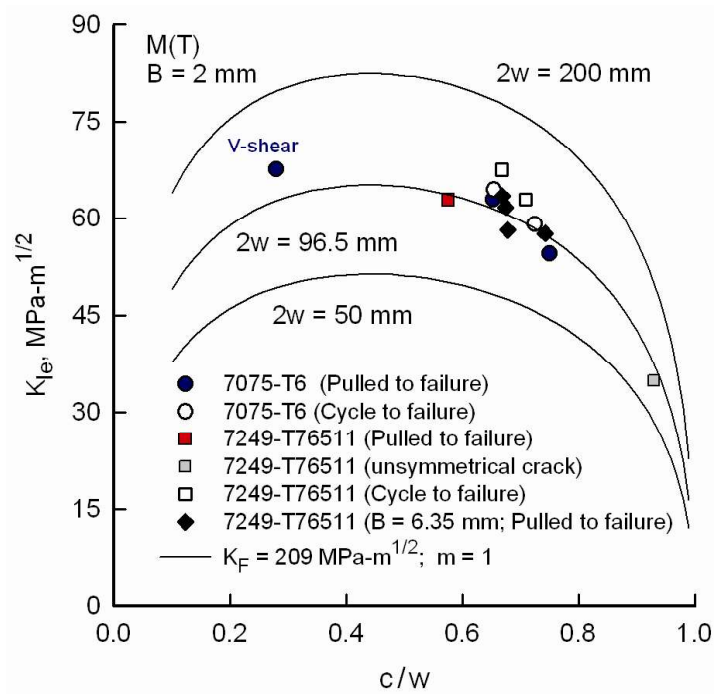


Figure 4. Elastic stress-intensity factors at failure for 7075-T6 and 7249-T76511 M(T) specimens and the TPFCA fracture analyses.

Contact K. Walker at [kevin.walker@dsto.defence.gov.au](mailto:kevin.walker@dsto.defence.gov.au)

## References

[1] [Newman, J., Jr.](#), Walker, K.F. and Liao, M. Fatigue Crack Growth in 7249-T76511 Aluminum Alloy under Constant-amplitude and Spectrum Loading. *Fatigue and Fracture of Engineering Materials and Structures*. Wiley-Blackwell, Vol. 38, 2015, pp. 528-539.

[2] Walker, K.F. and Newman, J.C., Jr. Development and Validation of Improved Experimental Techniques and Modeling for Fatigue Crack Growth in 7075-T6/T651 Alloy under Constant Amplitude and Spectrum Loading. In preparation.

[3] Donald, J. K. and Blair, A. Automated Fatigue Crack Growth Testing and Analysis – Series 2001. Version 3.09, 2009, Fracture Technology Associates, LLC, Bethlehem, PA.

[4] Newman, J.C., Jr. and Yamada, Y. Compression Precracking Methods to Generate Near-Threshold Fatigue-Crack-Growth-Rate Data. *International Journal of Fatigue*, Vol. 32, 2010, pp. 879-885.

[5] Newman, J.C., Jr. Fracture Analysis of Surface- and Through-Cracked Sheets and Plates. *Engineering Fracture Mechanics*. Vol. 5, No. 3, 1973, pp. 667-689.

## **2.10 Spectrum Truncation or Spectrum Compression? :When time and money matters and nothing less than a fraction of the original spectrum is acceptable; Chris Wallbrink and Beau Krieg [DST Group]**

Structural fatigue is principally driven by the cyclic load history (or load spectrum) experienced by a structure. The magnitude, frequency and order of the load cycles are all key factors affecting fatigue performance. The accurate development of a representative load spectrum is vital when testing the fatigue performance of a structure. Present day monitoring systems and data acquisition rates means that we now have access to measured structural loads data of far greater resolution than ever before. However, there is a fundamental problem in that data acquisition rates are orders of magnitudes higher than the cyclic load rates achievable with current generation structural test machines. While high fidelity load spectra provide a fantastic opportunity for insight and understanding of the loading environment, they may be too “load cycle dense” to be practical for fatigue testing purposes. The challenge is reducing the density of load spectra for test purposes while maintaining fatigue damage and fidelity.

This increase in spectrum fidelity has revealed the significance of large numbers of small cycles to fatigue damage [1, 2]. Thus, truncating small cycles within a spectrum could have unintended consequences and compromise the representative nature of the load sequence. An ongoing challenge within the aerospace community is to truncate recorded load spectra without adversely affecting its damage content or representativeness.

This work investigates two new DST Group approaches to significantly reduce the number of cycles within a spectrum without adversely impacting the damage content. These methods of “truncation” might be better referred to as spectrum “compression”. Rather than attempting to remove cycles that are perceived to be non-damaging, DST group is developing new approaches to compress the spectrum while preserving fatigue damage content and sequence effects. The algorithms are detailed in the accompanying ICAF paper [3].

Tests have been conducted on edge cracked specimens manufactured from 6.35mm thick 7075-T7351 aluminium sheet metal 100mm wide [4]. Presented in Figure 1 are results of coupon tests loaded with a transport aircraft load spectrum. The original spectrum contained over 430,000 cycles whereas the compressed spectrum contained ~40,000 cycles (a ~91% reduction of the original spectrum). As illustrated in Figure 1, this initial testing demonstrates the promise of

spectrum compression techniques in delivering equivalent fatigue damage using vastly smaller test load sequence. This reduction in spectrum size is impossible using traditional truncation methods without reintroducing damage through a scaling factor or other approach. To demonstrate this (using a fatigue crack growth algorithm) it can be shown that to achieve the same 91% spectrum reduction using traditional truncation through stress amplitude gating that a minimum of 58% of the damage content in the sequence would be lost.

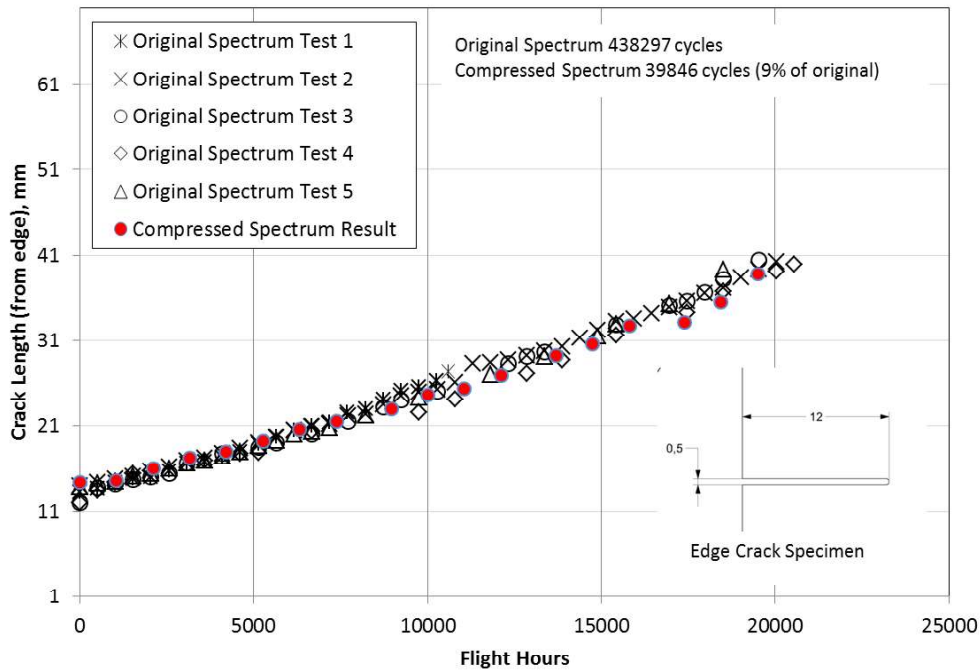


Figure 1: Crack growth under a transport load spectrum in 7075-T7351 Aluminium showing results for both the original spectrum (438297 cycles) and compressed spectrums (39,846 cycles).

Applications extend to full scale fatigue tests that typically take years to complete down to small component level tests where many specimens may be required. These methods can also be applied to verification of repairs (cold expanded holes, bonded repairs, etc) that may otherwise extend testing to impractical timeframes. There are also potential benefits to enhanced teardowns, where rather than applying arbitrary loading to grow damage, an approach could be taken to make the loading more meaningful.

To date the results of current testing has been positive and indicates that these “spectrum compression” methods can provide a superior approach to reducing the size of test load sequences [4]. It is anticipated that these methods will have a significant impact through reduced testing times and reduced costs. Although the art of truncation is old, DST group is endeavouring to reinvigorate this field with innovative new ideas that build upon the many advances in damage modelling.

#### References;

- [1] Wallbrink, C., P. Jackson, and W. Hu, Crack Growth Rate Curves: Which Part Dominates Life Prediction And When?, in *International Committee on Aeronautical Fatigue. 2011: Montreal, Canada.* p. 303-314.

- [2] Walker, K.F. and S.A. Barter. The critical importance of correctly characterising fatigue crack growth rates in the threshold regime. in *ICAF 2011 Structural Integrity: Influence of Efficiency and Green Imperatives - Proceedings of the 26th Symposium of the International Committee on Aeronautical Fatigue*. 2011.
- [3] Wallbrink, C. and Krieg, B. "Spectrum Truncation or Spectrum Compression? : When time and money matters and nothing less than a fraction of the original spectrum is acceptable" ?, in *International Committee on Aeronautical Fatigue*. 2015: Nagoya, Japan.
- [4] Chang, P., Heller, M., Wang, J., Opie, M. and Yu, X. "A New Approach for Hybrid Bonded Repair of Metallic Components" Journal article in preparation, 2017

Email: [Chris.Wallbrink@DSTO.defence.gov.au](mailto:Chris.Wallbrink@DSTO.defence.gov.au)

## 2.11 Improving fatigue life predictions with a crack growth rate material model based on small crack growth & legacy data; M. Burchill, S. Barter [DST Group]

The airframes of combat aircraft are typically designed to be both light weight and capable of bearing large and highly variable loads. Fatigue cracking is frequently a life limiting issue and critical crack sizes are often small, resulting in a substantial amount of the crack growth life occurring when the cracks are small [1]. Consequently many of the local cyclic stresses that grow these cracks are in the crack growth threshold region [2]. This leads to prediction problems since traditional crack growth rate data is often collected from long through section cracks where constant amplitude loads only are applied [3]. The crack growth rate curves produced by traditional methodologies, when used to predict total crack lives have been found to under predict the early crack growth rate observed for cracks in service structures. An example of typical standard crack growth rate data for AA7050-T7451 is presented in Figure 10A, where the crack growth extension ( $da$ ) per load cycle ( $N$ ) is plotted against the stress intensity range,  $\Delta K$  of that load cycle, for two typical load ratios ( $R = \sigma_{min}/\sigma_{max}$ ). Predictions (using the AFGROW crack growth code [4]) based on this data are shown in Figure 10B, along with measured growth from a series of small coupons tested to failure with a combat wing root bending moment (WRBM) variable amplitude loading spectrum. The over prediction of the total life and poor correlation for the rate of growth, in particular when the crack is small is evident.

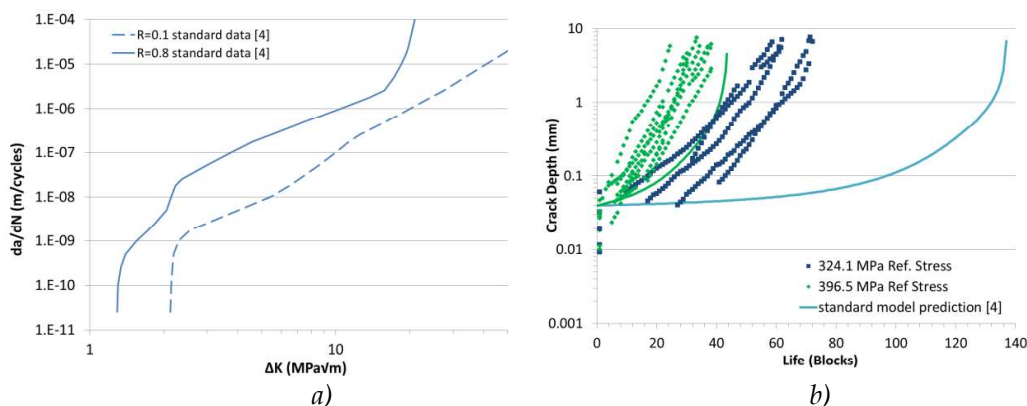
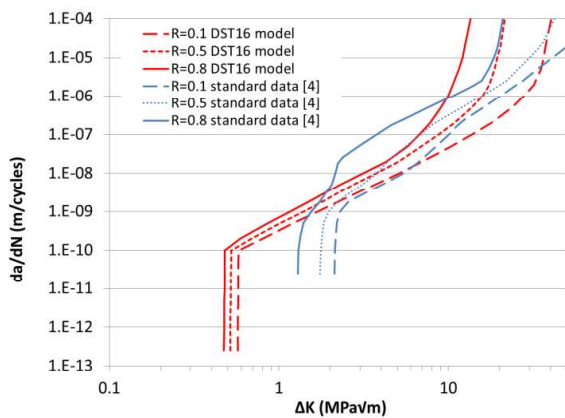


Figure 10 a) Standard AA7050-T7451 long-crack data sets, b) crack growth results from predictions and coupons tested with combat WRBM spectra at two stress levels (Ref Stress).

To address the problems highlighted above, the Defence Science and Technology (DST) Group has conducted a study that has combined the results from the Threshold And Small Crack (TASC) program [5][6] and various spectrum coupon test results drawn from support to RAAF aircraft structural integrity programs. Using measurements of small crack growth and copious legacy data from over 20 years of supporting F/A-18A/B Hornet aircraft, new crack growth rate curves were reverse engineered to produce material crack growth rate models of generic usefulness, although focused on combat WRBM loading. The common aluminium alloy, AA7050-T7451 was selected since it is used extensively in a wide range of combat aircraft airframes, including the RAAF's F/A-18A/B Hornet, F/A-18F Super Hornet, EA-18G Growler and the F-35 Joint Strike Fighter.

Fatigue crack data from over 160 coupons tested with ten (10) different F/A-18 A/B WRBM spectra were used to optimise the crack growth rate model set - referred to as DST16 shown in a) b)

Figure 11 (both compared to the traditional CGR set in Figure 10A and tabulated). A sensitivity study of DST16 model set was conducted by altering a range of parameters such as:  $\Delta K_{th}$ , gradient of the stage II period of the CGR curves; translation of the rate curves and dilation between different R models. The study provided confidence in the optimisation assumptions made in developing the DST16 model set, to characterise average growth rate observed in the experimental results.



a)

da/dN (m/cycle)	ΔK (MPa√m)		
	R=0.1	R=0.5	R=0.8
2.54E-13	0.57125	0.51578	0.47387
1.00E-10	0.57787	0.52210	0.47993
1.00E-09	1.69884	1.40106	1.16922
1.00E-08	5.10157	3.73162	3.10783
1.00E-07	13.7856	8.72491	6.75727
1.00E-06	27.8166	15.8432	9.95436
1.00E-05	36.4698	19.4669	12.0993
1.00E-04	40.3111	21.4704	13.5196

b)

Figure 11 DST16 growth rate model data for AA7050-T7451, a) compared to standard model data from Figure 1a and b) tabulated.

The DST16 model was then trailed for the prediction of fatigue crack growth produced by eight (8) different WRBM loading spectra and was shown to accurately predict both the total life and growth rates. (And was shown to be an improvement on a previously developed set of crack growth rate curves that are known as DST12 [5]). The average growth from over 100 coupons that were tested with this set of eight spectra were satisfactorily predicted by the DST16 model. An example is shown in a) b)

Figure 12 (along with comparisons to DST12 and the standard data) from very small crack sizes - less than 100μm

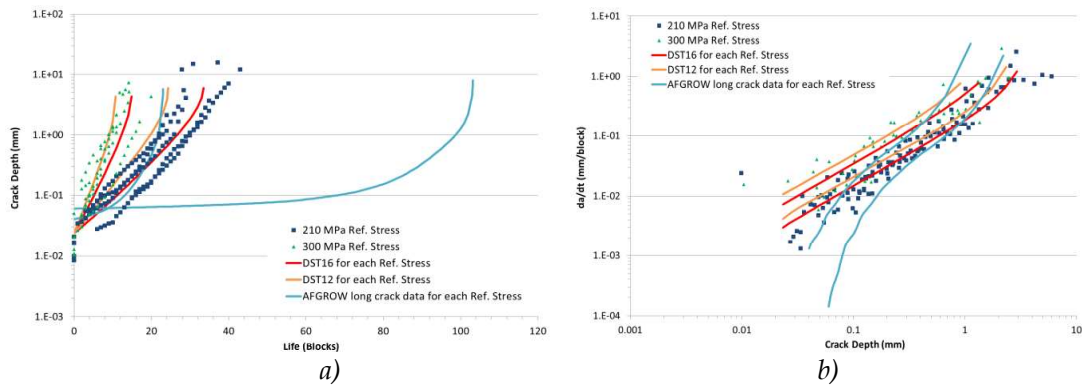


Figure 12 Crack growth data and predictions for a non-F/A-18A,B WRBM spectra at two stress levels show as a) crack depth vs. block and b) crack growth per block vs. crack depth

While this study was conducted mainly focusing on WRBM spectra, the DST16 curves could be further refined for other spectrum types with suitable adjustments to account for those aspects of the spectra that make them very different to the WRBM spectra. To identify what those spectra features maybe, the DST16 model was used to predict a spectrum derived from the direct measurement of helicopter transmission beam loading (Heli) (again compared with the DST12 model results) and gave a considerable improvement over both the standard material models and DST12 as shown in

a) b)  
Figure 13.

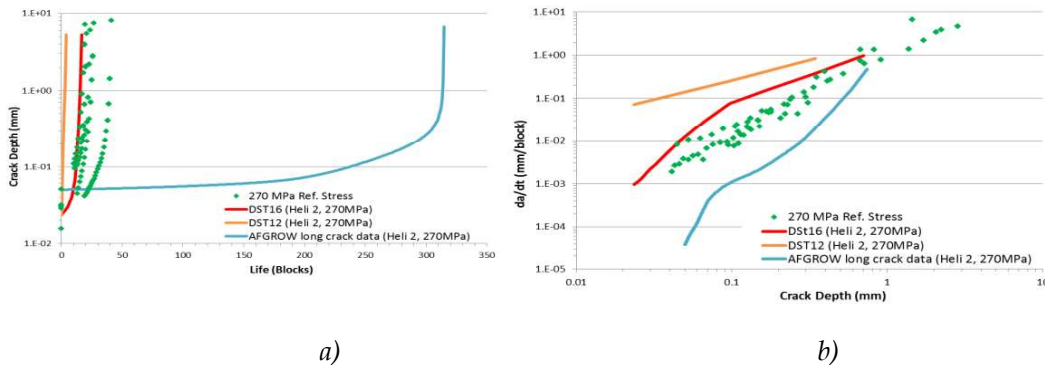


Figure 13 Crack growth data and predictions of non-WRBM spectra show as a) crack depth vs. block and b) crack growth per block vs. crack depth

Further effort will be made to identify and confirm the limitations of the DST16 crack growth rate model, particularly in seeking to account for spectra characteristics that drive crack growth rate changes. The outcomes may be used to further enhance prediction tools and make advancements in testing procedures, such as how to account for small cycles (with a high mean) and spectrum truncation. This work will continue to assist DST Group in developing a greater understanding of fatigue crack growth in typical structural alloys used in Australian Defence Force aircraft

## References

- [1] L. Molent, S.A. Barter, R.J.H. Wanhill. *The lead crack fatigue lifing framework*. International Journal of Fatigue, Vol 33, 2011, pp 323–331.
- [2] C. Wallbrink, P. Jackson, and W. Hu., *Crack Growth Rate Curves: Which Part Dominates Life Prediction and When?* ICAF Symposium, Montreal, Canada 2011.
- [3] ASTM E647-05 - Standard test methods for measurement of fatigue crack growth rates, ed: American Society for Testing and Materials, 2005.
- [4] J. A. Harter, *AFGROW Users Guide and Technical Manual*, Air Vehicles Directorate, Air Force Research Laboratory, WPAFB OH USA AFRL-VA-WP-TR-206, 2006.
- [5] K.F. Walker and S.A. Barter, The Critical Importance of Correctly Characterising Fatigue Crack Growth Rates in the Threshold Regime, in ICAF 2011 Structural Integrity: Influence of Efficiency and Green Imperatives, J. Komorowski, Editor. 2011, Springer Netherlands. p. 249-263.
- [6] M. Burchill, S.A. Barter, and M. Jones, The effect of crack growth retardation when comparing constant amplitude to variable amplitude loading in an aluminium alloy. *Advanced Materials Research*, 2014. **891-892**: p. 948-954.

### **2.12 The development of bar-coded marker band load sequences to enhance fatigue test outcomes; M. Burchill, S. Barter, M. McDonald [DST Group]**

Accurate crack growth data, from element, component or full-scale fatigue testing is a fundamental input into validating models used to predict fatigue damage in aircraft structures from service loading. Identifying, measuring and assessing fatigue cracks generated during testing therefore is of critical importance to aircraft operators, such as the Royal Australian Air Force (RAAF), to maintain aircraft structural integrity for the life of an airframe. The Defence Science and Technology (DST) Group commonly utilises a test enhancement methodology to mark the fracture surfaces of fatigue cracks during testing [1], allowing accurate and rapid determination of crack lengths post-test. With recent improvements in the understanding of fatigue crack growth, DST has proven a method by which these marks can be bar-coded successfully in a range of coupon and full-scale test programs on several different structural materials.

Based on observations that often a change in the crack path [2], along with topological changes, occur when there is significant change in the cyclic load ratio  $R$  ( $\sigma_{\min}/\sigma_{\max}$ ), bar-coded marker band load sequences, shown in Figure 14, have been designed [3]. Through the careful selection of the load amplitude ( $R$ ) and number of cycles ( $N$ ), highly contrasting patterns on fatigue crack fracture surfaces can be created in both aluminium and titanium alloys. These patterns, or marker bands, when included in various different types of load spectra, such as combat, transport and helicopter spectra enable accurate measurement of crack depth that corresponds to the time that the marker band load sequences were applied during testing.



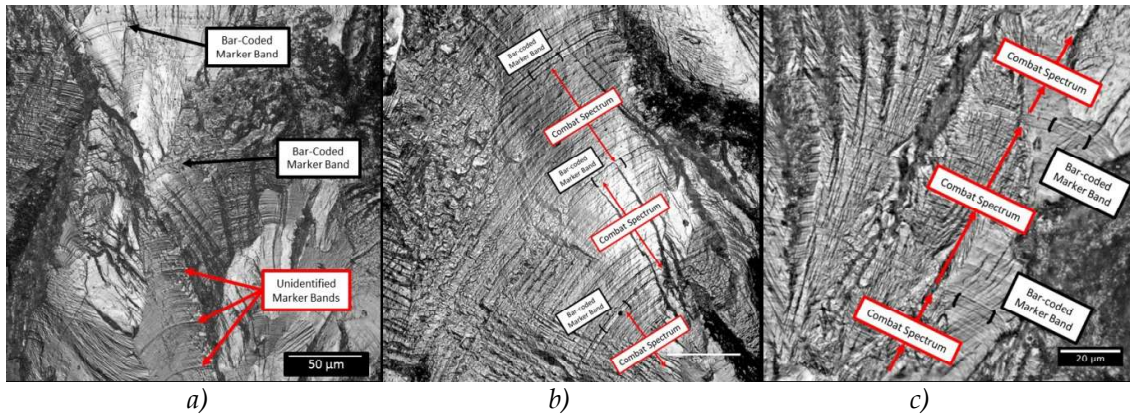


Figure 16 Examples of bar-coded marker bands in an aluminium alloy at crack depths of: (a) 0.1mm to 0.4mm, (b) 0.39mm to 0.55mm, and (c) 0.17mm to 0.24mm.

Typically DST uses marker bands which, in the examples shown, had a maximum load of 0.85 and a minimum load of 0.1 of the maximum spectrum loads. Testing has indicated that these load levels avoid the introduction of complex retardation or acceleration effects on subsequent flight load crack growth rates. Obviously, care must be taken to ensure changes in the load levels do not induce any unwanted crack growth effects to maintain the validity of the test. Through this work DST aims to improve prediction capabilities, through more accurate crack growth data for the prediction of fatigue damage in RAAF aircraft.

## References

- [1] S. Barter, L. Molent and R. Wanhill. Marker loads for quantitative fractography of fatigue cracks in aerospace alloys. 25th ICAF Symposium, Rotterdam, 2009.
- [2] P. White, S. Barter and L. Molent. Observations of crack path changes caused by periodic underloads in AA7050-T7451. Inter. J of Fatigue, Vol. 30, pp1267-1278, 2008.
- [3] M. McDonald, R. Boykett and M. Jones. Quantitative fractography markers for determining fatigue crack growth rates in aluminium and titanium aircraft structures, ICAS2012, Brisbane, Australia, 2012.

### 2.13 Fatigue crack path manipulation for crack growth rate measurement, S. Barter, P. White, M. Burchill [DST Group]

It is accepted that fatigue crack paths in metals that display confined slip, such as high strength aluminium alloys (e.g. AA7050-T7451 a common aerospace alloy) are responsive to loading direction and local microstructural orientation. It is less well recognised that crack paths in these alloys are also responsive to the loading history since certain loading sequences can produce highly directional slip bands ahead of the crack tip. By adjusting the sequence of loads, distinct fracture surface features or progression marks can result (for example Figure 17) and are evident even at very small crack depths. An investigation into the path a fatigue crack selects as it progresses through a material, when it is cyclically loaded with particular combinations of constant and variable amplitude sequences, has provided insight into the way these cracks grow. This makes it possible to design load sequences that allow very small advances of crack growth to be measured post-test by Quantitative Fractography. An outcome of which is that average growth rates can be more readily measured for rates well below the conventionally recognised threshold of the aluminium alloy examined here [1].

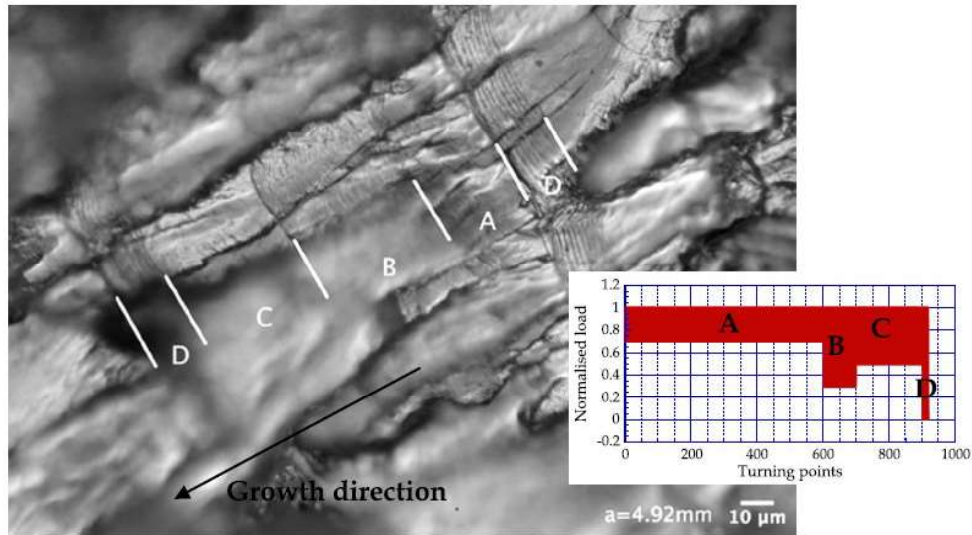
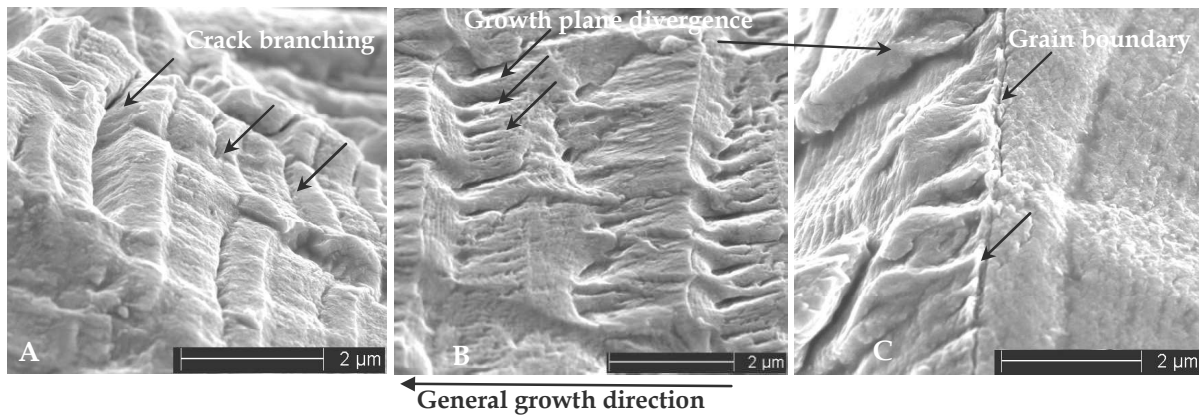


Figure 17 *Optical microscope image of AA7050-T7451 fatigue crack fracture surface – highlighted are features that relate to the test load spectra (insert), where A-D refer to the sub-blocks of constant amplitude with various load ratios.*

The post-test examination of fatigue cracks in coupons tested with various sequences (such as that shown in **Error! Reference source not found.** has allowed the measurement of bands of crack growth to produce local crack growth rates at very small crack depths and very low rates of growth in this alloy. The aims of this work were firstly to generate small-crack constant amplitude growth rate data and secondly, to achieve a greater understanding of the mechanisms of fatigue crack growth in this material. A particular focus of this work was the identification of possible sources of crack growth retardation, acceleration and path deflection in small cracks. The results suggest that for small cracks in this material, the rate of crack growth under variable amplitude loading will tend to be faster the more random the loading is. Consequently, predictions made based on the crack growth rates drawn from constant amplitude loading tend to under predict crack growth rates for spectra with more random loading. While the cause of this is still under investigation and is bound up with: the nature of the damage ahead of the crack tip as noted above and damage that is locally strongly influenced by the microstructural orientations, crack paths have clearly been seen to become more efficient (less path changes and an average path emerges that is closer to being perpendicular to the loading direction) due to random cyclic loading compared to constant amplitude cycling. **Error! Reference source not found.** shows constant amplitude sub blocks of growth that have produced local roughness, large path changes both within and between the sub-blocks and deflections at grain boundaries. Additionally, changing of the loading sequence from random to constant amplitude, results in path changes that can be controlled to a certain extent by the selection of the applied loading.



a) b) c)  
 Figure 18. Images of crack paths on the fracture surfaces of an AA7050-T7451 specimen loaded with a simple spectrum consisting of sequences of CA loading with different R ratios, but similar  $\sigma_{max}$  (the loading is shown schematically in Figure 17). a) and b) crack bifurcation/branching and crack front breakup after each change in R and c) crack path deflection at a grain boundary crossing.

In support of the above observation of less efficient crack growth for less random sequences, it has been observed that placing short blocks of constant amplitude cycles within a random sequence (based on the wing root bending moment load sequence for a combat aircraft), leads to progressive retardation of the growth of that block. Post-test observations suggest that for any sustained constant amplitude loading the crack tends to grow on one particular plane in one particular direction through each grain intersecting the crack front (see example of a grain boundary crossing with associated crack path deflection for a simple spectrum in **Error! Reference source not found**). It is postulated that a decrease in crack growth rate can be expected when that local plane and direction is not aligned to the overall crack front average growth plane. This also results in other retardation features such a roughness due to local crack bifurcation, which further retards crack growth on average. Using random loads results in growth that is less deflected since variation in load cycles produces a larger range of alternative crack paths at the crack tip. The alternate paths make the crack growth more efficient by at least facilitating crack front coalescence and suppressing bifurcation. This is of particular importance when the  $\Delta K$ s are low: for the examples presented here, for the aluminium alloy AA7050-T7451, where  $\Delta K$  is  $< 2.5 \text{ MPa(m)}^{0.5}$ .

The observations so far collected are important in aircraft design. They portend faster than expected growth for small cracks growing under random loading typical of aircraft service from the typical surface discontinuities in aircraft structural components, than may have been used in the design calculations or allowances for the structure. Consequently shorter structural fatigue lives than expected may be the result, and in turn produce unexpected failures and/or a requirement for costly repairs to maintain airworthiness. For this reason, although still requiring further development this work should be of interest to those involved in designing against fatigue in aircraft.

## Reference

- [1] Barter, S., White, P., Burchill, M. Fatigue crack path manipulation for crack growth rate measurement. *Engineering Fracture Mechanics*, 167, 2016. pp224-238, <http://dx.doi.org/10.1016/j.engfracmech.2016.04.020>

## 2.14 Automation of Quantitative Fractography for Determination of Fatigue Crack Growth Rates with Marker Loads; W. Hu, S. Barter [DST Group], A. Wiliem, B. Lovell, L. Liu [University of Queensland]

Quantitative fractography (QF) has recently been increasingly used for the determination of crack growth rates, especially under complex service loads, for small cracks and for cracks embedded in thick sections. Some of the challenges of this approach are: (1) it is labour-intensive; (2) it is time consuming, and; (3) it relies heavily on the level of expertise, experience and attention of the operator. These challenges lead to the possibility of subjectivity and inconsistency in the interpretation of results, in addition to the time and cost incurred. On the other hand, recent research in academia and industry has made great progress in applied digital image processing, such as geospatial feature mining, and fingerprint- and handwriting- recognition. It is therefore envisaged that an innovative technique could be developed by integrating the relevant methods in image processing, for the automation or semi-automation of QF for the determination of crack growth rates. A preliminary collaborative research project has been initiated between the DST Group and the University of Queensland.

Two image processing methods have been assessed so far, the edge detection method and the time series method. The time series method has shown great potential in correctly identifying progression marks on fracture surfaces, especially the multiple time series method. Figure 19 shows a schematic of applying the multiple time series method for determining crack growth rates. The work so far has been focusing on the identification of progress marks.

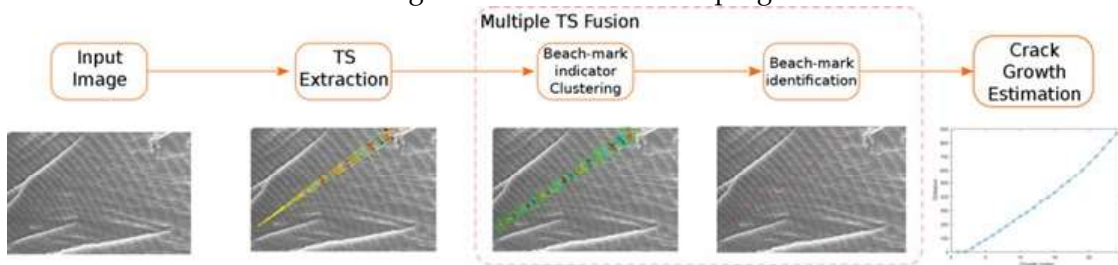


Figure 19. Schematic for constructing a crack growth history using the multiple time-series method.

In the multiple time series method, adjacent time series are analysed using a graph-based clustering algorithm called the Constrained Laplacian Rank (CLR) to cluster peaks in the time series that are possible candidates for progression marks. These possible peaks are further projected onto the direction of crack growth to determine the location of the progression marks. Figure 20 shows an example of the results of clustering using the CLR algorithm. On the image, each cluster represents the presence of a progression mark.

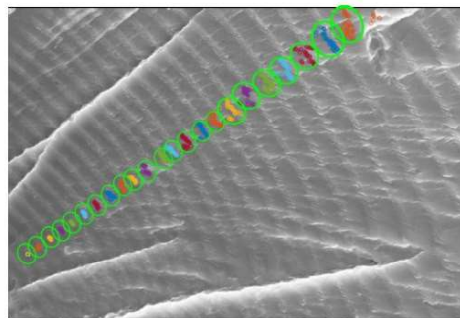


Figure 20. An example of clustering using the CLR algorithm.

Figure 21 shows a comparison of visual marked progression marks and those determined using the single and multiple time-series methods. The multiple series method performed much better in terms of miss rate and false positive of progression marks.

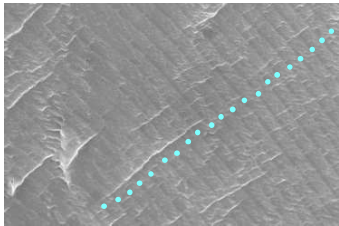
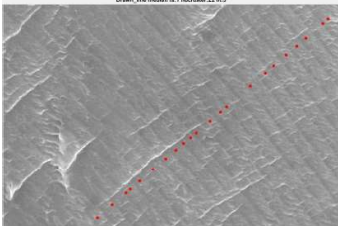
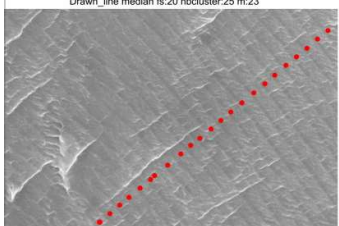
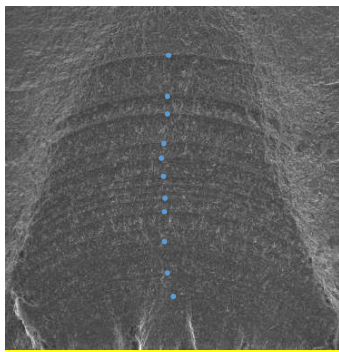
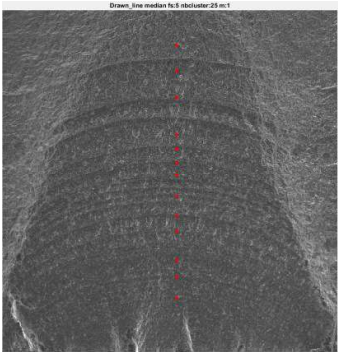
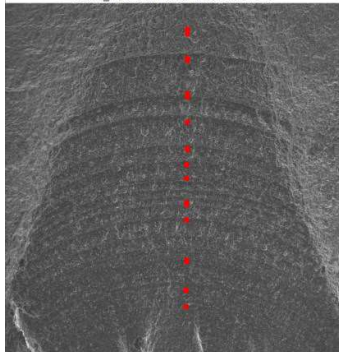
Imag	Ground truth	Single Time Series	Multiple Time Series
Sample 517a		 <small>Drawn_line median fs:1 ncluster:22 m:3</small>	 <small>Drawn_line median fs:20 ncluster:25 m:23</small>
Sample C72_c2_x10		 <small>Drawn_line median fs:5 ncluster:25 m:1</small>	 <small>Drawn_line median fs:30 ncluster:25 m:12</small>

Figure 21. Visual comparison of the performance of the multiple time-series and the single time-series method.

Further work is in progress in further reducing the effect of noise and verifying the results against those obtained with the current practice of using quantitative fractography for fatigue crack growth rate determination.

## 2.15 Automated Crack Growth Tracking Capability; Dr N. Rajic [DST Group]

Current fatigue certification practice for safety critical load-bearing components relies on detailed knowledge of material crack growth behaviour. Such knowledge is normally obtained empirically from exhaustive laboratory testing carried out on standardised coupons under controlled conditions. Relatively large sample sizes are typically required because of the variability in growth rate between samples, which can be up to a factor of 5 in certain situations. This sample-size requirement contributes to the generally high cost of material fatigue testing. Automation of crack length measurement can reduce the cost burden of fatigue testing. Methods based on elastic compliance and electrical potential drops (EPD) are the mainstays for such automation. Another disadvantage is the inability of these methods to identify irregular crack growth, such as angled cracking which if severe enough can invalidate a test result. The relevant standard stipulates that where irregular growth is possible a visual inspection must be used. A new automated visual crack growth tracking capability based on thermoelasticity and DST group has developed a system to conduct Thermoelastic Stress Analysis (TSA) called MiTE. Crack length measurements are derived from the thermoelastic response of the crack tip stress singularity imaged using a low-cost thermal detector robotically controlled using a high precision x-y translational stage under

feedback control. Results compare very well with visual methods, see Figure 1. The advantages of such an approach over established automation methods derive chiefly from its direct determination of the crack tip coordinates. As is the case for visual inspection, this enables testing of a wider range of specimen geometries and can cater for non-symmetric crack growth.

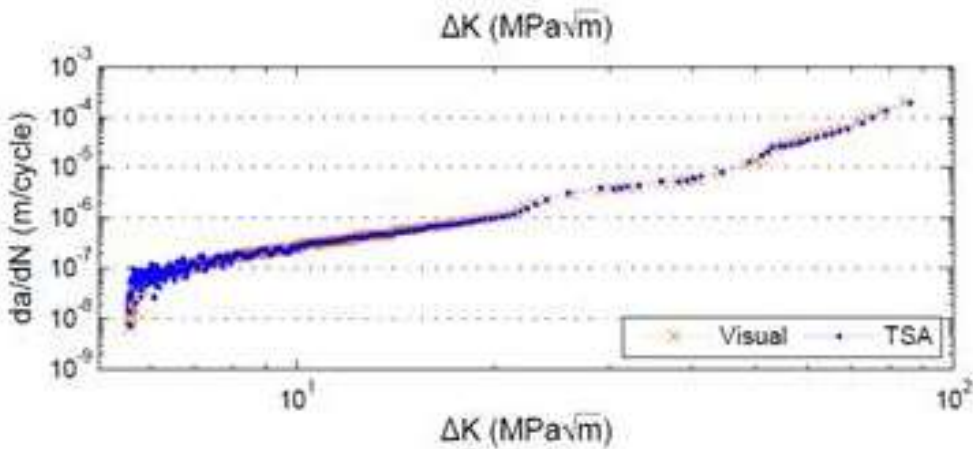


Figure 1 Example coupon crack growth measurement results using TSA and visual

The DST Group MiTE system information and freeware is available at <http://www.dst.defence.gov.au/opportunity/mite>

## 2.16 A bounded distribution model of equivalent initial flaw size distribution for structural risk analysis; R. Torregosa and W. Hu, [DST Group]

In the analysis of the probability of fracture of aircraft structures, unbounded distribution models such as the lognormal and the Weibull distributions are often used to describe the probability distribution of the equivalent initial flaw sizes of the components. These models tend to give an overly conservative prediction of risk due to their unboundedness in the right tail. In this paper, a bounded distribution model, the Beta distribution [1] is used to model the equivalent initial flaw size distribution. Crack data obtained from teardown inspection of a C-130H aircraft were compiled and used for EIFS distribution development. The derived EIFS distribution from TTCS method and Direct EIFS method using lognormal and Beta distributions are shown in Figure 1 and their corresponding risk curves are shown in Figure 2. It can be observed that the results from the TTCS method and Direct EIFS method using the Beta distribution are highly correlated up until  $SFPoF=1 \times 10^{-5}$  whereas the result from the lognormal based Direct model is very different from the other two.

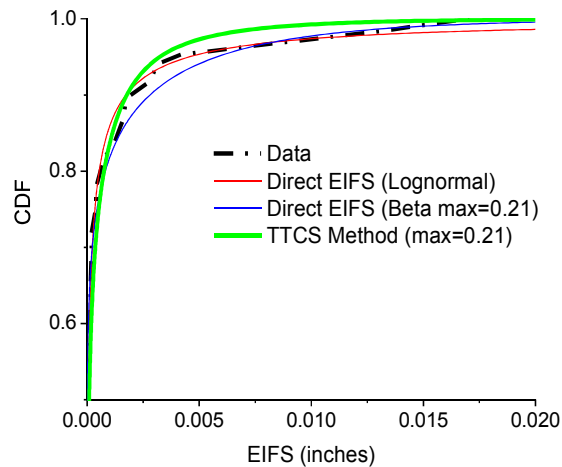


Figure 1 Comparison of EIFS distributions

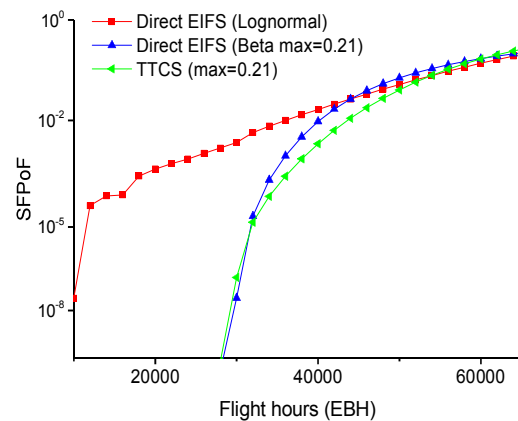


Figure 2 Comparison of SFPoF curves

## Conclusions and recommendation

Based on the investigation, the following may be concluded:

- a. Direct EIFS beta distribution model is superior to TTCS method in fitting its model to the data or regressed values at EIFS level.
- b. When using Direct EIFS method, Beta distribution shows better fitness to the observed or regressed EIFS values than the lognormal distribution.
- c. SFPoF curves from TTCS method are very sensitive to the assumed maximum EIFS.

Overall the Direct EIFS method using Beta Distribution seems to be a better option compared to the other two models since it showed superior results in terms of desirable characteristics of an EIFS distribution model. A future similar study will be conducted to other platforms such as FA-18 fighter aircraft.

## References

- [1] Ang, A.H.-S. and W.H. Tang, *Probability Concepts in Engineering Planning and Design*. Vol. 1. 1975: John Wiley & Sons.

## 2.17 A comparative evaluation of a deterministic and probabilistic approach for determining safety inspection intervals of airframe structures; R. Torregosa and W. Hu [DST Group]

The referenced paper [1] presents a comparative evaluation of a deterministic and a probabilistic approach applied to the analysis of two sets of test data obtained under laboratory conditions for the study of crack growth variability. The first set of data was from Virkler, et al., which used aluminium 2024-T3 mid-tension specimens subjected to constant amplitude loading. The second dataset was from experiments conducted by the authors on 7075-T7351 mid-tension specimens subjected to spectrum loading. Both the deterministic and probabilistic approaches were used to predict the safety inspection time for all coupons tested. For the probabilistic approach, a distribution of the initial flaw size and a master crack growth curve were derived from a number of randomly selected test results. The probability of failure is calculated based on the initial flaw size distribution, the master crack growth curve, the peak stress distribution and the material fracture toughness. A probability of failure of  $10^{-7}$  is used to determine the time for inspection. For

the deterministic analysis, the inspection time is determined by predicting the failure time then taking the inspection time as half of the predicted failure time. It was found that without the use of a factor of safety, probabilistic analysis is more conservative and that use of a factor of safety of 2 makes the deterministic prediction conservative but far from the exact values.

**Table I Comparison of deterministic and probabilistic safety inspection interval prediction using DST Group test data**

Test coupon fatigue lives (Load blocks)	Independent Trials	Deterministic analysis (FS=2.0)	Deterministic analysis	Probabilistic analysis (Fixed $K_C$ )	Probabilistic analysis (Variable $K_C$ )
		Predicted safe hours (Load blocks)			
12.1 (min) 16.1 (max)	1	7.7	15.4	11.5	9.9
	2	7.6	15.2	12.4	10.4
	3	7.3	14.6	11.1	9.7
	4	7.8	15.6	11.2	10.2
	5	7.5	15.0	11.6	10.2

**Table II Comparison of deterministic and probabilistic prediction using Virkler data**

Test coupon fatigue lives (Cycles)	Deterministic Analysis Safe life FS=2.0 (Cycles)	Deterministic Analysis Safe life (Cycles)	Probabilistic Analysis Fixed $K_C$ value	Probabilistic Analysis Mean $K_C = 25 \text{ Mpa-m}^{1/2}$	
			Safe life (Cycles)	St. dev.	Safe life (Cycles)
222000 (min) 320000 (max)	129700	259400	231117	1.5	188101
				1.0	210649
				0.8	215851
				0.5	223529

Based on the results of this study, shown in *Table I* and *Table II*, conclusions are as follows:

- Both the deterministic and probabilistic approach gave conservative predictions but the probabilistic approach predicts a life closer to the actual safe life;
- Without the use of a factor of safety, probabilistic prediction is more conservative;
- The application of both deterministic and probabilistic approach in predicting the safe fatigue life and inspection interval provides increased confidence in the prediction.

## Reference

- [1] Torregosa, R.F. and W. Hu, A comparative evaluation of a deterministic and probabilistic approach for determining safety inspection intervals of airframe structures, in 17th Australian Aerospace Congress. 2017: Melbourne.

## 2.18 Fatigue Crack Prognosis Using Bayesian iProbabilistic Modelling; W. Wang, W. Hu, and N. Armstrong [DST Group]

Prognosis of fatigue crack growth for mechanical and structural components is vital for aging military aircraft operated near or beyond their original design lives. For modern aircraft, prognostics and health management (PHM) is supposed to be a designed-in capability; however, prognosis of mechanical and structural damage is yet to fully mature. The objective of our study is to develop an unsophisticated, yet robust, methodology for crack size prognosis that is suitable for real-time PHM systems. A scheme adopting Bayesian probabilistic modelling, extended Kalman filter (EKF) in particular, was presented in [1] to predict fatigue crack growth for any given

number of cycles in common aircraft materials: 2024-T3 aluminum alloy for structural and AISI 9310 for dynamic components. In this scheme, the state model is the widely adopted Paris law in fracture mechanics (used to model the physics of crack growth), and the measurement model is a simple random walk model or an equation that relates the vibration feature with crack length plus random noise. The scheme was validated using a set of published crack growth test data – the Virkler fatigue crack growth data, where the state model parameters are derived from one half of the data and the crack length prediction is made on the other half of the data. The EKF framework is further validated using a set of gear tooth crack propagation test data, where the crack length is the unobservable (or hidden) state variable, and the observable variable is a feature extracted from the gear vibration signal. The state model is also derived from the Paris law and the measurement model is developed using the observed relationship between the known crack length, the applied stress, and the energy of the impulsive signature extracted from an optimized sinusoidal model for gear vibration signals. Using the recursive EKF solution, we were able to achieve promising prognostic results in terms of the accuracy of the prediction, and demonstrate the method’s robustness in dealing with uncertainties in the parameters defining the Paris law and the uncertainties in the measurements. Compared to other studies, the proposed method is a much simpler and more robust approach to the prognosis of fatigue crack size in mechanical structures and rotating components.

The Virkler crack growth test data were employed to validate the methodology. The tests were funded by the US Air Force and conducted at Purdue University in 1977. The main objective of the test was to investigate the statistical characteristics of metal fatigue behavior, specifically, the variability of fatigue crack propagation properties for 2024-T3 aluminum alloy under constant amplitude loading. There were 68 specimens tested to grow the initial crack of 9 mm to the final crack of 50 mm. The number of cycles ( $N$ ) for each specimen to reach the final crack length was very different due to the variability in material properties. The plot of crack length ( $a$ ) versus  $N$  for all 68 tests is shown in Fig. 1. From a portion of the data, we estimated Paris constants to be  $m = 2.9$  and  $C = 8.586 \times 10^{-11}$  (with  $DK$  in  $\text{MPa}\sqrt{\text{m}}$ ). Assuming  $C$  is Gaussian distributed with a standard deviation of  $C_{\text{std}} = 0.619 \times 10^{-11}$ , we used the developed EKF scheme to estimate the crack length at a given number of cycles. A guesstimate of the initial crack length is  $a_{0|0} = 8.95$  mm as opposed to the true value of 9.00 mm. The predicted results are displayed in Figs. 2 ~ 4. The reason why we focused on the predicted estimate instead of the updated estimate is because in reality we tend to be more interested in the predicted crack length of an aircraft structure in the next 50 or 100 flight hours without the future measurement data for the updated estimate. Future development would be required to adaptively predict the DN (e.g. number of flight hours) when an aircraft structure fails.

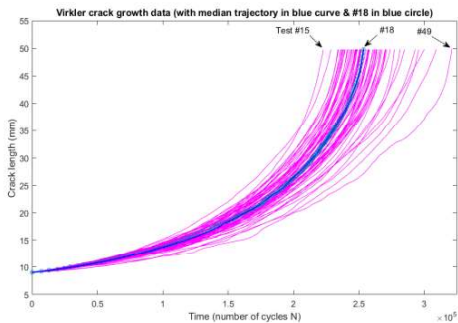


Fig. 1 The plot of crack length ( $a$ ) versus cycle counts ( $N$ ) for Virkler crack growth data.

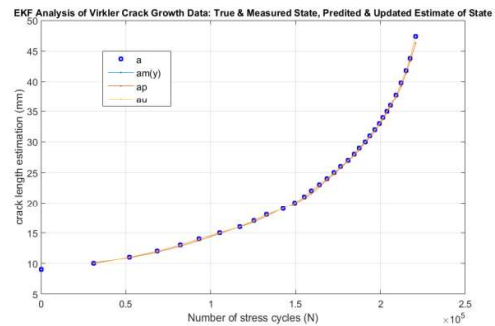


Fig. 2 EKF analysis of Virkler Test #15 ( $m=2.9$ ).

In Fig. 2, we can see that the predicted estimate of the crack lengths ( $a_p$  – the red line in the Figures) are very close to the *true* crack lengths, probably with the exception of the last few points. From the

error variance of predicted estimate, we found that the last 5 time-steps have relatively big errors whereas the errors for the rest are well contained. The results for Test #18 (the median growth rate) shown in Figs. 3 are similar to those for Test #15 (the fastest growth), despite the fact that the two crack growth trajectories are quite different as displayed in Fig. 1. Apparently the prediction error for Test #49 (slowest growth) as shown in Fig. 4 is much bigger than those for Test #15 and Test #18.

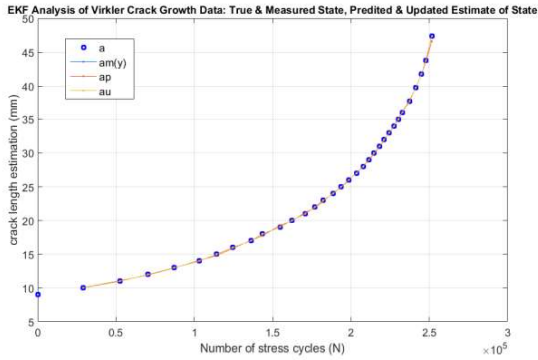


Fig. 3 EKF analysis of Virkler Test #18 ( $m=2.9$ ) ( $m=2.9$ ).

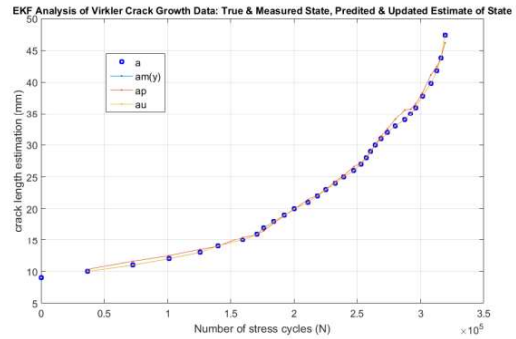


Fig. 4 EKF analysis of Virkler Test #49

In all three examples the error variance for the later time-steps seems to be bigger than the early time-steps. This is probably because the Virkler data was sampled at an increasing  $\Delta a$ , i.e.  $\Delta a$  was increased from 0.2 mm to 0.4 mm when crack length  $a$  reached 36.2 mm then to 0.8 mm when  $a$  reached 44.2 mm. The magnitude of the prediction error is very similar for these different crack growth trajectories. If the data were sampled at an equal  $\Delta a$  of 0.2 mm (with DN getting progressively smaller though), we would expect to see smaller and more consistent errors across all time-steps.

We also applied the methodology to a set of gear tooth crack propagation data where we could only measure the crack length indirectly through vibration features. With a reasonable assumption that the Paris exponent  $m=3.0$  for the EN36A (or AISI 9310) steel in the core of gear teeth, we estimated the other parameters in the Paris model (i.e. the state transition and physics-based damage progression model) from the test data. Figs. 5 and 6 show the predicted and updated crack lengths under two different variances for the crack growth (or state) equation. The result in Fig. 5 suggests that the physical model is under estimating but the measurement model is over estimating. If the error variance for the state model is reduced to  $Q=0.001$  as shown in Fig. 6, which means that the state model becomes more accurate and should be trusted more, the predicted estimate from the state equation will weigh more in the final updated estimate of the state. In Fig. 6, the updated estimate at #155 is closer to the predicted estimate than that in Fig. 5. This illustrates the effect of error terms in the state space model on the final estimation.

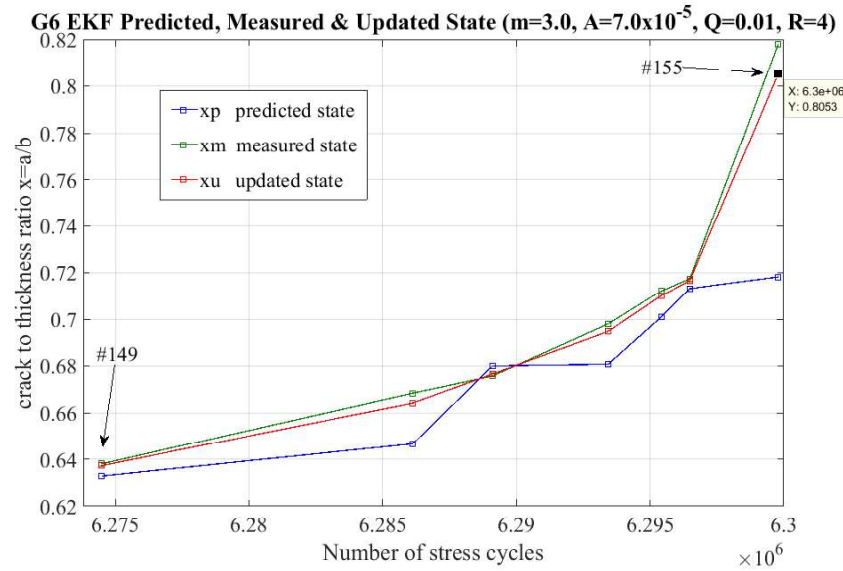


Fig. 5 Estimation of the tooth crack length/depth with Paris state model at file #155 – the end of the G6 series testing (state variance  $Q=0.01$ )

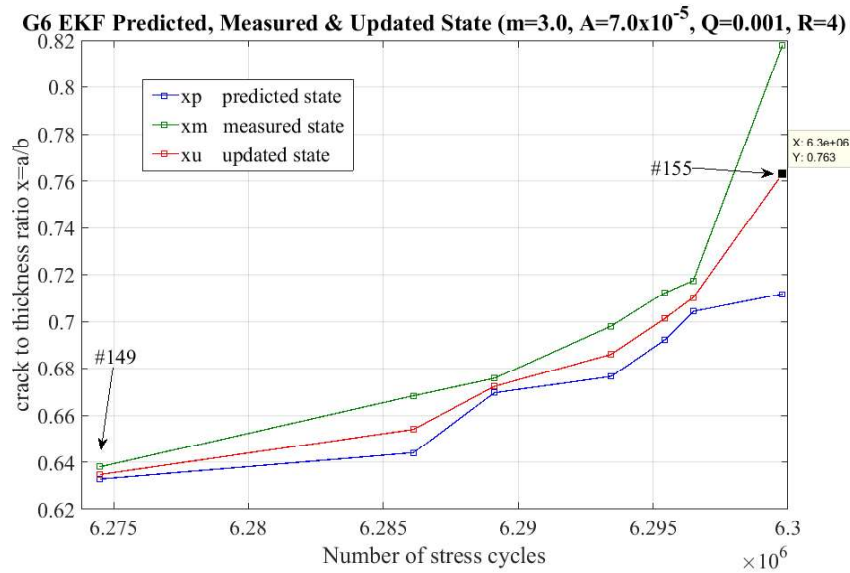


Fig. 6 Estimation of the tooth crack length/depth with Paris state model at file #155 – the end of the G6 series testing (state variance  $Q=0.001$ )

In summary, we proposed an EKF-based Bayesian scheme for crack growth prognosis, which was validated using the Virkler data and gear tooth crack growth data. Using the recursive EKF solution, we were able to achieve effective prognosis of fatigue crack growth in terms of the accuracy of prediction and the robustness in dealing with uncertainties in material property parameters used in the Paris Law and with the measurement uncertainty. Comparing to the methods used in the literature, the EKF-based approach is much simpler, and the state space modelling format is probably much more readily adaptable for researchers in the fracture mechanics community. Future work will include multivariate normal statistics for the state variables.

## Reference

W. Wang, W. Hu and N. Armstrong (2017), *Prognosis of Fatigue Crack Growth using Bayesian Probabilistic Modelling*. Accepted for publication in The Bulletin of Japan Society of Mechanical Engineers (JSME), special issue on Fracture and Strength, July 2017 (published in advance online by JSME: DOI:10.1299/mej.16-00702).

## 2.19 Aeronautical Fatigue and Structural Integrity Activities at Boeing Aerostructures Australia (BAA); A. Garg, A. Pipilikas, A Sheppard [BAA Melbourne], S. Georgiadis [Boeing Research & Technology, Melbourne]

### 2.19.1 Introduction

Boeing Aerostructures Australia (BAA) is a centre of excellence for the design and manufacture of composite flight controls and flaps for commercial aircraft. BAA currently manufactures flight controls and flaps for the 737, 747, 777 and 787 aircraft. The

components built by BAA are fabricated using either pre-impregnated CFRP (Carbon Fibre Reinforced Plastic) or Resin Infused CFRP. In addition, BAA engineers have been involved in the design of various other components for Boeing aircraft fabricated from CFRP solid laminates and CFRP honeycomb sandwich panels.

Some of the key focus areas and initiatives developed by the BAA engineering team have been on the development and understanding of the behaviour of CFRP structures within the field of damage tolerance and durability for Principle Structural Elements (PSE). A mixture of coupon, element, sub-component and full scale component level testing has been performed to substantiate the analysis methodologies developed by the team.

### 2.19.2 CFRP Joint Durability with Bolts

As CFRP materials are applied to more applications with higher load carrying requirements, CFRP structural joint durability must be validated for different bolt type/diameters, CFRP materials, joint thicknesses and shim configurations.

To support a number of aircraft programs, BAA has conducted cyclic fatigue tests at coupon level through to full scale component level. Joints tested include metal-to-CFRP joints and CFRP-to-CFRP joints with varying parameters to substantiate the design of critical joints and to develop empirical parameters for an analytical prediction method.

Testing demonstrated that joints subjected to alternating in-plane shear loads may fail either by CFRP hole damage (hole elongation, delamination around hole edge, fibre damage, or bearing of hole) or by fastener failure through bending induced cracking. In some cases both hole damage and bolt cracking was observed. The joint failure mode was compared against the different joint design parameters. It was determined that the joint stack thickness to diameter ratio ( $T/d$ ) has a significant influence on joint durability and failure mode. In general, low  $T/d$  joints are associated with CFRP hole bearing damage and high  $T/d$  joints are associated with bolt cracking and failure, this is illustrated qualitatively in Figure 1.

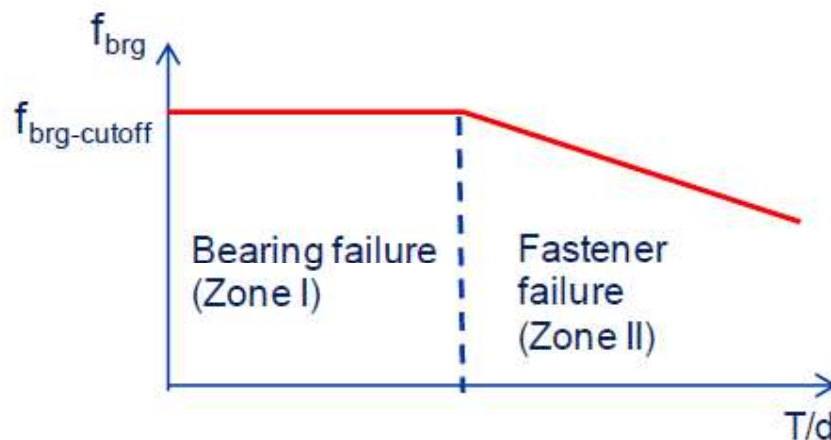
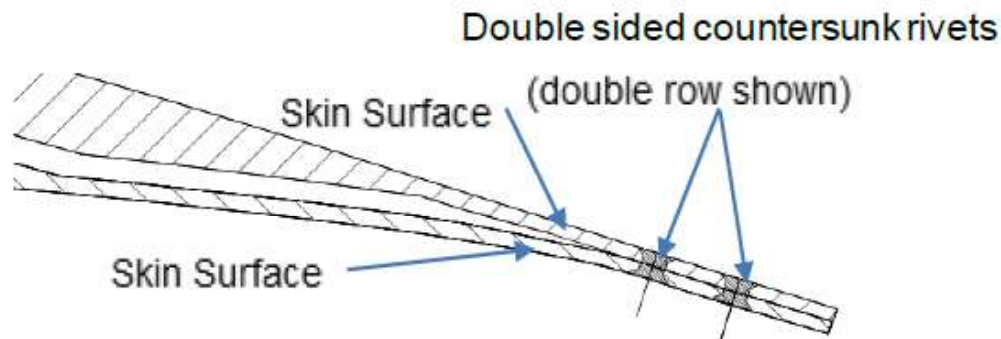


Figure 1 Qualitative Representation of Bearing Stress,  $f_{brg-max}$  vs  $T/d$

### 2.19.3 CFRP Joint Durability with Rivets

Typical wing or empennage control surfaces and flaps may utilise double sided countersunk rivets for trailing edge skin closeout joints to minimise aerodynamic drag as illustrated in Figure 2.



*Figure 2 Typical Trailing Edge Skin Closeout Joint*

Fatigue tests were performed on CFRP-to-CFRP joints with double sided countersunk rivets in both pre-impregnated CFRP laminates and resin infused CFRP laminates to develop a design allowable stress and fatigue methodology for the evaluation of this type of joint configuration. Two approaches for the analysis were defined; one approach presents a "Reserve Factor" approach which requires calculations to be undertaken to generate fatigue margins for each rivet. A second approach is a simplified "Endurance Limit" approach which provides rivet shear load cut-off endurance limit values, which can be easily applied by the stress analyst to determine a "pass" or "fail" assessment of the joint. The evaluation of the applied riveted joint shear maximum fatigue stress,  $f_{max}$  or the fatigue bearing load,  $P_b$ -max is made against a prescribed cut-off endurance value ( $f_{max}$ -comp-runout or  $P_b$ -runout) which determines that the closeout joint had a life beyond 1 million cycles.

Fatigue analysis for the riveted joints loaded in out-of-plane tension was also determined, based on cyclic data from shear-tension interaction test coupons and elements which combine shear and tension loading onto the joint, Figure 3.

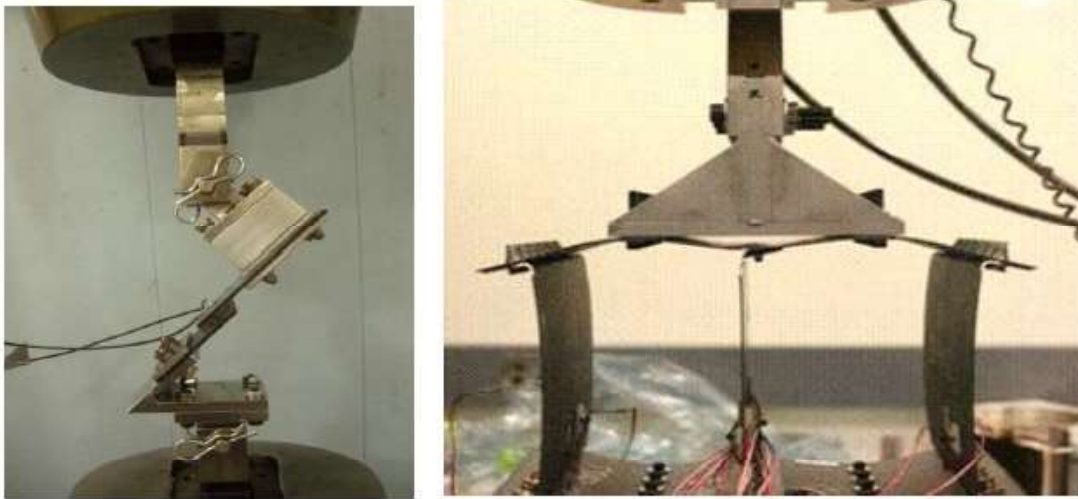
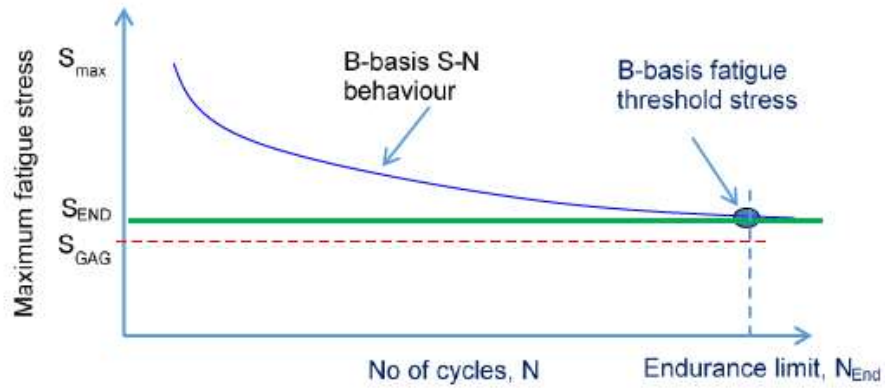


*Figure 3 Shear-Tension Interaction Test Coupon and Element*

The riveted joint fatigue tension capability was determined by an “Endurance Limit Approach” in which the rivet tension load cut-off and endurance limit ratio are based on a 1 million cycle threshold.

#### 2.19.4 Notched Fatigue Behaviour of CFRP Pre-Preg and Resin Infused Laminates

The strength evaluation of CFRP laminates with initial manufacturing flaws or other undetectable defects during the aircraft life are typically assessed by static strength analysis of these structures. The ability for undetectable defects to degrade the strength and capability of aircraft during operational service is evaluated through a no detrimental growth damage philosophy. This approach considers potential undetectable manufacturing flaws or impact damage is present and demonstrates through analysis methods substantiated by test that the damage will not grow detrimentally. Validation testing was conducted at coupon level through to component level with artificial barely visible impact damage (BVID) or damage equivalent to a 0.25” diameter open hole (OH). To demonstrate the no detrimental growth philosophy, the endurance limit/threshold approach (Figure 4) was developed.



Endurance limit approach:  $S_{GAG} \leq S_{END}$   
 Where  
 $S_{END}$ : Endurance limit Stress  
 $S_{GAG}$ : Maximum ground-air-ground (GAG) stress

Figure 4 Typical endurance limit approach for fatigue Aeronautical Fatigue and Structural Integrity Activities at BAA for ICAF 2017

For coupons with a 0.25" diameter open hole, a cyclic loading ratio of  $R=-1$  was tested to 1 million cycles to establish no damage growth design strains with a high reliability and confidence level (95/95), to allow evaluation of different CFRP structures through an analytical approach. In addition, coupons with simulated BVID were also cyclically loaded with maximum fatigue loads at  $R=-1$ . Based on these tests, run out strain values were established, one for compression loaded structure which is critical for BVID and one for tension load structure which is critical for open hole fatigue. Figure 5 illustrates a typical endurance limit strain behaviour for open hole fatigue of CFRP pre-preg or resin infused laminates with varying percentage of fibres in the loading direction.

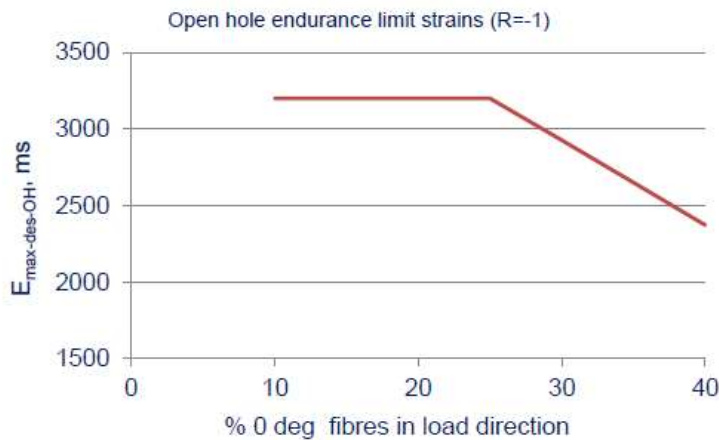
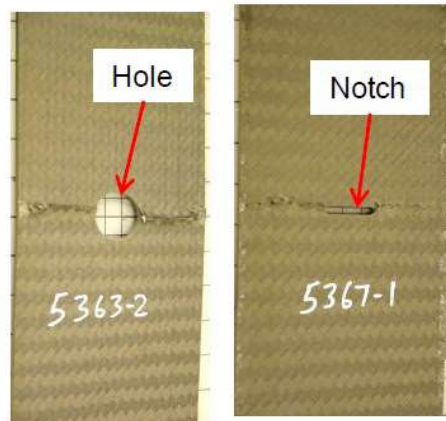


Figure 5 Endurance Limit Strains vs % 0 deg. fibres in load direction for CFRP OH Fatigue

Analysis methods development and testing (element level and full scale level) has also been conducted into larger visible damage in CFRP panels, Figure 6. The approach for

visible damage is to demonstrate limit load static strength capability and no detrimental damage growth over the applicable maintenance inspection interval.



*Figure 6 Fatigue Coupons with Visible Notches after End of Life Residual Strength Testing Aeronautical Fatigue and Structural Integrity Activities at BAA for ICAF 2017*

#### 2.19.5 High Cycle Vibration Fatigue

Wing and empennage components are subjected to aero-acoustic environments that include sonic and/or aerodynamic buffet fatigue. For the 787 aircraft the fatigue impact from an aero-acoustic environment was substantiated through an analytical approach and validated by full scale sub-component testing. This validated analytical approach is also being used to support the latest 777 derivatives.

A finite element based frequency response analysis was developed which determines the Power Spectral Density Function (PSD) and Cumulative RMS curves for all elements of the structure (refer to Figure 7 for an illustrative example). The Cumulative RMS plot produced by the frequency analysis is used to determine which part of the analysed frequency range contributes most power to a measured quantity, and therefore which part of the response will cause the greatest amount of damage to the structure. In addition, the results are qualitatively used to assess the behavior of the structure and determine the life of key features from a 300-hour overall sound pressure level and demonstrate that fatigue cracks will not develop. The 300 hour level is consistent with the design life goal of the 787 and 777 derivative aircraft.

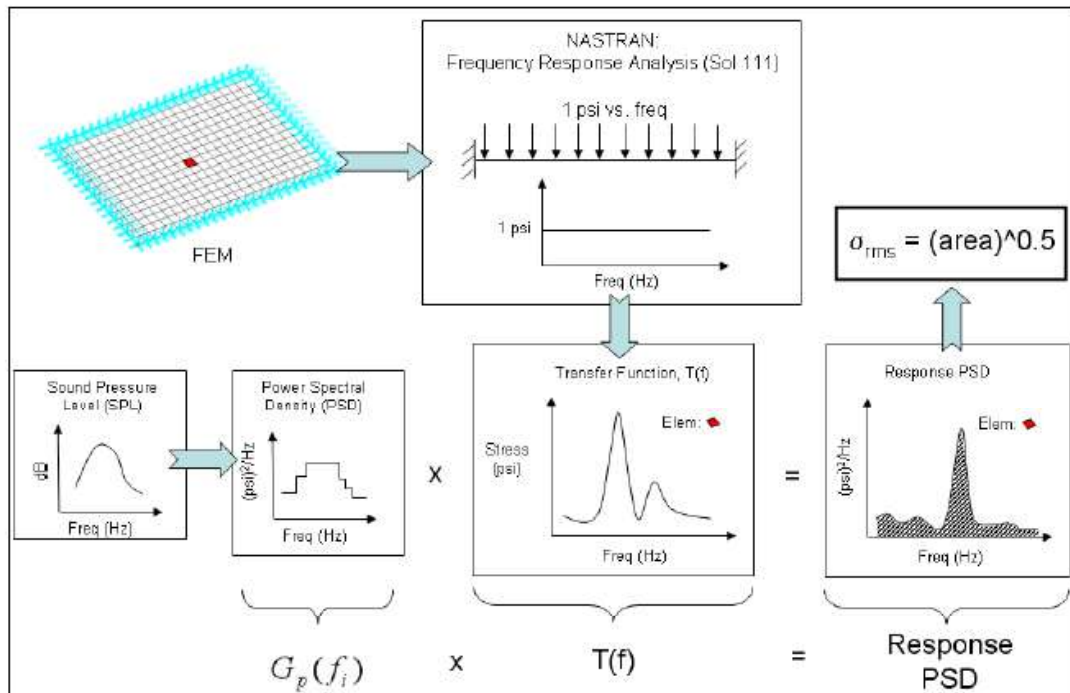


Figure 7 Frequency Response Analysis and PSD Determination for an Element of Interest

### 2.19.6 Integrated Co-cured Structures and New Materials

On site at BAA is a Boeing Research and Technology Australia (BR&T-A) office. BAA Engineers assigned to BR&T-A are identifying new resin infused CFRP materials and are developing next generation integrated co-cured structural designs to reduce fabrication cost, maximise structural performance and provide an uncompromised level of operator safety.

To identify the right combination of material type and integrated structural detail, a balance is required between environmental durability (thermal cycling of co-cured joint details to validate no detrimental crack development), damage tolerance (impact resistance) and structural integrity. A combination of new analysis methods and testing is being developed and applied to rapidly screen tough resin systems, interlayer tougheners and novel fibre architectures to support selection of the appropriate combination of materials and structural design approach.

For detailed design, the co-cured joints of integrated structures must be damage tolerant to delaminations and flaws at the co-cured interface between structural elements (e.g. interface between skin and spar) and within the individual laminated elements in the region of the joint which react critical through-thickness loads. To analytically assess delaminations/flaws at these locations within the co-cured joint, fracture mechanics is used with a strain energy release rate approach. The application of this fracture analysis approach is being refined to maximise efficiency and is validated by test using a no damage growth approach.

### 3. Full Scale Test Activities

#### 3.1 C-130J Wing Fatigue Test Teardown and Forensic analysis; D. Williams [DST Group]

Following successful completion of 62 456 fatigue test hours and demonstration of residual strength under appropriately factored design limit load conditions, the collaborative Royal Air Force (RAF) and Royal Australian Air Force (RAAF) C-130J Wing Fatigue Test Program is currently focused on test article teardown and forensic analysis. Completion of the forensic analysis will effectively represent the end of the collaborative program, with both the RAF and RAAF electing to pursue individual test interpretation approaches cognisant of their respective airworthiness management frameworks.

The RAAF Test Interpretation (TI) methodology has been defined in accordance with the endorsed durability and damage tolerance certification basis for the RAAF C-130J-30. It will propose instructions for continuing airworthiness based upon an assessment of when damage is likely to be observed at each fatigue critical location; what inspection program is necessary to assure safety; and when structure may require modification or replacement to ensure continued safe operation.

To achieve the stated TI outcomes, the results of the forensic analysis of the test article play a significant part. To ensure the forensic analysis received the necessary inputs, DST have taken the lead role in managing the stakeholders involved in the teardown, as shown in Figure 22. DST have significant experience in both aircraft teardown and forensic analysis; has provided direct input into the Statement of Requirement (SOR) for the teardown conducted by Airbus Group; defined the necessary outputs for TI; and provides ongoing leadership of the activity to ensure timely delivery of TI outcomes.

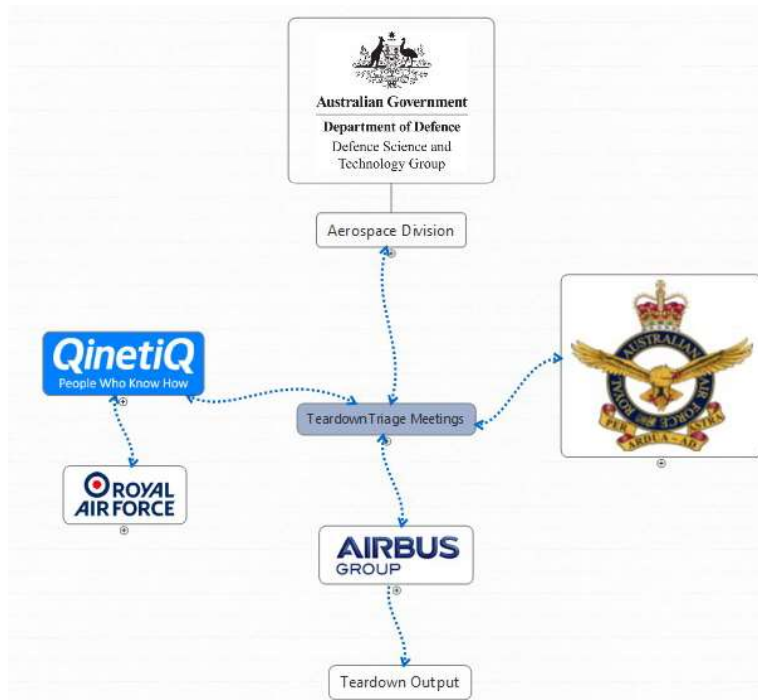


Figure 22 Teardown stakeholder interaction

The teardown output shall ultimately be captured in an Airbus Group Teardown Report, a DST Group Forensic Investigations Report, and a DST designed online database. Details of the teardown activity conduct may be found in [1].

An example of a part removed from the test article during the teardown process is shown in Figure 23. The crack was first identified during the fatigue testing phase, but was allowed to grow un-altered until the end of test. Airbus Group NDT technicians inspected and quantified the crack characteristics after it had been removed from the test article and reported the results to DST. The part was shipped from Airbus to DST where a full forensic examination of the fracture was conducted. DST broke open and cleaned the part to reveal a fracture surface as shown in Figure 24.

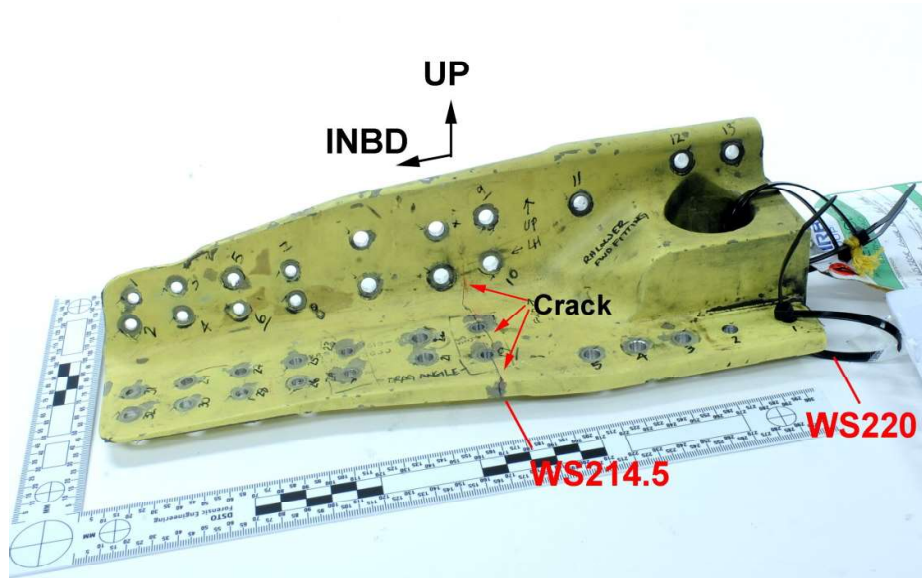


Figure 23 C-130J-30 WFT centre wing forward lower corner fitting

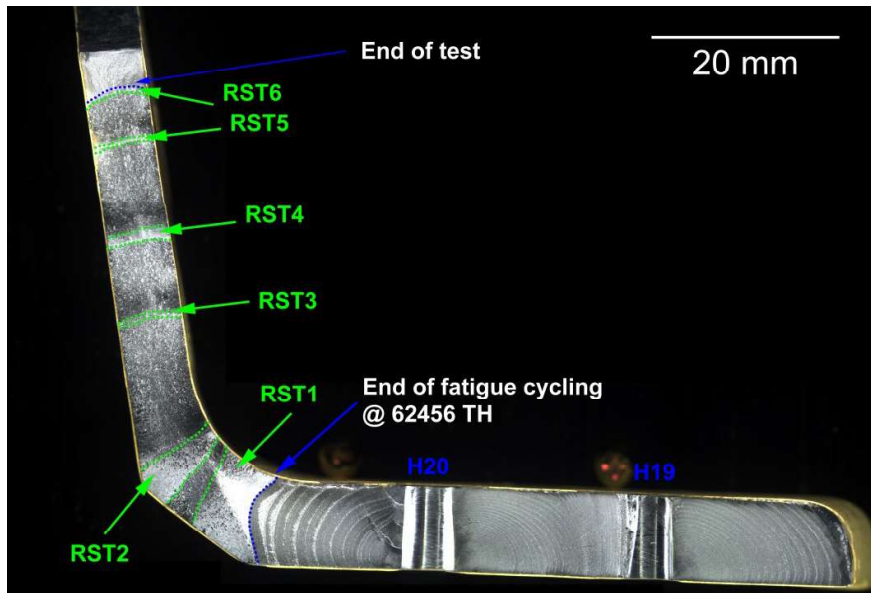


Figure 24 Centre wing forward lower corner fitting fracture surface

It has been possible to characterise the crack growth on the fracture surface, as shown in Figure 24, as a result of a carefully crafted test load spectrum. The test load spectrum for the WFT comprised 120 “Superblocks” of repeated load sequences, which was followed up with a series of residual strength test load applications and an accelerated test spectrum. A Superblock, consisted of 5 repeated blocks of exactly the same load sequence and 1 block of the same load sequence with the inclusion of rare high load events. The repeated nature of the loading - in particular the high load events, has generated very distinguishable crack growth marks on the fracture surface, allowing for a detailed understanding of the progression of the crack against test hours. Figure 25 clearly identifies the repeated pattern left on the fracture surface by the high load events in each superblock.

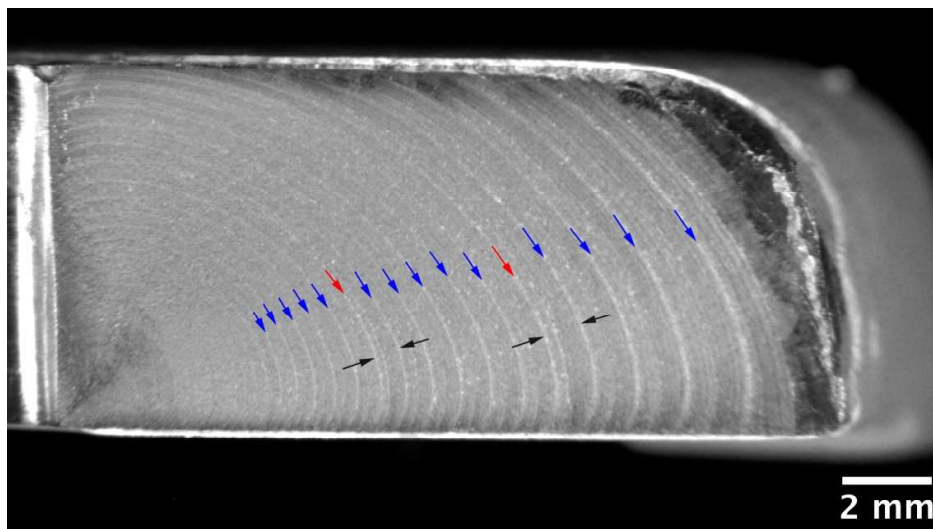


Figure 25 Fatigue progression marks

By plotting the crack growth against test hours, it has been possible to generate test demonstrated crack growth rates which are then used as inputs to the models developed and calibrated in reference [2]. The output of these models is utilised in the generation of TI output, as described in [3], which translates the result from test hours to the RAAF fleet. The TI phase of the C-130J WFT Program is currently still ongoing and is not part of the collaborative arrangement struck with the RAF. Discussion on this topic shall be made available at the completion of the activity.

#### **References**

- [1] D. Williams (2016), *C-130J Wing Fatigue Test Program – Teardown Volume 1: Management Plan*, DST-Group-TN-1552, Defence Science and Technology.
- [2] M. McCoy, K. Maxfield, R. Ogden, *Royal Australian Air Force C-130J Wing Fatigue test Analytical Tool Calibration and Verification (FASTRAN 5D & FAMSH 1.6)*, DSTO-TR-3099, Defence Science and Technology.
- [3] K. Maxfield, R. Ogden, M. McCoy (2017), *Australian Test Interpretation Guide (Phase 1) for the C-130J Wing Fatigue Test*, DST-Group-TR-3350, Defence Science and Technology.

### **3.2 Distributed Fibre Optic Strain System for Full-Scale Fatigue Testing; C. Davis, M. Knowles, N. Rajic and G. Swanton, [DST Group]**

The Defence Science and Technology Group has been conducting full-scale fatigue tests of ex-service F/A-18 Hornet centre fuselages in support of the Royal Australian Air Force's structural integrity management programs, for its frontline fighter fleet for over 12 years. Historically, conventional electrical resistance foil strain gauges have been used extensively on these tests to monitor and record the structural response to loading; however, there are limitations with these in terms of cost, installation times and physical complexity when handling and routing many gauges. Developments in commercially available, distributed fibre optic strain measurement systems have presented the opportunity to overcome these limitations. This has been demonstrated on the most recent centre fuselage test article [1]. Based on Rayleigh scattering, the system ('ODiSI B' by Luna Innovations) was trialled, which allowed comparisons of strain response, spatial resolution and noise levels with conventional foil gauges. Comparisons were also made of the full-field strain mapping capability of the system with full-field stress mapping by thermoelastic stress analysis (TSA). Furthermore, the distributed fibre optics demonstrated their potential to detect crack propagation in a coupon with a growing fatigue crack during cyclic loading, see Figure 2.

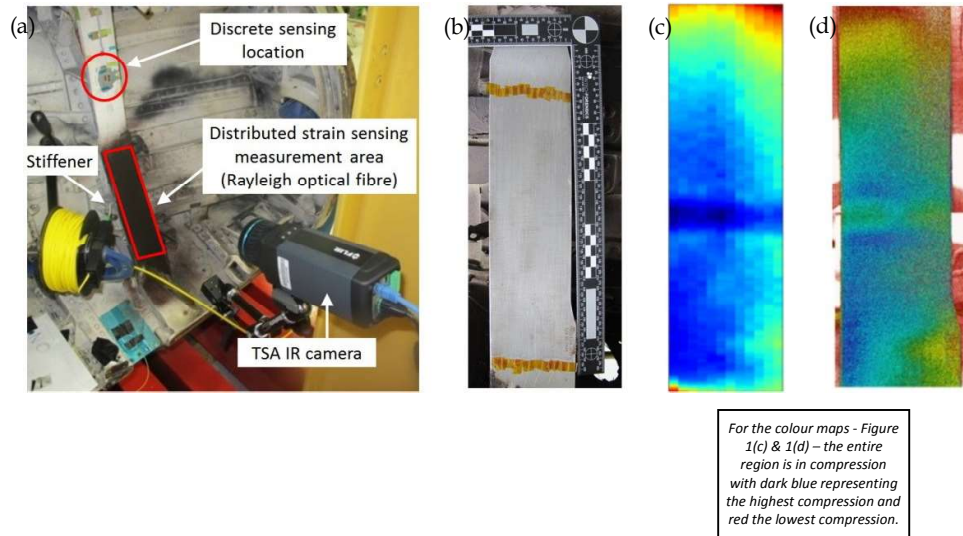


Figure 1: (a) Location of distributed fibre optics on F/A-18 centre barrel (b) Layout of optical fibres (c) Distributed fibre optic strain output (d) TSA output

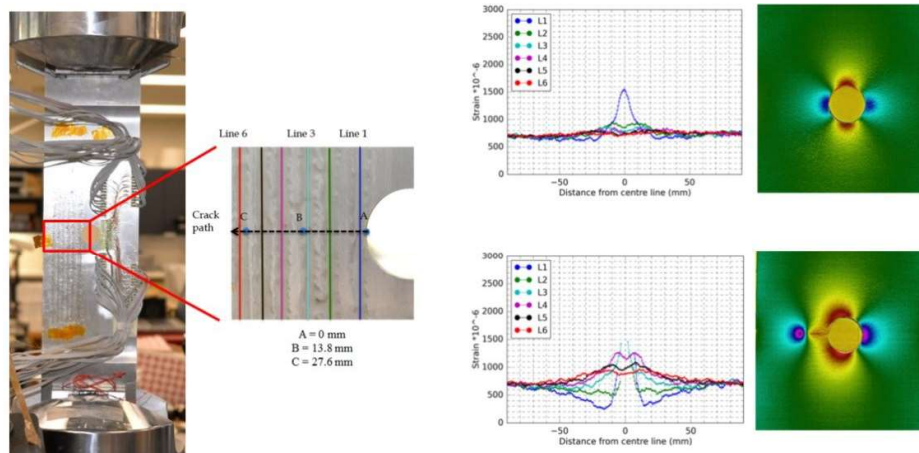


Figure 2: (left) coupon set up with six lines of the same optical fibre. (middle) Detail of fibres next to hole (right) Strain distributions and corresponding TSA scans at two different crack locations "A" and "B"

**References:**

[1] Davis, C., Knowles, M., Rajic, N., and Swanton, G., *Evaluation of a Distributed Fibre Optic Strain Sensing System for Full-Scale Fatigue Testing*, in: Proceedings of the 21<sup>st</sup> European Conference on Fracture, ECF21, Catania, Italy, 2016.

[geoff.swanton@dsto.defence.gov.au](mailto:geoff.swanton@dsto.defence.gov.au)

### **3.3 Sample Heading Level 2 Blueprint TITANS: A Roadmap towards the Virtual Fatigue Test through a Collaborative International Effort; A. K. Wong [DST Group]**

The term Virtual Fatigue Test entered our lexicon a little over a decade ago ([1, 2]) and has gained increasing currency as the fidelity and sophistication of numerical models continue to improve, keeping pace with advances in computing hardware that have been unabated from Moore's Law. At the same time, growing labour and real estate costs, as well as increasing complexity of aircraft designs and the introduction of new materials and processes, have all contributed to the mounting costs of physical testing. Both of these factors have conspired to drive towards an increasing reliance on analyses. In the 2009 NATO ATO Report titled "Qualification by Analysis" [3], it wastes no time in setting the rationale for turning towards analyses in its Executive Summary's opening sentence: "The time and cost associated with designing, developing and qualifying new military air vehicles is prohibitive..." In this same report, however, it concedes that "... Full Scale Fatigue Tests (FSFTs) continue to produce premature fatigue cracking, demonstrating the current inadequacies of the fatigue analysis process. Until a time is reached when FSFTs do not reveal significant premature failures or cracking, designers and regulators alike will not have enough confidence in analysis methods to allow deletion of full scale testing."

Such inadequacies have certainly been borne out by any number of FSFTs that DST has been involved with and serve only too well to reinforce the importance of full scale testing. Unplanned failures have continued to emerge in full scale tests, often well in advance of the scheduled test duration, that have led not only to tremendous program cost and schedule penalties, but have certainly pushed the idea of eliminating the necessity for full scale testing further into the distant future. A valid question is why does this still happen in this modern era and despite some 70 years of knowledge and experience with aeronautical fatigue? The reasons are many, both from the programmatic and technological perspectives, including cost and schedule pressures as well as the limitations of modelling. Whilst the former depends much on judgment, culture and processes (any experienced program manager would know that cutting corners in the beginning is invariably counterproductive at the end), why the latter has made so little apparent progress despite significant advances in our ability to model and predict fatigue at the material/coupon level is worthy of some pondering. In trying to understand this, we looked internally at the various FSFT programs with which DST has had involvement and quickly came to the realization that the reason lies much in their purpose and therefore our approach. Invariably, each of these has/had a well-defined goal (such as establishing a life-of-type for the purpose of qualification) that is/was funded by our military clients and driven by costs and schedules. Consequently, these have/had been approached single-mindedly in pursuance of that goal rather than treating these as science experiments that may be used to hone our predictive skills (incidentally, the term "science experiment" is often used by our clients to describe any of our work that may lack focus - their focus). Importantly and until recently, even the identification of fatigue critical regions could not be confidently predicted or validated until the fatigue tests have essentially run their course thus making the problem space for life prediction possibly too large to handle (as the number of possible critical locations to analyse can be overwhelming). In recent years, however, DST has developed a critical piece of technology that could fundamentally

change this position. It has been proposed [4] and duly demonstrated [5] that the microbolometer-based Thermoelastic Stress Analysis (TSA) technology can be used to effectively identify fatigue critical locations and to provide direct validations on the computation of stresses at these locations at the early stages of full scale testing. The arrival of this important tool has suddenly made the problem space of aircraft fatigue life predictions under FSFT conditions much more manageable.

With the foregoing realization, DST is proposing a concerted and systematic effort to progressively develop and improve on our ability to predict aircraft lives undergoing FSFTs. Launched as Blueprint TITANS (Transglobal Integrated Tests & Analyses Network on Structures), it aims to:

- a. encourage national and international participations in forming a network of scientists and engineers to work in a collaborative and coordinated fashion to pursue the below objectives,
- b. make every FSFT a learning exercise in the prediction of aircraft lifing, thus leading to progressive improvements in all aspects of modelling,
- c. work progressively towards an increasing reliance on modelling and, by inference, a decreasing reliance on full scale testing, for the purpose of airworthiness design and qualification
- d. drive improvements on present, or development of new, techniques for the identification of fatigue critical regions as well as for the validation of stress models.

Figure 1 shows a schematic of how tests and analyses are integrated to produce the desired outcomes. In this diagram, the normal process of undertaking a FSFT is shown linearly along the bottom (represented by the green boxes), from its initial cycling through to its completion after Residual Strength Test (RST) and teardown assessments (note that some details or variations such as repairs made to the test article when damage is found have been omitted for simplicity). Incidentally, this whole process for a military aircraft type can take up to (and sometimes beyond) a decade to accomplish. In the middle row and at the upper left-hand corner are the various forms of analyses and modelling (blue boxes), often accompanied by coupon testing to calibrate the models (grey box). On the left-hand side of the middle row, the TSA technology is shown (in orange) as the “Hotspot Finder” that can be deployed to the FSFT at its commencement (represented by the dotted line). This generic description is used as this initiative is open to adopting any other technologies that can be effectively demonstrated.

In the past, at least from our own experience, models have been used to inform inspection locations on FSFTs (shown by the dotted lines), but have usually stopped short of proceeding to the prediction of actual test lives. Furthermore, no effort has ever been made to produce any prediction on crack distributions that may be expected to be found during teardown inspections. Within the new paradigm under Blueprint TITANS, such predictions will be a requirement. The other important requirement is the feedback loops that compare the predictions to what are actually found – these are the deltas that will be used as metrics to drive improvements in the various models which, in turn, should drive down the deltas themselves.

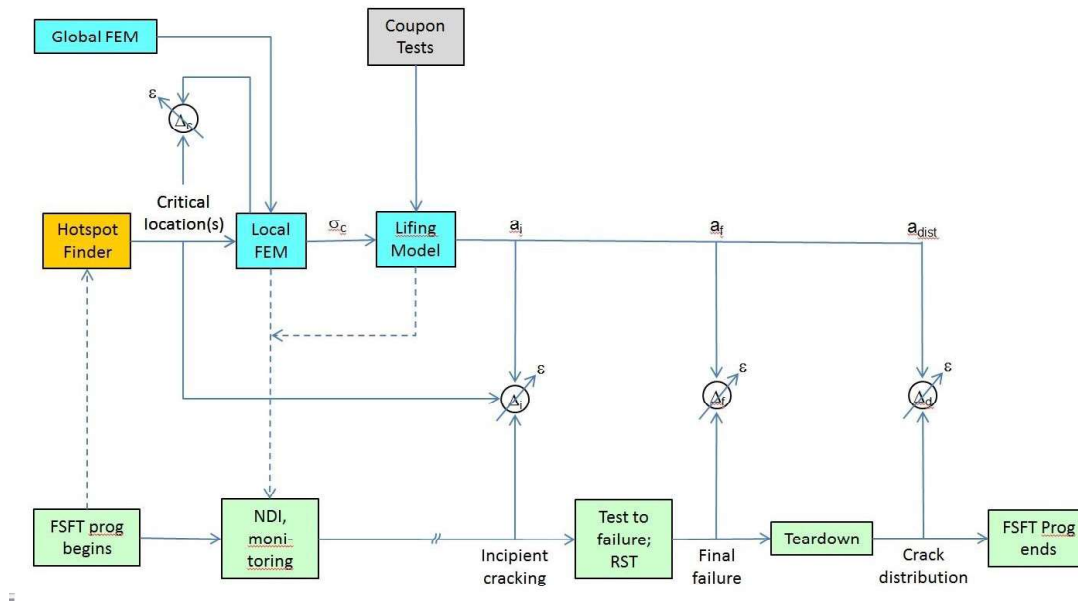


Figure 1. Schematics of Blueprint TITANS

The motivation for undertaking this systematic approach can now be easily seen by exploring some possible scenarios. Suppose that, after many years of concerted effort in this pursuit, the deltas ( $\Delta_i$ ,  $\Delta_f$ , and  $\Delta_d$  in Fig. 1) can be consistently shown to be sufficiently small or suitably conservative. Under this scenario, there will then no longer be a requirement for the FSFT to continue beyond the first green box. This would represent a tremendous cost and schedule saving as a typically 10-year FSFT program can potentially be reduced to just months! Taking this to the next (and ultimate) step, if in addition to the preceding,  $\Delta_c$  (i.e., the errors in the prediction of critical locations by the models) can be consistently shown to be sufficiently small, then there will be no need for the FSFT at all.

Blueprint TITANS presents a systematic roadmap towards the ideals of a Virtual Fatigue Test. At best, the ultimate goal to remove any requirement for FSFTs could be achieved eventually, even if this may take many years/decades. In reality, many factors (such as build quality or rogue flaws) may work against this goal from being ever achieved. A more likely prospect is that the FSFT may not be required to run its full course, thus still representing significant savings in program costs and schedule. At worst, even if neither of these goals turn out to be achievable, the concept of a concerted international effort to make every FSFT a learning exercise in aircraft life prediction will undoubtedly improve our modelling capabilities and add to our understanding of aircraft fatigue in general.

## References

- [1] Tikka, J. (2002) "Fatigue life evaluation of critical locations in aircraft structures using virtual fatigue test", Proc 23rd ICAS, 8-13 Sept, Toronto, Canada.
- [2] Farahmand, B. (2004) "Virtual testing versus physical testing for material characterisation", Proc 45th AIAA/ASME/ASCE/AHS/ASC Struct, Struc Dynamics & Mat Conf, Apr 19-22, Palm Springs, California.
- [3] NATO RTO (2009) "Qualification by analysis", NATO-RTO Report RTO-TR-AVT-092 AC/323(AVT092)TP/229.
- [4] Wong, A.K. (2013) "Making the invisible visible: taking a look at stresses in aircraft fatigue analysis and testing" Proc ICAF Symposium, 5-7 June, Israel.
- [5] Rajic, N, McSwiggen, D. McDonald, M. Whiteley, D. (2015) "In situ thermoelastic stress analysis of the F-35 - an improved approach to airframe structural model validation", 2015 Aircraft Structural Integrity Program Conference, Dec 1-3, San Antonio, TX, <http://www.meetingdata.utcd Dayton.com/agenda/asip/2015/proceedings/presentations/P8675.pdf>

## 4. In-Service Structural Integrity Management

### 4.1 Innovative Repair of Classic Hornet Centreline Pylons based on Optimal Shape Reworking; Xiaobo Yu<sup>1</sup>, Jaime Calero, Simon Barter, Michael Opie [DST Group], Matt Gordon [Defence Aviation Safety Authority]

The SUU-62 centreline pylon as shown in Figure 26 of F/A-18 classic hornet aircraft is a critical load path item that serves to connect external stores to the fuselage. It has a fatigue history at one of the forward attachment points as illustrated in Figure 27. To ensure the structural safety of the centreline pylons, the Royal Australian Airforce Force (RAAF) had implemented a safety-by-inspection scheme using in-situ liquid dye penetrant based Non-Destructive Inspection (NDI). Towards the end of 2014, following a review of the in-situ NDI results, it was found that the cracking could become critical – with the potential of pylon loss – at a crack size smaller than the accepted lower limit of the NDI method. Consequently, RAAF suspended all F/A-18 operations with the SUU-62 fitted.

The centreline carriage is a highly desirable capability for the F/A-18 aircraft. For instance, a centreline fuel tank can be attached to extend the range of the aircraft, increase the time on station and decrease the reliance on aerial refuelling assets. Prior to the present work [1], two options were considered to restore the centreline carrying capability: (i) purchasing new pylons, however the lead-in time was too long to meet the operational needs; and (ii) performing an industry standard repair, however the stress at the fatigue critical region would be significantly increased such that the “repaired” pylons would still be unsafe to use.

Hence, a third option as presented [1] was pursued by the authors and their colleagues – that is, to develop an innovative repair solution based on optimal shape reworking, which has been proved to be highly effective in repairing primary aircraft structural components [2]. In this application, the optimal shape reworking was integrated with the high precision inspection to achieve the target fatigue life. The key features of the present repair solution are illustrated in Figure 28. Its success was enabled by two innovations summarised as follows:

- a. Iterative finite element based rework shape optimisation. This innovation enabled a tightly controlled optimal rework shape at the critical location that reduced stress concentration while removing cracks. In this application, an optimal rework shape with a nominal 1 mm deep cut was designed using unique in-house rework shape optimisation software [2], a purposely developed 3D general mesh morphing scheme [3] and iterative 3-D computational structural analyses. The peak stress at the fatigue critical location was minimised and was kept lower than that of a blue-print configuration. The optimal rework shape was designed to accommodate fleet geometric variations and many non-blueprint issues found in the critical areas of these SUU-62 support frames, as determined by precise measurements. It is a precise shape, which would not have been achievable by conventional semi-controlled blending-based repair.

- b. High precision inspection. A highly sensitive precision replica-based inspection method was implemented to assess the in-service damage and repaired components. It was used to detect cracks at far smaller sizes, by an order of magnitude, than the standard in-service NDI inspection. This enabled a precise determination of the extent of any cracking and therefore allowed a minimum amount of rework cutting to guarantee crack removal. Additionally, the improved crack size and distribution information (number of frames cracked) allowed a more precise estimate of remaining fatigue life based on a Weibull analysis with an assumption of much smaller initial crack sizes.

With the lower-than-blue-print peak stress and the confidence of much smaller initial crack sizes, the present repair solution has led to a significantly extended fatigue life of approximately 1000 flight hours. The optimal rework shape was CNC-machined into the frames after rapid jig development and prototyping. A total of 23 pylons have been repaired and returned to service in two batches, of which the first batch of 12 pylons were returned to service within seven weeks to support urgent operational needs.

In conclusion, the repair solution presented here is an innovative and highly effective solution proved to be achievable to meet the tight delivery schedule. **Future** applications include: (i) the innovative repair solution can be applied to worldwide F/A-18 classic hornet fleets, and (ii) the innovative technologies can be readily applied for repair of other primary aircraft structures.

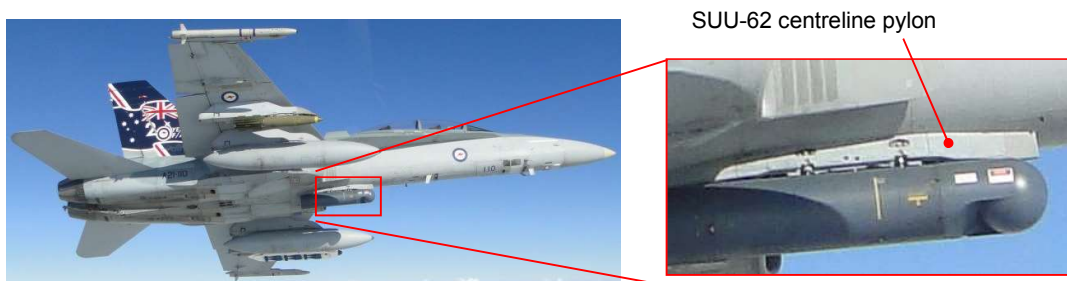


Figure 26. SUU-62 centreline pylon on aircraft with forward- and aft-fairing



Figure 27. (a) SUU-62 centreline pylon frame; (2) Typical crack locations next to the forward LHS mounting attachment.

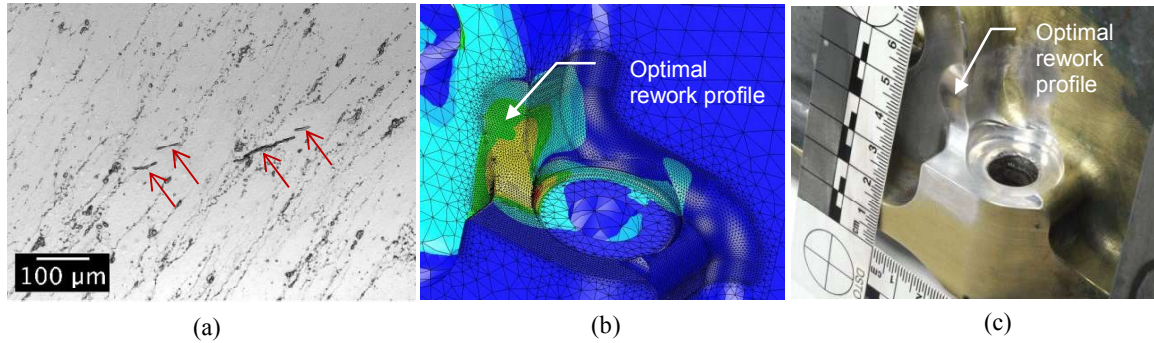


Figure 28. Key features the current innovative repair technology. (a) Very small cracks revealed by high precision inspection; (b) Reduced stress distribution at critical area (reflected by uniform colours); and (c) L/H forward attachment critical region after precise shape rework.

#### References:

1. Yu X, Calero J, Barter S, Gordon M and Opie M, *Innovative repair of classic hornet centreline pylons based on optimal shape reworking*, accepted for oral presentation, 29th ICAF Symposium, 7-9 June 2017, Nagoya, Japan.
2. Heller M, Burchill M, Wescott R, et al., *Airframe life extension by optimised shape reworking – overview of DSTO developments*, 25th ICAF Symposium, Bridging the Gap between Theory and Operational Practice, 27-29 May 2009, Rotterdam.
3. Yu X, *A new mesh evolution algorithm to enable improved rework shape optimisation of complex 3-D structures*, presented at: WCSMO11, 7-12 Jun 2015, Sydney.

## 4.2 F/A-18A/B Shear Post Coupon Design and Critical Crack Size Estimation, R Evans and X Yu [DST Group], D Tata [QinetiQ]

The shear post (or shear tie) of the F/A-18A/B Classic Hornet aircraft is 48 mm in diameter and is integral to the Y508 centre fuselage former, refer to Figure 1. It is a machined component and transfers shear (vertical) loads from the wing, via a bearing within the wing aft closure rib, into the fuselage. To ensure flight safety of the aircraft and to assess the potential for unexpected cracking under a new, more representative spectrum, a coupon fatigue test program is to be carried out for the RAAF. This test spectra has been drawn from operational flying and has been found to be considerably more severe than the full-scale fatigue test (FSFT) spectra at this location. The fatigue crack growth characteristics and critical crack size ( $a_{crit}$ ) of cracking in the shear post will be investigated by this test program. The Structural and Damage Mechanics team within the DST Group has been tasked to perform detailed design of the test coupon, which is documented in [1].

Finite element analysis (FEA) of the coupon design was undertaken in order to match peak stress and stress decay curve data determined by L-3 Communications (now L3 Technologies). StressCheck® was used to create and analyse detailed 3D parametric FE models of the shear post, due to its convenience in analysing cracked bodies. This code uses the variable order polynomial elements method (p-element) approach, as compared

to h-version software. The use of p-elements allows a relatively coarse geometric mesh to be used, enabling quick mesh creation with a high level of accuracy. Key geometry dimensions were changed, such as coupon length and thickness, and the resultant effect on stress and crack data was assessed. The representation of loading was also examined; via contact or bearing. The model was relatively insensitive to the changes. The stress results of the coupon design matched within 1 % of the full Y508 former model from L-3 Communications which was as desired. This was obtained primarily by adjusting the location of the load application on the post. Figure 2 shows the principal stress distribution of an uncracked shear post FE model.

To estimate  $a_{crit}$  and to understand the natural progression of crack growth to  $a_{crit}$ , an iterative process was used. This process was based on an initial discontinuity size and  $da/dN$  data of the shear post material. The critical crack was chosen to be the crack where the stress intensity factor (SIF) was relatively constant around the crack front and equal to the fracture toughness (conservative value) of the aluminium alloy material of the coupon. The origin and orientation of the cracks were commensurate with the location of the maximum principal stress and the direction of the highest stress decay gradient. Cracks of various sizes and offset elliptical shapes were incorporated into the models. Sample crack shapes are shown in Figure 3. SIFs were extracted around the crack front for these numerous cracks, refer to Figure 4.

#### Reference

- [1] R Evans, D Tata and X Yu, "F/A-18A/B Shear Post Coupon Design and Critical Crack Size Estimation", DST Group Technical Report in preparation, Objective ID: AV12659849, December 2016.



Figure 1 The F/A-18A/B Y508 shear post

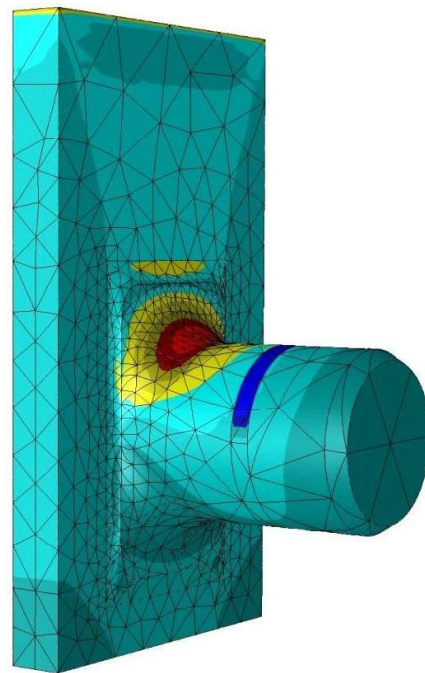


Figure 2 Max principal stress distribution for uncracked FE model

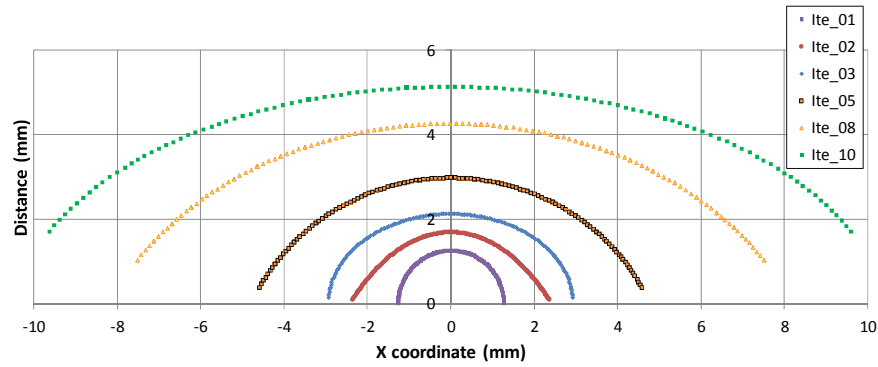


Figure 3 Crack geometry of selected cracks iterative method

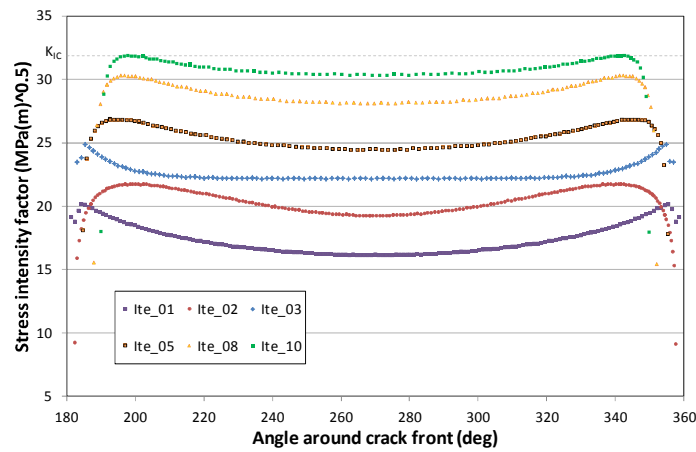


Figure 4 SIF variation around selected crack fronts

### 4.3 Fatigue Analysis of Transport Aircraft Structures using Advanced Cyclic Plasticity Models - an Assessment; D. Agius, [RMIT], C. Wallbrink, W. Hu [DST Group], K. Kourousis [University of Limerick] and C. Wang [UNSW]

Strain-Life methodologies have routinely been used in the aerospace industry for many years to manage aircraft structural integrity. Despite the availability of advanced cyclic plasticity models in the literature, surprisingly fairly basic models are mostly used in software tools in the aerospace industry. Although speculative, the reasons are most likely related to stability of the solution and historical reasons. Basic models such as the Masing model [1] rudimentarily estimate the cyclic hysteresis responses using the stabilised cyclic stress strain curve. While this is a reasonable approach for high cycle fatigue, its validity is questionable if significant amount of fatigue damage occurs under non-stabilised material behaviour.

With more advanced models for cyclic plasticity, transient behaviours such as strain ratchetting and mean stress relaxation may be captured, giving a more accurate characterisation of the material behaviour. So the question remains: how do these models perform when applied to real world problems? The DST Group, as part of the 2010 structural management plan review for the P-3C Orion, conducted an extensive coupon

testing program [2]. Crack nucleation (initiation) data was obtained for a wide range of spectra obtained from identified fatigue critical locations for both the Royal Australian Air Force and the United States full scale fatigue test.

In this work, these data were used to evaluate the performance of a number of cyclic plasticity models including, Masing (Mas) [1], Multicomponent Armstrong-Frederick (MAF) (commonly known as Chaboche et al model) [3,4], MAF with Threshold term (MAFT) [5], Multicomponent Armstrong-Frederick with Multiplier (MAFM) [6] and Ohno-Wang (O-W) models [7].

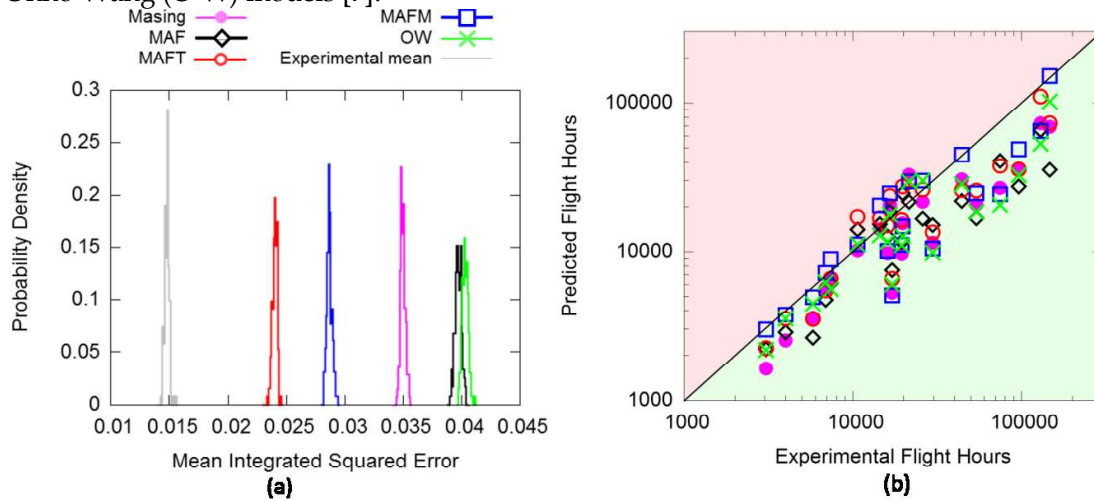


Figure 1: (a) Mean Integrated Square Error distributions formed by each of the cyclic-plasticity models (b) plot of geometric means from simulated fatigue lives versus their corresponding experimental values for a variety of transport aircraft load spectra.

Four advanced nonlinear kinematic hardening models were assessed using fatigue life predictions under transport aircraft fatigue load spectra relative to the Masing model. The assessment of the cyclic plasticity models was conducted using the Mean Integrated Square Error as a metric, based on the statistical distribution of the experimental and the numerical results, Figure 1a). The assessment showed that the MAFT and MAFM nonlinear kinematic hardening models coupled with the Prager back stress and isotropic hardening improved fatigue life predictions when compared to the Masing model. As can be seen from the plot of geometric means in Figure 1 (b), the majority of the simulation results are located in the lower “green” portion of the chart indicating conservative predictions. In this investigation the MAFT model demonstrated the best fatigue predictions.

The optimisation process also highlighted an issue in achieving a parameter set that simulated both ratcheting and mean stress relaxation phenomena. As a consequence of this, the parameter selection for this study was based on the improved ratcheting simulation accuracy. Future work will be aimed at determining the difference in fatigue life predictions when the model’s parameters are optimised for mean stress relaxation.

The results of this investigation [8,9] will influence the development of future structural integrity management programs that require crack nucleation as part the management strategy. In many case the strain-life methodology forms an integral part of airframe management strategies. It is foreseen that the outcomes of this investigation will have a significant positive impact to future management of aircraft in the Australian Defence

Force. Further new innovative technologies such as virtual fatigue testing could greatly benefit from enhanced understanding of the stress strain evolution offered by these plasticity models considered in this investigation.

## References;

- [1] G. Masing, "Self stretching and hardening for brass (in German)," in Second International Congress for Applied Mechanics, Zurich, Switzerland, 1926, pp. 332-335.
- [2] D. Phillips, R. Hartley, and R. Amaratunga, "DSTO Coupon Testing Documentation in Support of the P-3 SLAP," 2005.
- [3] J. L. Chaboche, K. Dang-Van, and G. Cordier, "Modelization of the strain memory effect on the cyclic hardening of 316 stainless steel," in Fifth International Conference on SMiRT, Berlin, Germany, 1979.
- [4] P. J. Armstrong and C. O. Frederick, "A Mathematical Representation of the Multiaxial Bauschinger Effect," G.E.G.B. Report RD/B/N, vol. 731, 1966.
- [5] J. L. Chaboche, "On some modifications of kinematic hardening to improve the description of ratchetting effects," International Journal of Plasticity, vol. 7, pp. 661-678, // 1991.
- [6] Y. F. Dafalias, K. I. Kourousis, and G. J. Saridis, "Multiplicative AF kinematic hardening in plasticity," International Journal of Solids and Structures, vol. 45, pp. 2861-2880, 5/15/ 2008.
- [7] N. Ohno and J. D. Wang, "Kinematic hardening rules with critical state of dynamic recovery, part I: formulation and basic features for ratchetting behavior," International Journal of Plasticity, vol. 9, pp. 375-390, 1993.
- [8] D. Agius, M. Kajtaz, K. Kouriousis, C. Wallbrink, C. H. Wang, W. Hu, F. S. Silva "Sensitivity and optimisation of the chaboche plasticity model parameters in strain-life fatigue predictions". Materials & Design vol. 118, pp. 107-121, 2017
- [9] D. Agius, C. Wallbrink, W. Hu, K. Kouriousis, C. H. Wang, M. Kajtaz "Fatigue analysis of transport aircraft structures using advanced cyclic plasticity models - an assessment". In: 10th International Conference on Structural Integrity and Failure (SIF-2016): 13-15 July, 2016

Email: Chris.Wallbrink@DSTO.defence.gov.au

## 4.4 Simulated Aircraft Spectrum Loading Behavior on 7075-T6 and 7249-T76511 Aluminum Alloys used on the P-3 Aircraft; K.F. Walker [DST Group Australia] and J.C. Newman Jr., [Mississippi State University USA]

The wings on the P-3C Maritime surveillance aircraft are made from 7075-T6 aluminium alloy. The current wings for the United States fleet have been replaced with 7249-T76511 alloy due to its improved corrosion resistance over the 7075 alloy. The P-3C fleet in Australia has maintained the 7075 alloy wings. The objectives of this study were to conduct fatigue-crack-growth tests on middle-crack-tension, M(T), specimens made of thin-sheet 7075 and 7249 alloys under constant-amplitude loading to compare with test data previously generated on compact, C(T), specimens, and to conduct fatigue-crack-growth tests on middle crack tension, M(T), specimens under a simulated P-3C wing spectrum. The spectrum was derived from a full-scale fatigue test (FSFT) program conducted at Lockheed-Georgia [1, 2] under contract to the U.S. Navy. But the large FSFT spectrum was reduced by eliminating stress ranges less than 15% of the maximum range. This spectrum, 301FSFT15tc, was used to conduct crack-growth tests on a thicker 7249 alloy [3]. In the current study, the spectrum was further modified to have only tension-tension loading (301FSFT15tt). Thus, the spectrum tests were conducted without anti-

buckling guides. These spectra had about 300,000 cycles, and they were repeated until failure or the test was terminated.

There were five (5) M(T) specimens made of the 7075-T6 and 7249-T76511 alloys each that were 96.5 mm (2w) wide and 2 mm (B) thick. All specimens had an electrical-discharged notch that was 10 mm in length and all specimens were fatigue pre-cracked under constant-amplitude loading ( $R = 0$ ), as shown in Figure 1. The initial crack was grown to a half-length of 6.35 mm, and then the spectrum loading was applied. Part of the spectrum loading is shown in Figure 1, where the applied loads have been normalized by the maximum spectrum load and the minimum load was zero. The modified tension-tension spectrum has the same sequence and load ranges as the tension-compression spectrum but a higher mean load to maintain the minimum load of zero. The test frequencies ranged from 4 to 7 Hertz. Prior to conducting the spectrum tests, the load frame was tuned and the FTA crack-monitoring system [4] was trained on a similar M(T) specimen of the same initial stiffness and under the same spectrum loading sequence and magnitude. Crack lengths were monitored with two crack-mouth-opening displacement (CMOD) gages (front and back). As the crack grew and the specimen stiffness changed, the FTA system modified the correction file to maintain accurate loading. (A validation file with the actual loading was also created for use in validating the accuracy of the target spectrum loading.) These gages were removed when the crack length reached about 60% of the width. Visual measurements were then made on crack length against cycles until either failure or the crack length reached about 70 to 75% of the width, and then the specimen was pulled to failure to obtain some fracture toughness data.

Figure 2 shows the spectrum results on the 7075-T6 alloy. Two maximum stress levels in the spectra were used: (1)  $S_{\max} = 128$  MPa and (2)  $S_{\max} = 156$  MPa. The first test experienced a power outage after about 1-million cycles. This specimen was then used as a fracture test with a crack-length-to-width ratio of about 0.27. The second test at 128 MPa lasted for nearly 7-million cycles (14 days). The initial portions of the first and second tests agree well. The stair-casing results were due to the severe overloading applied around 86,000 cycles. The third test was conducted at a maximum applied stress on 156 MPa. Surprisingly, these results agree well with the lower applied stress case. It is suspected that more plane-stress behavior is induced by the higher maximum stress level, which would cause more crack-growth retardation.

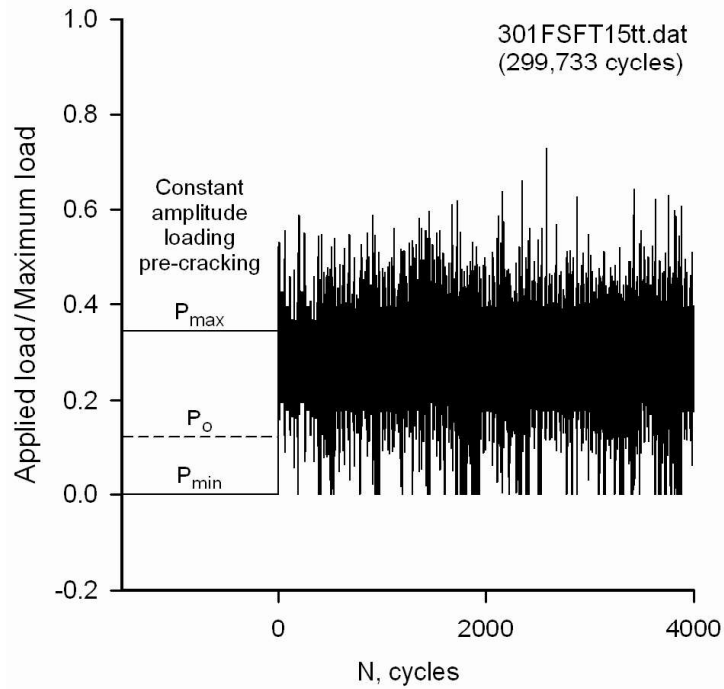


Figure 1. Fatigue pre-cracking loads and part of the modified P3-C simulated spectrum loading.

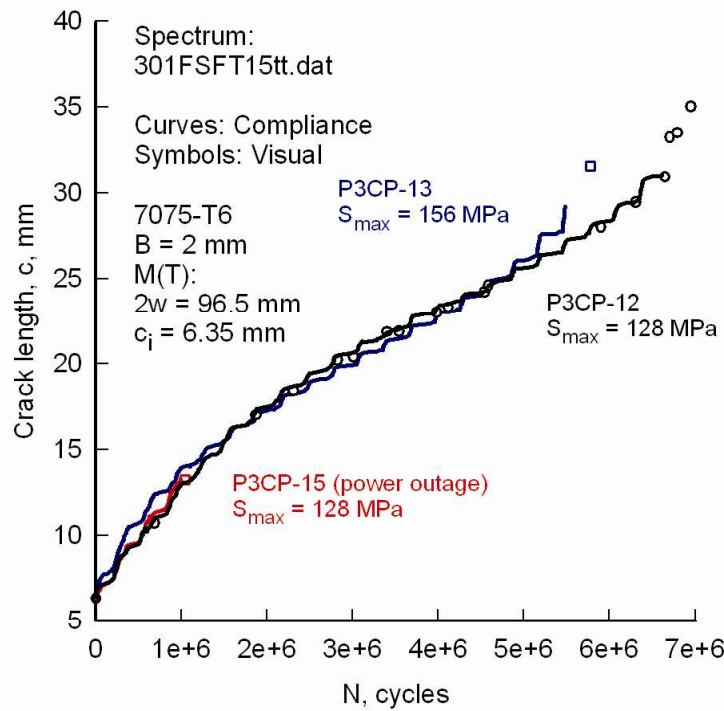


Figure 2. Crack-length-against-cycles under the modified P3-C simulated spectrum loading for the 7075-T6 M(T) specimens.

Figure 3 shows similar results on the 7249-T76511 alloy under the same spectrum loading. Again, two maximum stress levels were used: (1)  $S_{max} = 128$  MPa and (2)  $S_{max} = 156$  MPa in the spectra. Here two tests were conducted at the highest maximum applied stress level, and these results showed some scatter between the two tests (about 20% near failure). Surprisingly, the test at the lower applied stress level (128 MPa), gave longer life initially, but crossed over the test results for the higher stress level, and the final life agreed with one of the higher applied stress level tests. Again, it is suspected that more plane-stress behavior is induced by the higher maximum stress level, which would cause more crack-growth retardation. The spectrum life for the 7249 alloy was about *one-half* of the live for the 7075 alloy. This behavior was caused by the fact that the 7249 alloy has much faster crack grow at the lower stress-intensity factor ranges (lower threshold) than the 7075 alloy [3]. Further study is underway using the FASTRAN life-prediction code [5] using the variable-constraint option to see if the model can predict the behaviors observed in these tests.

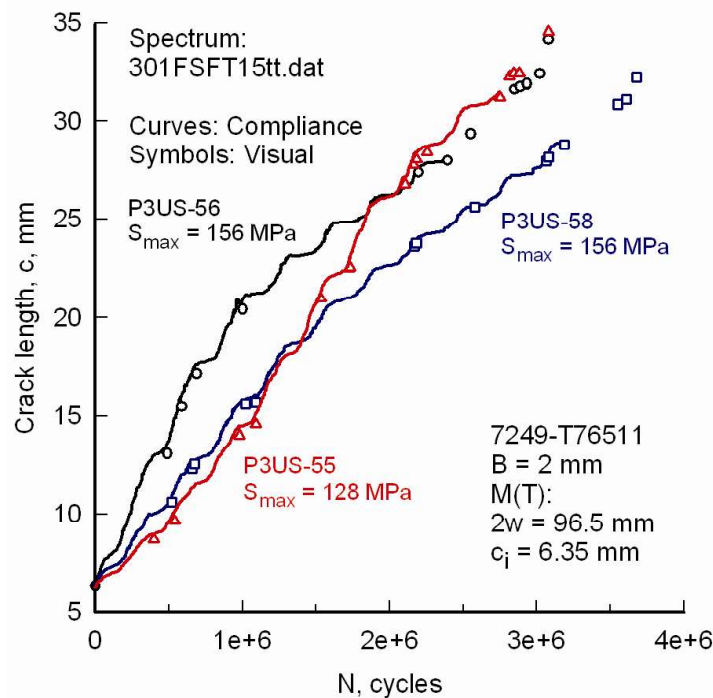


Figure 3. Crack-length-against-cycles under the modified P3-C simulated spectrum loading for the 7249-T76511 M(T) specimens.

#### References:

- [1] Lamas, J. and Edwards, M. P-3C Service Life Assessment Program - Full-Scale Fatigue Test. International Committee on Aeronautical Fatigue, 22nd Symposium, Lucerne, Switzerland, 2003.
- [2] Shah, B. P-3C Service Life Management, United States Air Force, Aircraft Structural Integrity Program (ASIP) Conference, Memphis, TN, USA, 2004.

[3] [Newman, J.C., Jr.](#), Walker, K.F. and Liao, M. Fatigue Crack Growth in 7249-T76511 Aluminum Alloy under Constant-amplitude and Spectrum Loading. *Fatigue and Fracture of Engineering Materials and Structures*. Wiley-Blackwell, Vol. 38, 2015, pp. 528-539.

[4] Donald, J. K. and Blair, A. Automated Fatigue Crack Growth Testing and Analysis – Series 2001. Version 3.09, 2009, Fracture Technology Associates, LLC, Bethlehem, PA.

[5] Newman, J. C., Jr. FASTRAN – A Fatigue Crack Growth Life Prediction Code based on the Crack-Closure Concept. Version 5.4 User Guide. 2012, Fatigue and Fracture Associates, LLC, Eupora, MS.

Contact K. Walker at [kevin.walker@dsto.defence.gov.au](mailto:kevin.walker@dsto.defence.gov.au)

#### **4.5 Research Program Outcome: Interaction of Fatigue and Intergranular Corrosion in the AP-3C Dome Nut Holes; T. J. Harrison, B. R. Crawford, C. Loader, D. Goudie, A. Walliker [DST Group]**

Maritime Platforms System Program Office and the Defence Aviation Safety Authority have recently ruled that some instances of Intergranular Corrosion (IGC) can remain on Royal Australian Air Force (RAAF) AP-3C aircraft. This is a result of two parallel research programs conducted by DST Group into the initiation [1] and growth [2] of fatigue cracks from Intergranular Corrosion (IGC), which showed that the presence of IGC did not void the current airworthiness practice. This has increased the operational capability of the RAAF AP-3C fleet while significantly reducing maintenance time and costs.

The RAAF has been concerned by the presence of IGC in the AP-3C Orion for some time. There have been cases of IGC fissures forming from the bores of particular fastener holes (Dome Nut Holes (DNH)) in the wing skin of the AP-3C to depths approaching 10 mm. Due to the large size of this IGC, removal and subsequent repairs were costly and reduced aircraft availability as the originally approved repair required the complete removal of the IGC.

The DST Group research programs investigated the fatigue implications of IGC. One program investigated the causes underlying fatigue initiation from IGC through a combination of experimental work and numerical modelling. This program culminated in a PhD dissertation which was accepted by RMIT University on the 28<sup>th</sup> of August, 2014 [1]. The second program, the DST AP-3C Orion Intergranular Corrosion project, investigated the interaction and growth of multiple fatigue cracks in the presence of IGC [2].

These programs, as reported in [3], both showed that fatigue cracks initiate from Dome Nut Hole locations containing IGC either at pitting corrosion, which is the precursor to IGC, or at corroded inclusions along the IGC fissure [4]. A predictive model was developed to predict initiation depth (Figure 1) [5] and relate this to a knock-down factor on life for fatigue crack initiation (Figure 2). The reductions in fatigue life from the understood initiation mechanisms did not impact on the lifeing of the DNH locations and did not invalidate the inspection techniques used in maintenance of the AP-3C by a shifting of the

site of fatigue crack initiation. Finally, IGC fissures were found to not accelerate fatigue crack growth (Figure 3) [2].

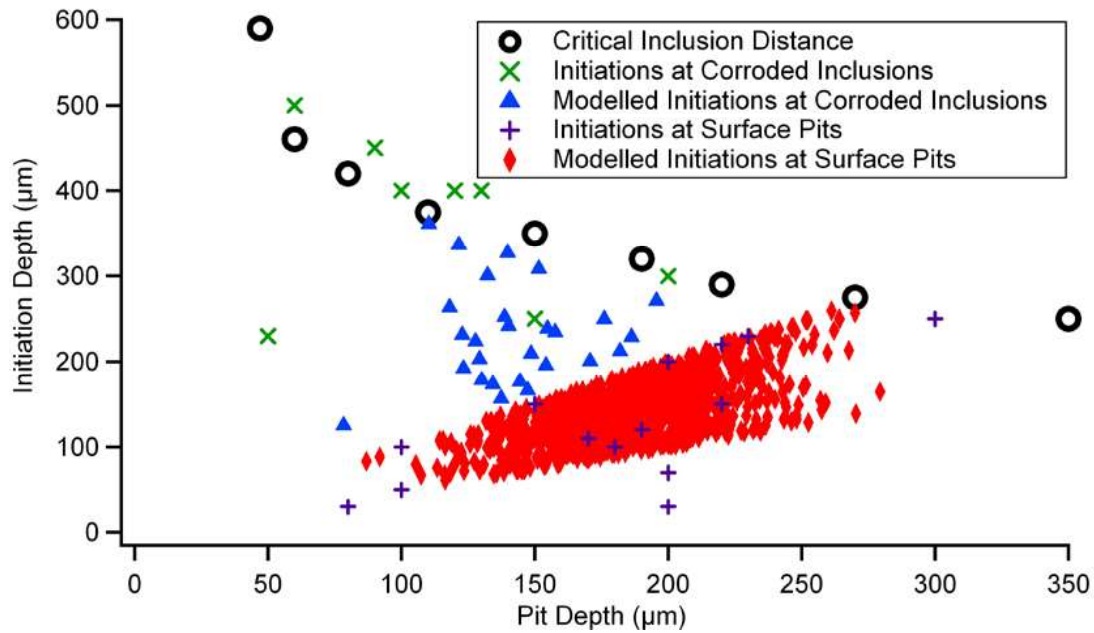


Figure 29: Predictive model and fatigue test results for fatigue initiation depth and how that relates to pit depth. Also shown is the Critical Inclusion Distance, whereby a corroded inclusion has to be within that depth to be a fatigue initiation; this shows a limiting initiation depth of approximately 750  $\mu\text{m}$

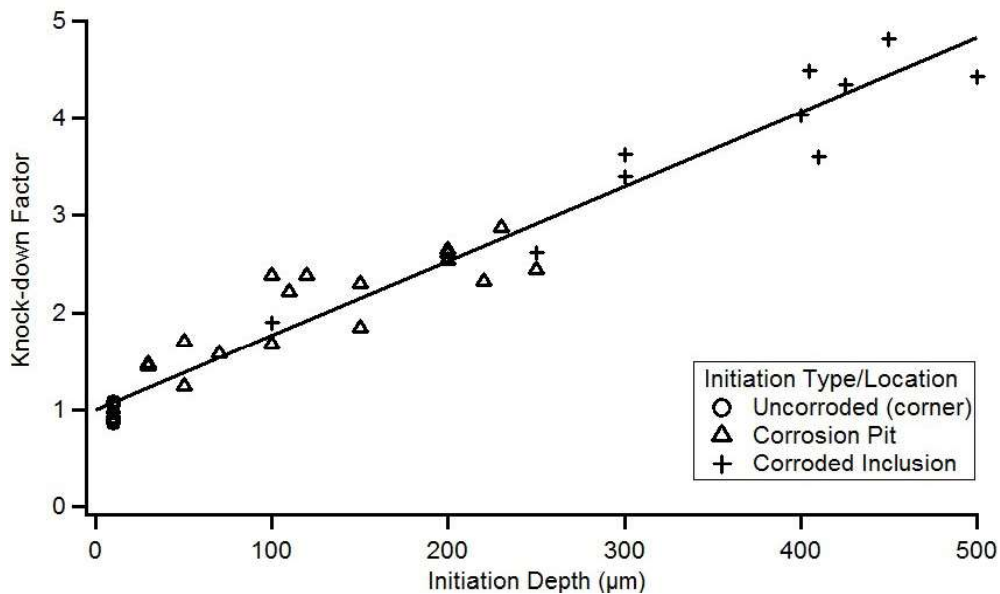


Figure 30: Relationship between a knock-down factor based on the number of cycles to fatigue initiation (in constant-amplitude testing) and initiation depth of the same test samples, highlighting a linear relationship between initiation time and depth for this form of IGC.

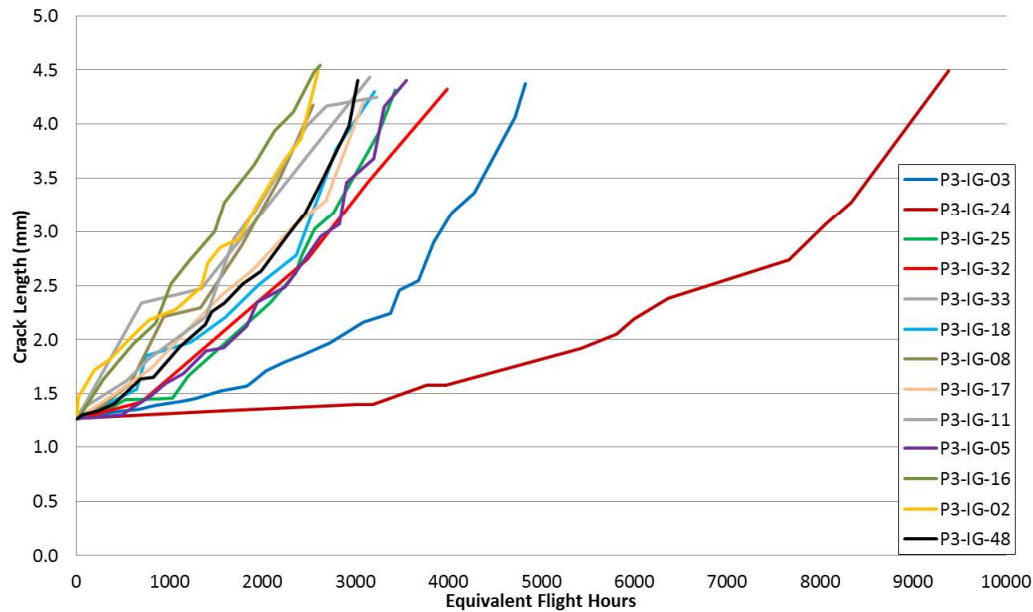


Figure 31: Fatigue crack growth from 1.27 mm until approximately 4.5 mm (failure of the ligament between the main hole and satellite hole within the DNH configuration) with application of FCA352 (most severe) spectrum loading, showing a number of specimens having similar crack growth to each other (as well as to an uncorroded specimen), with one outlier that is actually slower crack growth than the uncorroded specimens.

## References

- [1] T. J. Harrison. *Predicting fatigue crack initiation due to the presence of intergranular corrosion in extruded 7075-T651 aluminium alloy*. PhD thesis. School of Aerospace, Mechanical and Manufacturing Engineering, RMIT University, Victoria, Australia; 2014.
- [2] C. Loader, D. Goudie, M. Salagaras, J. Underwood, A. Walliker. *RAAF AP-3C interaction between intergranular corrosion and fatigue*. Melbourne, Victoria: DSTO-TR-3048; 2014
- [3] P. Jackson, C. Wallbrink . *A Review of Australian and New Zealand Investigations on Aeronautical Fatigue During the Period April 2013 to March 2015*. Melbourne, Victoria: DST-Group-TN-1460
- [4] T. J. Harrison, B. R. Crawford, C. Loader, M. Brandt. *The effect of Intergranular Corrosion on Fatigue Crack Initiation*, submitted to International Journal of Fatigue, 2017
- [5] T. J. Harrison, B. R. Crawford, C. Loader, G. Clark, M. Brandt. *Predicting the likely causes of early crack initiation for extruded aircraft components containing intergranular corrosion*. International Journal of Fatigue. 2016;**82**:700-707

## **4.6 A Study of the Effectiveness of porosity as a fatigue crack initiator in AA7050-T7451; S. Barter and B. Dixon [DST Group]**

### **Introduction**

The F/A-18 A-D Centre Barrel (CB), Figure 1a, is a primary load bearing member, which comprises three bulkheads that contain the wing attachment points. Small voids, herein referred to as porosity, form during the casting of the AA7050-T7451 plates from which these bulkheads and other F/A-18 parts are made and these are potential sites for fatigue crack initiation. Porosity is most prevalent in the centre of such plates, is typically associated with intermetallic inclusion particles, and the limited reduction in thickness when the plates were rolled means that there was limited healing of the porosity that was present.

One of the manufacturers implemented process improvements for the F/A-18 A-D AA7050-T7451 plates supplied in the 1980s to reduce the amount of porosity present [1]. This resulted in a reduction in the number of large porosity discontinuities present in the plates and an improvement in average fatigue life. Despite this work, porosity has been identified as a cause of fatigue cracks in F/A-18 Full-Scale Fatigue Tests (FSFTs) and is therefore worthy of further assessment. Consequently, there was interest in quantifying how rapidly fatigue cracks grow from porosity.

### **Method**

Cylindrical coupons were manufactured from near the wing attachment locations (Figure 1b) of 6 bulkheads from two ex-service F/A-18 A-D CBs. The coupons (Figure 1c) were polished to remove all potential crack starting surface discontinuities apart from porosity. They were fatigue tested to failure under one of two fighter wing root bending moment spectra. The fracture surface of each coupon was examined using quantitative fractography, which allowed the cross-sectional area and maximum depth of the crack starting porosity discontinuities to be measured, as illustrated in Figure 2. A crack growth curve was derived for each coupon and this allowed the effectiveness of the porosity as a crack starter to be quantified according to its Equivalent Pre-crack Size (EPS) [2], which compared the crack growth from porosity to that from a fatigue crack of the same size. In this manner, the fatigue severity of the porosity in the CB bulkheads was quantified via the measurements made for 116 coupons.

### **Results**

As illustrated in Figure 3, the EPS of porosity was much smaller than its physical size. On average, the porosity had the effectiveness of a fatigue crack one tenth its maximum depth. For other typical aircraft component discontinuities, there is usually a much better match between the depth and EPS. Furthermore, the porosity's two-dimensional size (i.e. area and depth) predicted its crack-like effectiveness poorly, with unquantified factors such as the three-dimensional size and shape, and collocated inclusion particles appearing to have a significant influence.

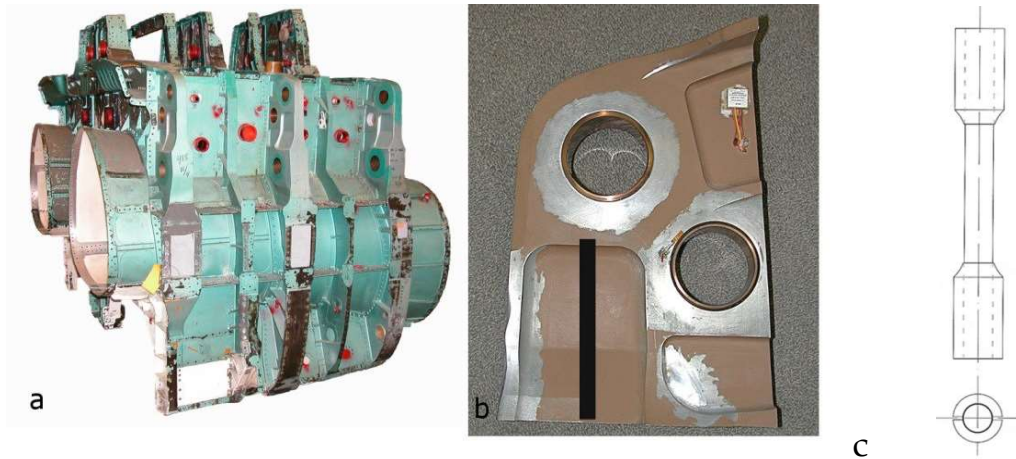


Figure 32. Polished coupons made from the F/A-18A-D centre barrel (CB) bulkheads. a. Shows a F/A-18 A-D CB. b. Shows the orientation in which coupons were cut from near the wing attachment locations. c. Shows the cylindrical design of the polished coupons with bonded grips.

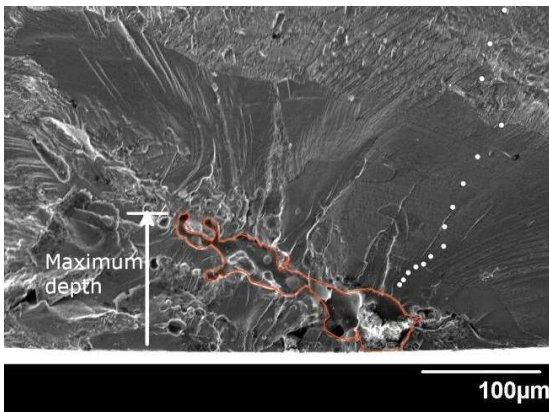


Figure 2. Porosity at the start of a fatigue crack in one of the coupons. The maximum depth that was measured for each coupon is illustrated. The porosity boundary area (red) was also measured.

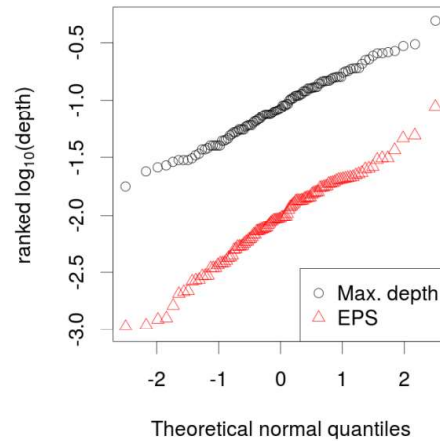


Figure 3. Comparison of the maximum depth and EPS of the porosity via a normal probability plot of the  $\log_{10}$  depths.

## References

- [1] Owen, C., Bucci, R. and Kegarise, R. (1989) Aluminum Quality Breakthrough for Aircraft Structural Reliability. *Journal of Aircraft* **26** (2) 178-184
- [2] Dixon, B., Barter, S. and Mazeika, R. (2016) *Quantification of the Fatigue Severity of Porosity in the AA7050-T7451 Thick Plate Used in the F/A-18A/B*. DST Group-TR-3295, Melbourne, Australia, Defence Science Technology Group.

#### **4.7 An Investigation of the Effectiveness of Adhesively Bonded Doubler Repairs on Existing Fatigue Cracks in Typical Combat Aircraft Structures; G. Swanton, L. Robertson and S. Barter [DST Group])**

An inherent consideration for the integrity of a fatigue damaged structure using adhesively bonded doublers is the existence of any remaining cracking prior to the bonding on of the doubler. The limitations of non-destructive inspection techniques or insufficient 'confidence cutting' make this scenario a distinct possibility. In the case of highly loaded, fracture critical details typical of combat aircraft structures (e.g. bulkhead flanges), this risk is compounded by the presence of the doubler itself limiting the sensitivity of future inspections for fatigue cracking.

An F/A-18 original equipment manufacturer doubler modification was used as the basis for a Defence Science and Technology Group coupon study [1] to assess the effectiveness of doublers bonded over existing totally embedded fatigue cracks in a highly stressed location. The fatigue damage in this study consisted of two types: naturally grown cracks and electrical discharge machining (EDM) slots to simulate such cracks. One set of coupons were cycled to grow fatigue cracks before a doubler was installed, and then subjected to continued fatigue cycling. Another set of coupons had simulated fatigue cracks inserted via EDM slots of different configurations, sizes and at a selection of locations; a smaller one to approximate natural cracks and a larger size to assess damage tolerance aspects. The EDM coupons also had a doubler bonded over the top and were fatigue cycled to grow cracking from these slots.

For the naturally grown fully embedded cracks, the doublers were very effective in reducing the fatigue crack growth rate. Post-test quantitative fractography (QF) showed the rate reduced by several orders of magnitude, which resulted in an extension of over five coupon lifetimes compared to a reference set of unrepaired coupons. The doublers weren't as effective on the EDM coupons, as these typically failed at between one to two lifetimes. QF indicated that the corner 'cracks' that were included in these coupons grew faster than the embedded surface 'cracks'. In all cases the doubler was successful in reducing the crack growth rates by varying degrees through the reduction of section stresses. The outcomes of this research are expected to support future structural integrity management decisions involving bonded doubler modifications to ADF aircraft.

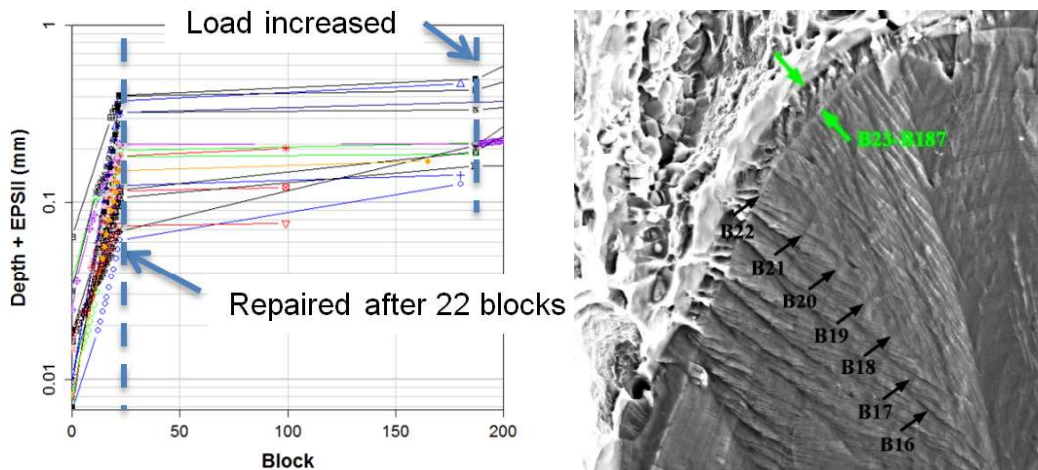


Figure 1: Crack growth curves for repaired SEM image of partial fracture coupons

#### References:

[1] Swanton, G., Robertson, L., and Barter, S., *The Effect of Adhesively Bonded Doubler Repairs on Existing Fatigue Cracks in Typical Combat Aircraft Structures*, in: 17<sup>th</sup> Australian International Aeronautical Congress, Melbourne, Australia 2017.

geoff.swanton@dsto.defence.gov.au

#### 4.8 Recent Developments in SHM for Aircraft Structures - an Australian Defence Perspective; S. Galea, N. Rajic, C. Davis, C. Rosalie, J. Smithard, C. Brooks, S. van der Velden and P. Norman; [DST Group]

As aircraft fleets get older there is a greater reliance on safety-by-inspection (SBI) programs to manage the aircraft structural integrity (ASI) of the fleet. As the number of structural 'hot spot' findings increase within an ageing fleet, more SBI programs are required to maintain ASI thus consuming a greater portion of the operator's resources available for through-life-support, as well as the possibility of significantly reducing aircraft availability. SBI approaches traditionally rely on the application of conventional NDI at set intervals, which can be costly and time-consuming especially if applied to difficult to access regions. One way of reducing costs and increasing aircraft availability is through the introduction of in-situ NDI or structural health monitoring (SHM) using structurally-integrated transducers which facilitates an inspection on demand approach. SHM is another airframe diagnostics approach available within the NDI toolbox allowing ASI managers greater flexibility when developing SBI programs for the fleet.

The Australian Defence Science and Technology (DST) Group has a program of work aimed at developing autonomous, robust, reliable SHM systems with the specific aim of retro-fitment to existing aircraft. This paper describes some of the current SHM techniques being developed, evaluated and demonstrated at DST, which include the application of (1) acousto-ultrasonic techniques using low profile piezotransducers and optical fibre sensors and (2) thermoelastic stress analysis (TSA) using miniature micro-bolometer based thermal imagers.

#### **4.9 F/A-18 Inner Wing Step Lap Joint Phased Array Ultrasonic (PAUT) Inspection Development; S. Trezise [QinetiQ Australia]**

The F/A-18 Hornet aircraft employs carbon epoxy composite upper and lower wing skin panels. At the wing root, each skin panel is spliced to a titanium plate via a bonded stepped lap joint. The discovery of disbonds in these joints in a foreign fleet wing led to a requirement for inspection of the RAAF fleet wings. QinetiQ developed a phased array ultrasonic inspection technique to inspect the both the inner and outer mould lines of the joint. Phased array ultrasonic inspection is not commonly used within the RAAF NDT community, and as such training in the method, its application to the inner wing step lap joint, and critically the interpretation of results, was required and delivered to the RAAF. Implementation of this inspection is allowing the RAAF to understand the condition of the joint in fleet wings and to monitor and manage any defects identified.

#### **4.10 C-130J WFT Test Interpretation; M. Richmond [QinetiQ Australia]**

DST Group participated in a joint Royal Australian Air Force (RAAF) / Royal Air Force (RAF) project to conduct a wing fatigue test (WFT) of the C-130J to loading representative of the usage of both fleets. Using the existing, and significant, body of knowledge collected through operation of previous models of the C-130, the WFT aim is to optimise the aircraft structural inspection program through sound analysis that is supported by test based evidence relevant to the RAAF C-130J configuration, role and environment.

The testing phase was completed at the end of 2015 and the program has now moved into the test interpretation phase. The test interpretation process has been developed by DST Group, with QinetiQ conducting an independent validation and verification on behalf of the RAAF to ensure the process output will meet RAAF C-130J type certification requirements. Initial test interpretation effort is directed at deterministic evaluation of inspection threshold and inspection interval. Subsequent analysis will focus on probabilistic methods to determine limits of validity and derive the structural life of type for the RAAF C-130J fleet.



#### 4.11 Rotary Wing - Best Practice Fatigue Management; Anthea Mills [QinetiQ Australia]

The Australian Defence Force (ADF) applies Aircraft Structural Integrity (ASI) principles to the management of both its fixed and rotary wing fleets. However, a variety of technical and cultural challenges mean that ASI Programs for helicopters are currently less mature than those for fixed wing aircraft. In addition, although changes within military airworthiness regulations are expected to lead to long term improvements, in the short term there may be some confusion as the acceptable means of compliance for the new regulations are bedded down. Regardless of potential developments in ASI, Fatigue Management (FM) will be a fundamental requirement within future ADF programs, providing regular confirmation that the certification bases of ADF helicopter fleets remain valid. FM must ensure that the risk of structural failure does not exceed the accepted risk which is inherent within the aircraft's certification basis, unless that risk is clearly understood and appropriately mitigated or consciously retained. To achieve this, stakeholder collaboration is required to enable appropriate data collection, assessment and ongoing system improvement, see Figure 1.

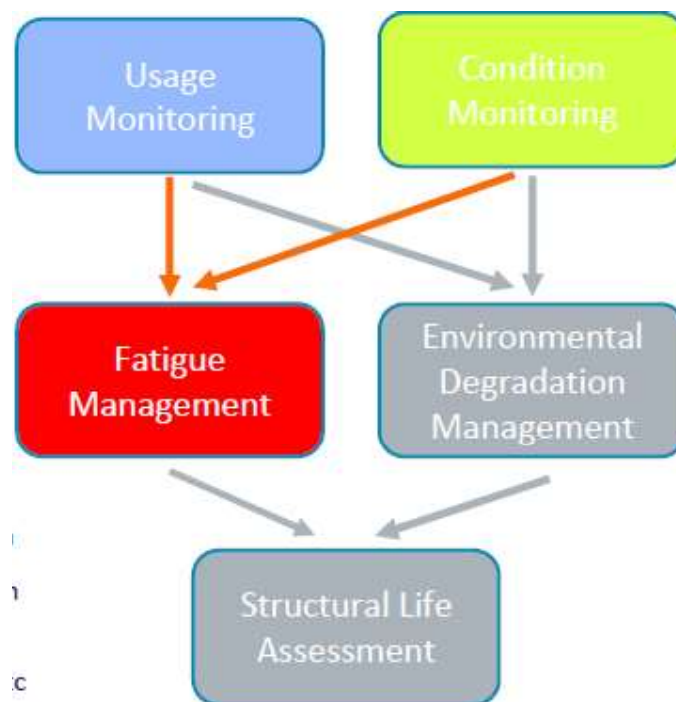


Figure 1 Elements of Structural Integrity Management

The elements of the theoretical system for achieving these goals, and the best practice approaches to these for rotary wing aircraft, include Flight Manoeuvre Recognition and Health and Usage Monitoring Systems. Added complexities also arise in through life management approaches currently being employed by the ADF include the different design standards employed by the various helicopter manufacturers, the use of commercial maintenance organisations and joint programs with foreign military operators.

## 4.12 Non-intrusive Flight Test Instrumentation (NIFTI) for Aircraft Structural Integrity Management; S. Galea [DST Group]

Many military services operate aircraft with planned withdrawal dates (PWD) well past the design life or life of type (LOT). For example the F/A-18 Classic Hornet operated by the ADF has a PWD about 20 years beyond its design life. A PWD extension requires the maintainer to reassess the fatigue life of critical components of the aircraft, along with the associated structural certification basis, to determine the fatigue management requirements to maintain the integrity of the structure to the revised PWD. Consequently a number of fatigue critical components may need to be managed on a safety-by-inspection (SBI) basis. To assist in the PWD assessment and/or in the development and validation of SBI programs knowledge of the operational aircraft loads and usage is essential. The collection of such data can be an expensive and time consuming exercise if existing commercial-off-the-shelf (COTS) flight test instrumentation (FTI) systems are employed. NIFTI is a small rapidly configurable system which utilises a bespoke wireless communications technology, instead of a COTS alternative such as WiFi or Bluetooth. Physically, the system comprises a single recorder (gateway) and 50+ wireless sensors that are designed to adhere to any surface, while having negligible influence on aircraft handling qualities, performance or operating limits. NIFTI was successfully demonstrated, using ten accelerometer modules, on a proof-of-concept flight trial on an AWC PC-9A. The future development path flight includes demonstrators on a fast jet.



Figure 1 NIFTI Phase I system of the type trialled on the PC-9

## 5. Fatigue Investigations of In-Service Aircraft

### 5.1 Propeller “falls off” a Saab 340B Commuter Aircraft; [Civil Aviation Safety Authority]

On 17 March 2017 a Regional Express Saab 340B aircraft registered VH-NRX was forced to make an emergency landing after the right propeller fell off mid-air. The propeller was found a few days later in bushland in Sydney's south-west, Figure 2. In its preliminary report, the Australian Transportation Safety Board (ATSB) stated that a fatigue crack had formed in the propeller mounting flange, where the propeller attaches to the gearbox, and transitioned into the shaft section. The crack originated at the bore of a dowel pin near the forward face of the propeller hub flange, see Figure 4. The dowel pin bore was corroded in parts and corrosion pitting was found near the fracture. Further work is ongoing to ascertain whether the corrosion or other factors contributed to the fracture initiation.



Figure 1 View of the aircraft after landing



Figure 2 Propeller as found

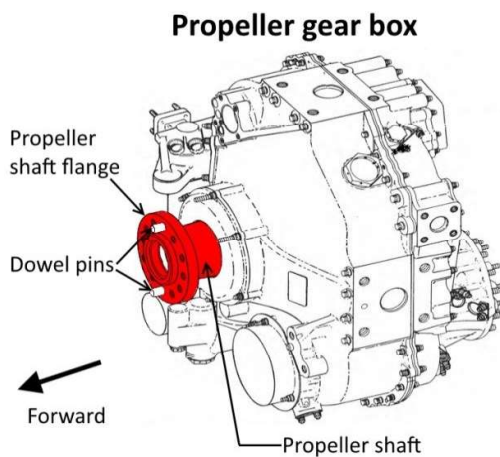


Figure 3 Gear box schematic



Figure 4 Section of propeller shaft

According to the ATSB this is the first known critical failure of this type, initiating within the propeller hub flange of the GE Aviation CT7-9B engine. The same propeller gearbox is fitted to multiple variants of the CT7 engine and SAAB 340 and EADS CASA CN-235 aircraft

There is currently no maintenance requirements specified in existing maintenance manuals for routine inspection of dowel pin bores. Inspection for surface defects only occurs when the gearbox is disassembled for overhaul. Both the operator and the engine manufacturer have already taken proactive safety action in response to the ATSB's safety advisory notice.

## Reference

Australian Transport Safety Bureau report AO-2017-032

## 5.2 RAAF F/A-18 Auxiliary Power Unit (APU) Turbine Hub Cracking; [N. Athinotis DST Group]

The Royal Australian Air Force (RAAF) operates the F/A-18 aircraft. An APU had been in overhaul due to a shaft leak. Non-destructive inspection on the turbine revealed cracks at three of the blade roots and in the hub. Cracking at the blade roots is a known issue. The US Navy had previously reported an uncontained APU turbine failure in 2003. DST examination of the APU turbine revealed four cracks were present between blades on the hub and six cracks were present on the aft face at the trailing edge blade roots. Examination of the fracture surfaces of seven cracks revealed they were consistent with fatigue.

Primary carbides rich in tantalum, titanium and niobium were frequently present at crack origins. Oxides of aluminium and chromium were also frequently present at crack origins. The majority of the trailing edge blade tips showed evidence of rubbing which was also heat-tinted, indicating the rubbing had occurred during operation. This could have increased stresses at the blade roots and led to crack initiation in the trailing edge blade roots. The aft faces of the blades also showed evidence of rubbing that resulted in the formation of a stepped surface, and this rubbing may have contributed to the initiation of cracks at the hub in the nominally low stress regions. The presence of aluminium and chromium oxides within the cast turbine could have been responsible for the initiation of fatigue cracks during normal APU operation.

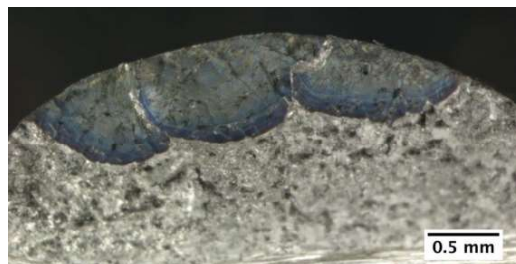


Figure 1 Hub crack location

Figure 2 Fracture surface of the hub crack

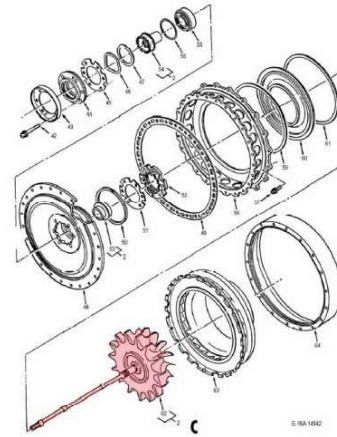
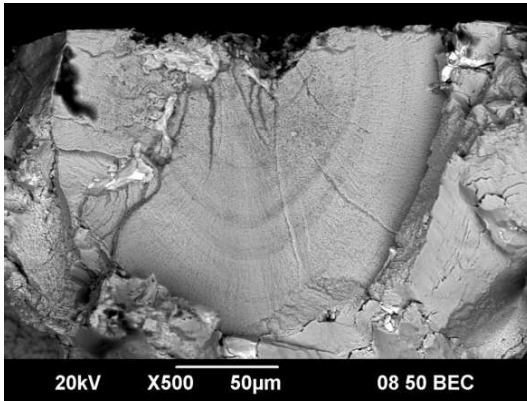


Figure 3 SEM micrograph of a fatigue crack origin

Figure 4 Schematic

### 5.3 Helicopter Horizontal Driveshaft Intermediate Bearing Cracked Assembly; [N. Athinotis DST Group]

During after-flight inspection of an aircraft it was discovered that a crack had developed on the right-hand support of the intermediate bearing housing. Further investigation revealed that the crack had propagated through the entire right-hand support. Due to the extensive damage on the fracture surface, the crack origins could not be identified; however cracking appeared to initiate from the forward and aft edges of the supports and propagate towards the central flange, indicating the application of forward and aft loading. Examination of the bearings revealed that the aft bearing suffered extensive rolling contact fatigue damage, and evidence of axial loading of the bearings in the forward and aft directions was observed. Examination of the intermediate bearing housing assembly components revealed wear damage to the aft bearing inner race, spacer and flange that indicated the installation preload on the assembly had been lost, introducing a degree of play that permitted axial movement of the spacer and flange on the splined shaft. Loss of preload and axial movement of components on the shaft assembly is considered to have resulted in excessive axial loading being transferred to the bearings, resulting in the observed rolling contact fatigue damage. Excessive forward and aft axial loading is considered to have transferred to the housing, resulting in the observed fatigue cracking observed.

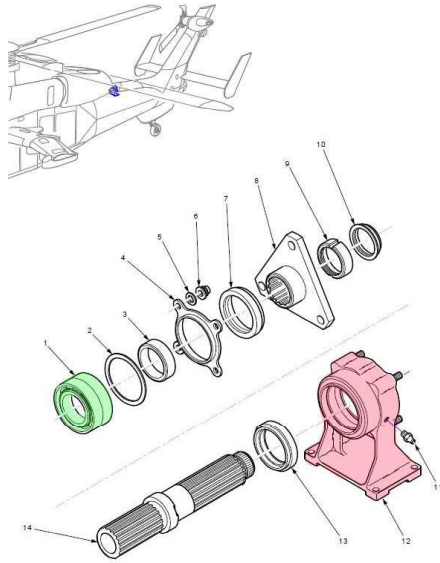


Figure 1 Schematic, bearing housing in red

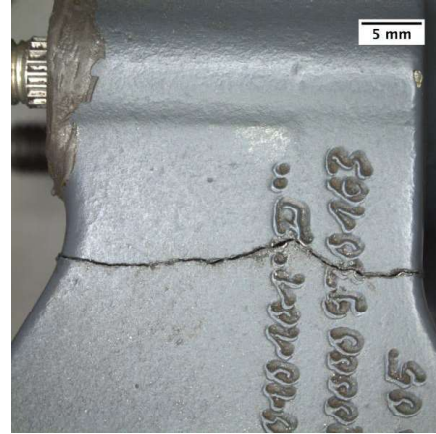


Figure 2 RHS of the bearing housing



Figure 3 spalling damage on the outer race

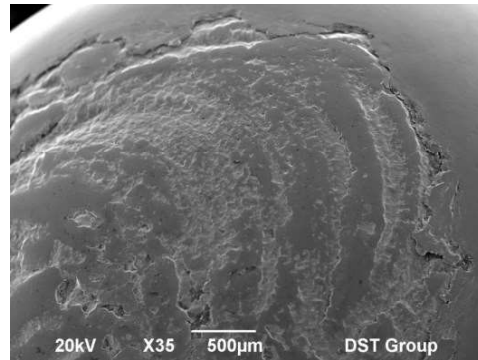


Figure 4 SEM showing spalling

#### 5.4 PC-9/A Frame 11 Left Hand Top Fastening Bracket Stress Corrosion Cracking; [N. Athinotis DST Group]

The Royal Australian Air Force operates the Pilatus PC-9 trainer aircraft. During an inspection of a PC-9/A aircraft, the Frame 11 Left Hand Top Fastening Bracket (LHTFB) was found to contain multiple cracks. A Special Technical Instruction was released shortly thereafter to inspect the fleet. This inspection found multiple cracked brackets. Destructive examination of the two Frame 11 LHTFB submitted for investigation found that all cracks observed in the components were due to stress corrosion cracking, which had propagated

in the long-transverse direction (the direction corresponding to the outboard-inboard direction on the component). The investigation revealed that the cracks initiated in the area where the Heli-Coil hole joined the outboard surface of the component. Although no specific crack origins were observed, the cracks most likely initiated from areas where the protective coating was damaged or absent, such as during installation of the Heli-Coil and fitting of the bracket to the aircraft.

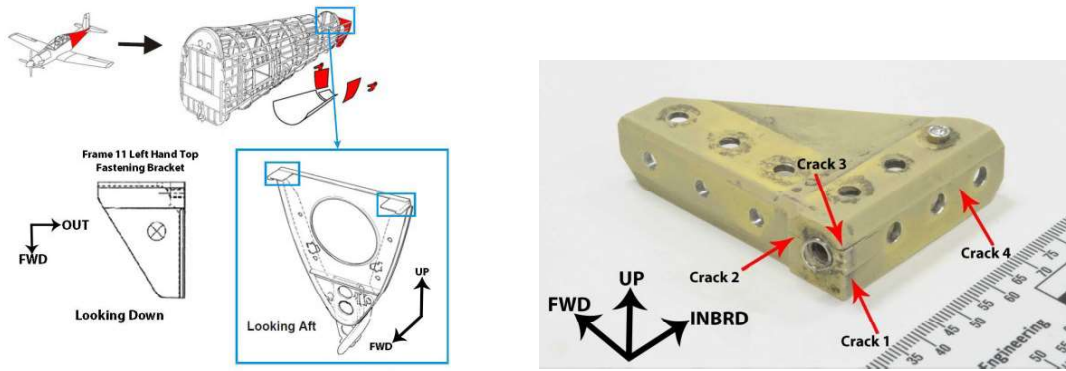


Figure 1 Schematic showing frame 11      Figure 2 Frame 11 LHTFB with cracks identified

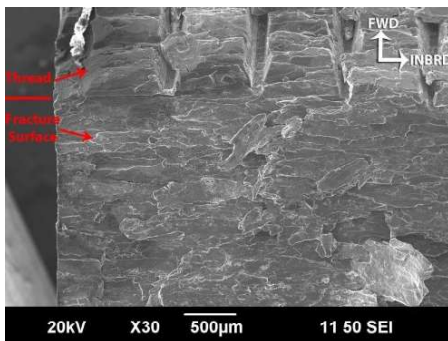


Figure 3 SEM image of fracture surface

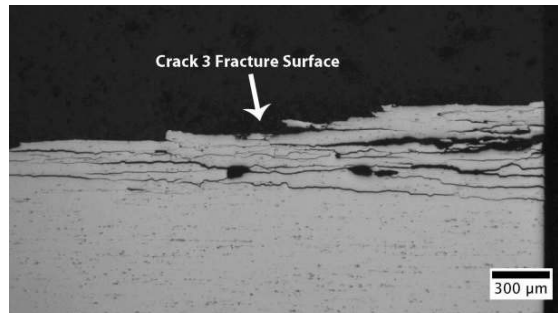
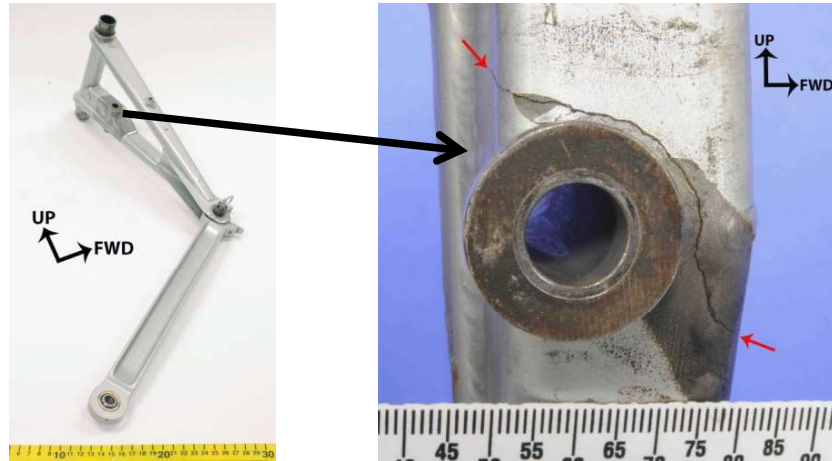


Figure 4 Cross section

## 5.5 PC-9/A Nose Landing Gear Folding Strut Cracking; [N. Athinotis DST Group]

Cracking occurred at the weld of the upper section of two NLG Folding Strut actuator attachment lugs. Undetected cracks via post-flight visual inspection and underestimation of cracks using Liquid Penetrant Inspection (LPI) prompted this investigation. Multiple fatigue cracks initiated at the weld toe of the actuator attachment lug and joined rapidly to form a stable single crack front. Similar crack growth rates were determined for each of the two struts. This together with the fact that the components had experienced a large difference in number of landings and had similar material properties/defects meant that cracking was likely triggered by a specific event in the life of the component. Surface decarburisation observed in the vicinity of cracking in both struts and the corresponding reduction in hardness and strength equated to a lower fatigue strength in these areas. The

limited access to the strut when installed in the aircraft, the tightly closed cracks on both the aft and rear faces of the box structure and the presence of paint and dirt, likely contributed to the cracks not being detected via visual inspection and the underestimation of crack length via LPI.



*Figure 1 Photograph of the NLG Folding Strut from A23-017 showing the orientation of the crack which extends around the weld circumference of the actuator attachment lug*